

Modeling and estimation of pedestrian flows in train stations

THÈSE N° 6876 (2016)

PRÉSENTÉE LE 18 MARS 2016

À LA FACULTÉ DE L'ENVIRONNEMENT NATUREL, ARCHITECTURAL ET CONSTRUIT
LABORATOIRE TRANSPORT ET MOBILITÉ
PROGRAMME DOCTORAL EN GÉNIE CIVIL ET ENVIRONNEMENT

ÉCOLE POLYTECHNIQUE FÉDÉRALE DE LAUSANNE

POUR L'OBTENTION DU GRADE DE DOCTEUR ÈS SCIENCES

PAR

Flurin Silvan HÄNSELER

acceptée sur proposition du jury:

Prof. N. Geroliminis, président du jury
Prof. M. Bierlaire, directeur de thèse
Prof. S. P. Hoogendoorn, rapporteur
Prof. W. H. K. Lam, rapporteur
Prof. U. Weidmann, rapporteur



ÉCOLE POLYTECHNIQUE
FÉDÉRALE DE LAUSANNE

Suisse
2016

Acknowledgements

First and foremost, I would like to thank my supervisor Michel Bierlaire. This thesis would not have been possible without his guidance and vision, as well as his incredible mentoring and support. He has always been there when I needed his advice, for which I'm deeply grateful. We've had countless profoundly inspiring scientific discussions, as well as other enriching moments while skiing, playing volleyball, hiking, or at conferences.

I am grateful to William H.K. Lam for welcoming me to the Hong Kong Polytechnic University between July and December 2014. His great intuition for compelling research, his genuine curiosity, and his scientific experience and knowledge have made this stay – truly memorable already for many other reasons – a very enriching one. I keep many fond memories of my interaction with him and his group, which has given me insight in a culture and lifestyle that is so different from the one that I grew up with. I appreciated immensely these exchanges, which have shaped my perspective of life far beyond research.

I would like to extend my heartfelt thanks to my current and former colleagues at EPFL for the warm and friendly atmosphere and their friendship. Among them, I would like to particularly thank Antonin Danalet, Marija Nikolić, Riccardo Scarinci, Bilal Farooq, as well as Anna Fernández, Bilge Atasoy, Eva Kazagli, Stefan Binder, Tomáš Robenek, Matthieu de Lapparent, Shadi Sharif, Yousef Maknoon and Prem Kumar, with whom I've been directly involved in research, shared office, spent countless evenings and weekends, or otherwise had a very pleasant interaction. This also holds for Nicholas Molyneaux, Thomas Mühlematter and Gael Lederrey, with whom I've been working particularly closely during their stay at the lab, and who contributed greatly to this thesis and have become friends.

Beyond EPFL, I wish to thank various other researchers whose work, knowledge or opinion has been a great influence. Among them, I would

like to mention Gunnar Flötteröd, Stefan Seer, as well as several people from TU Delft, in particular Femke van Wageningen-Kessels, Jeroen van den Heuvel and Winnie Daamen.

Besides Michel Bierlaire and William H.K. Lam, I would also like to thank the other members of the jury for their time, and their valuable and constructive input. The many comments by Serge Hoogendoorn, both regarding mathematical subtleties and fundamental aspects of the thesis, have been most helpful. The remarks by Ulrich Weidmann have been equally appreciated. I would also like to thank Nikolas Geroliminis for his constant advice over the years, and for presiding the committee.

This thesis has been supported by the Swiss National Science Foundation, as well as by the Swiss Federal Railways (SBB). Several people have contributed to its successful outcome by bringing in practical experience and ‘field data’, in particular Nicolas Anken, Aurelius Bernet, Beat Hürzeler, Herbert Kessler, Sonia Lavadinho, Michael Moos, Bonnie Qian, Michael Schürch, Uri Schtalheim, Zina Singer, Oliver Specker, Michaël Thémans, and Jasmin Thurau. Their contribution is greatly appreciated.

Lastly, I could not have come this far without the unconditional support of Gemma, my family, and my closest circle of friends in Switzerland, Spain and elsewhere in Europe. I am greatly indebted to all of them.

Lausanne, February 29, 2016

Flurin Hänseler

Abstract

This thesis addresses two modeling problems related to pedestrian flows in train stations, namely that of estimating pedestrian origin-destination demand in rail access facilities, and that of describing the propagation of pedestrians in walking facilities. For both problems, a mathematical framework is developed at the aggregate level, describing pedestrians in terms of groups with the same departure time, origin and destination.

The proposed demand estimator is probabilistic and accounts for within-day dynamics as well as for natural fluctuations across days. It is inspired by estimation methodologies that are used in the context of vehicular traffic. Critically, the proposed methodology takes the train timetable and ridership data into account, significantly improving the accuracy of the estimates. Other information sources, such as link flows or sales data, can also be incorporated.

To describe the propagation of pedestrians, walkable space is considered as a network of pedestrian streams that interact locally. Based on the continuum theory for pedestrian flow and the cell transmission model, a computationally efficient model is obtained that can be used under a wide range of traffic conditions. An optional extension allows considering anisotropic flow, where the walking speed depends on the walking direction. Such a formulation is advantageous in particular at high densities.

Throughout the thesis, a case study of Lausanne railway station is considered. A detailed discussion of the usage and level-of-service of its rail access facilities is provided, underlining the performance and practical applicability of the proposed modeling framework.

The contribution of the thesis is fourfold. First, it provides a dedicated estimation methodology for pedestrian OD demand in train stations. Second, it proposes a novel macroscopic network loading model for congested and multi-directional pedestrian flows. Third, it presents a detailed case

study of a Swiss train station, for which a rich data set is collected. Finally, it applies the aforementioned modeling framework to that case study, and provides practical guidance for its use in the planning and dimensioning of rail access facilities.

Beyond train stations, the developed modeling framework can be readily applied to various other pedestrian facilities, such as airports, shopping malls, stadiums or urban walking areas. For instance, it may be used to support the organization, planning and design of such facilities, to safely and efficiently manage pedestrian flows using real-time monitoring and control, or to assess and optimize the safety both during normal use and in case of emergency.

Keywords: Public transportation, pedestrian flow, demand estimation, network loading, train station, infrastructure planning.

Résumé: Ce travail porte sur la modélisation des flux de piétons dans les gares, et en particulier sur l'estimation de matrices origine-destination et sur la modélisation des flux avec une approche continue. Les deux problèmes sont étudiés en détail pour le cas de la gare de Lausanne.

Zusammenfassung: Diese Arbeit befasst sich mit der Modellierung von Fussgängerströmen in Bahnhöfen. Insbesondere wird die Schätzung von Quelle-Ziel-Matrizen und die Modellierung von Strömen mittels eines Kontinuum-Ansatzes diskutiert. Beide Probleme werden am Beispiel des Bahnhofs Lausanne ausführlich erläutert.

Contents

Acknowledgements	i
Abstract	iii
1 Introduction	1
1.1 Motivation and objectives	1
1.2 Contributions	4
1.3 Thesis structure	6
2 Context and case study	9
2.1 Literature review	9
2.2 Pedestrian data	12
2.3 Lausanne railway station	16
3 Demand estimation	23
3.1 Introduction	23
3.2 Methodological framework	25
3.3 Case study	40
3.4 Concluding remarks	47
4 Traffic assignment	49
4.1 Introduction	49
4.2 Literature review	51
4.3 Model framework	53
4.4 Model specification	64
4.5 Isotropic case studies	71
4.6 Anisotropic case studies	77
4.7 Discussion	85
4.8 Concluding remarks	90

5	Application and practical guidance	91
5.1	Introduction	91
5.2	Estimation of origin-destination demand	92
5.3	Level-of-service assessment	96
5.4	Planning guidelines	101
5.5	Concluding remarks	106
6	Concluding remarks	107
6.1	Main findings	107
6.2	Practical recommendations	108
6.3	Future research directions	110
	Appendices	115
	Bibliography	125
	Curriculum Vitae	143

Chapter 1

Introduction

1.1 Motivation and objectives

There is a general need to better understand pedestrian flows in public spaces. Notably, such knowledge is required for optimally planning and designing pedestrian facilities, involving aspects like infrastructure dimensioning or route signage. It is equally required for the management of pedestrian flows, such as the real-time monitoring, prediction and control of human crowds.

An optimal design and operation of pedestrian facilities aim at enabling efficient, comfortable and safe pedestrian flows. Efficiency usually means the minimization of walking times, but may also imply maximizing the length of stay of customers in a shopping mall. Comfort can be measured in terms of level-of-service indicators such as pedestrian density, or in terms of ambient factors that take into account the aesthetics of a facility. Safety involves aspects such as the rapid evacuation in case of emergency, the risk-free mobility of disabled people, or the avoidance of injuries on train platforms.

In pedestrian flow theory, a distinction is made between free-flow conditions at low densities, and congested conditions at high densities. In the free-flow regime, pedestrian flows are characterized by phenomena of self-organization, such as spontaneous lane formation in conflicting traffic. These yield a high flow performance even in multi-directional flow. In the congested regime, self-organization breaks down and the friction between pedestrians increases, incurring a significant drop in flow performance.

For optimal performance, a pedestrian facility should be operated in the

free-flow regime. This may be achieved by two ways. First, by ensuring an infrastructure dimensioning that can cope with the expected pedestrian demand without congestion. This option is feasible if pedestrian demand is homogenous across time, and if providing enough infrastructural capacity is economically viable. Second, by using a crowd management system that actively avoids congestion. Crowd management systems may for instance impose a limit on the inflow to a system, or reroute pedestrians away from busy areas. This option is particularly interesting if important demand peaks occur, such as during the simultaneous arrival of multiple large trains in a train station.

For both infrastructure assessment and crowd management, the availability of an appropriate pedestrian dynamic model is critical to reach efficient flow conditions. The development of such models has been the subject of research since the early 1990s, demonstrating the importance of the issue. A variety of pedestrian facilities have been considered, ranging from simple crosswalks (Lam et al., 2002) to shopping areas (Lam and Cheung, 2000), entire shopping districts (Borgers and Timmermans, 1986), metro stations (Lee et al., 2001), train stations (Daamen, 2004), airports (Solak et al., 2009; Lee et al., 2012), music festivals (Naini et al., 2011), university campuses (Danalet et al., 2014), museums (Yoshimura et al., 2014), or religious sites (Al-Gadhi and Mahmassani, 1990).

Among these facility types, rail access facilities are particularly relevant. Rail access facilities provide pedestrian access to trains, and have been subject to a strong increase in demand due to population growth, increase in mobility, and the installation of sales and service points within train stations (Nio, 2012). As a consequence, phenomena like congested walking facilities, delays of trains due to overcrowded platforms, or safety violations during boarding and alighting have emerged, putting the smooth operation of entire public transportation systems at risk (Hoogendoorn and Daamen, 2004; Buchmüller and Weidmann, 2008; Jiang et al., 2009a). Understanding these issues is challenging from a research point of view, and their alleviation highly relevant both for economic welfare and for mitigating climate change.

In that context, the objectives of this dissertation are threefold.

1. To provide a detailed yet ‘operational’ model of the usage and level-of-service of rail access facilities, describing when and where pedestrian flows occur, how these flows are influenced by the train timetable, whether congestion arises, and how the performance of a train station is affected.
2. To collect, consolidate and analyze a rich set of data for a complex train station including pedestrian flow counts, pedestrian trajectory data, the train timetable and delay data, as well as ridership information, and to explore this data in order to obtain an empirical understanding of pedestrian flows in train stations at a concrete example.
3. To provide an application of the developed modeling framework at the example of the aforementioned case study, to assess the practical applicability of the framework, and to provide practical guidance on its use for the planning and dimensioning of pedestrian facilities in further train stations.

Despite the growing importance of the field, the scientific literature associated with these three aspects of pedestrian flows in rail access facilities is still limited, and may be summarized as follows. A more detailed review of the relevant literature is provided in subsequent chapters.

Models: Fundamentally, two model types may be distinguished. A first type of models is concerned with the assessment of the *usage* of a pedestrian facility, which are typically referred to as demand estimation models. Activity-based models belong to that type. They consider demand as the result of an underlying need to perform activities, such as ‘buying a ticket’, or ‘boarding a train’ (Hoogendoorn and Bovy, 2004). Another approach consists in estimating demand at the scale of origin-destination (OD) flows, such as ‘North entrance to Platform #5’. A lower computational cost and reduced data requirements make such estimators of OD demand viable for real-time applications and long-term prediction. A second type of models is referred to as pedestrian traffic assignment models, which are useful for assessing the *level-of-service (LOS)* of pedestrian facilities. They typically consist of a route choice and a network loading model. Route choice models assign OD demand to routes,

typically using utility-based approaches (Borgers and Timmermans, 1986; Cheung and Lam, 1998; Hoogendoorn and Bovy, 2004). Network loading models describe the propagation of pedestrians along these routes. Even though many such models have been presented in the literature, there is still a lack of network loading models that are at the same time accurate and computationally efficient (Duives et al., 2013).

The two model types, demand and assignment models, are complementary. For a given infrastructure and data, the demand model takes the level-of-service as input and predicts the usage, whereas the assignment model takes the usage as input, and predicts the level-of-service.

Data: Various forms of data have been collected in rail access facilities. These range from density and speed measurements in walking facilities for the estimation of density-speed relationships (Daly et al., 1991), recordings of train arrival and departure times for the estimation of train delays (Higgins and Kozan, 1998), pedestrian flow measurements obtained from CCTV networks (Ganansia et al., 2014), automated fare collection data to study pedestrian arrival time distributions, route choice and waiting times (van den Heuvel and Hoogenraad, 2014), or capacity measurements of train doors to estimate access and egress times associated with public transport vehicles (Fernández et al., 2015). In most cases, typically only a single type of data is collected, i.e., cases in which multiple data types have been collected for the same train station are rare.

Applications: In the literature, a large set of case studies involving pedestrian flows in train stations are available. These concern light rail and underground stations in Hong Kong (Lam et al., 1999; Lee et al., 2001), train stations in Lisbon and Bern (Hoogendoorn and Daamen, 2004; Rindsfüser and Klügl, 2007), a subway station in Paris (Kaakai et al., 2007), as well as further examples from Vienna, Beijing and Amsterdam (Seer et al., 2008; Jiang et al., 2009a; Starmans et al., 2014).

1.2 Contributions

Within the aforementioned literature, the main objective of this thesis is to develop a modeling framework for the usage and level-of-service of pedes-

trian facilities in train stations. Real data is collected and used for its calibration and validation. The resulting framework can be directly applied for the planning and dimensioning of rail access facilities, and in the long term for an active and passive management of pedestrian crowds.

The contributions of this thesis include

- the development of a dedicated demand estimation methodology for pedestrian OD demand in rail access facilities, in particular taking the train timetable into account;
- the development of a pedestrian network loading model that is capable of accurately describing multi-directional and congested flows in large facilities and at low computational cost;
- the collection of a rich set of data for a large Swiss train station, comprising multiple data sources for a single site;
- the application of the aforementioned models to that case study in order to study their performance, and the formulation of a planning guideline to facilitate their practical application.

Despite the focus on train stations, most of the developed methodologies can also be applied to other pedestrian facilities, such as airports, museums, or urban pedestrian areas. Specifically, the developed model framework can be used to support the planning, organization, design and control of pedestrian facilities by (i) assessing new designs of stations, buildings, stadiums and other facilities, (ii) testing operational schemes such as train timetables or flight schedules with respect to the expected pedestrian flows, (iii) assessing evacuation plans for buildings, and (iv) implementing crowd management and control measures and strategies, including real-time solutions.

The main challenge in addressing these issues is to develop pedestrian models that can reproduce and predict flow dynamics under a variety of circumstances and conditions. In particular, this entails tackling research challenges such as (i) the identification of key dynamics and phenomena to be modeled, (ii) the choice of an appropriate theory to represent these phenomena, (iii) their mathematical formulation, and finally (iv) the calibration and validation of the developed models based on real data.

1.3 Thesis structure

The remainder of this thesis is structured as described in the following. Figure 1.1 provides a graphical representation of the structure.

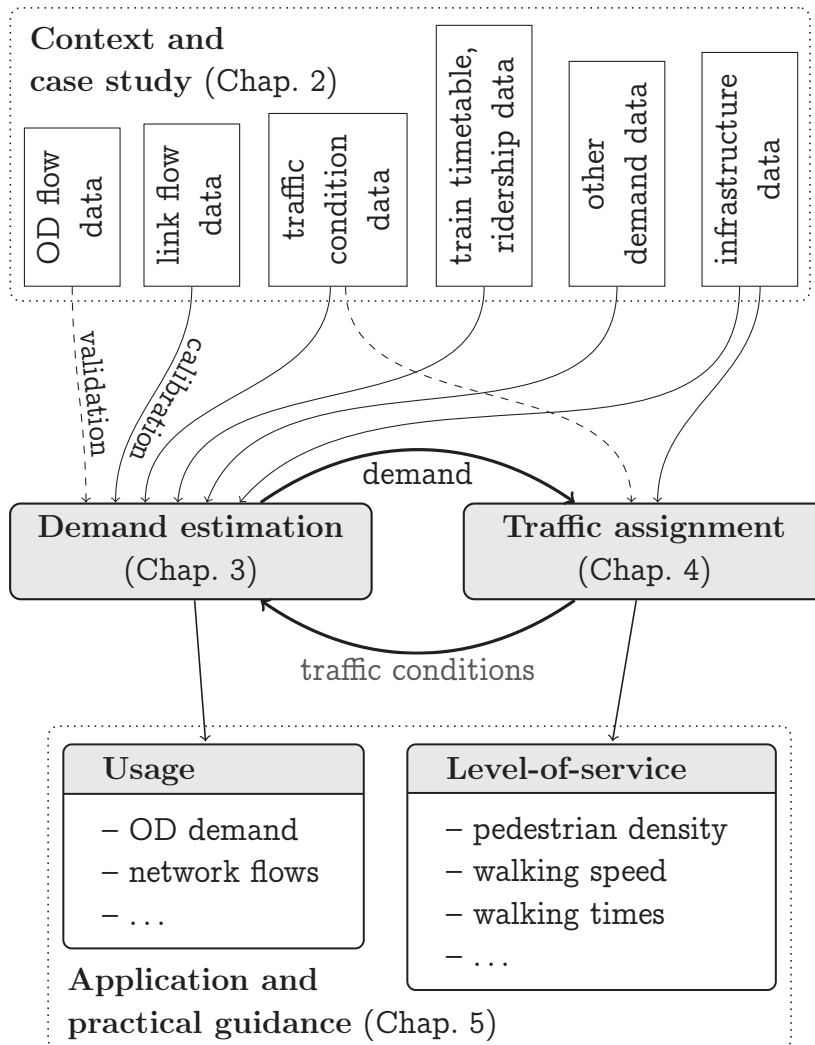


Figure 1.1: Thesis structure.

Chapter 2 provides a review of the literature associated with pedestrian flows in rail access facilities, and a classification of data that is available in that context (see rectangles in Fig. 1.1). This data is useful to calibrate (solid arrows) and validate (dashed arrows) the envisaged

modeling framework. A case study of Lausanne railway station is introduced, to which reference is made throughout the thesis.

Chapter 3 presents a framework for estimating pedestrian OD demand within a train station (left shaded rectangle in Fig. 1.1). It takes into account ridership data, and various direct and indirect indicators of demand such as link flow counts, density measurements or survey data. The problem is considered in discrete time and at the aggregate level, i.e., for groups of pedestrians associated with the same origin-destination pair and departure time interval. The formulation is probabilistic, allowing to consider the stochasticity of demand. A key element of the framework is the use of the train timetable, and in particular of train arrival times, to better capture demand peaks. A case study of Lausanne railway station shows that, compared to a classical estimator that ignores the notion of a train timetable, the gain in accuracy in terms of RMSE is between 20% and 50%.

Chapter 4 outlines a pedestrian traffic assignment model (right shaded rectangle in Fig. 1.1), and presents in particular a novel macroscopic loading model for multi-directional, time-varying and congested pedestrian flows. Walkable space is represented by a network of streams that are each associated with an area in which they interact. Due to its aggregate character, the model is computationally cheap, which is advantageous for studying large-scale problems. Two specifications are considered.

Isotropic density-speed relationship: A well-established isotropic pedestrian density-speed relationship is used. Two case studies involving Lausanne railway station and a Dutch bottleneck experiment are presented. A comparison with the social force model and pedestrian tracking data shows a good performance of the proposed model with respect to predictions of travel time and density.

Anisotropic density-speed relationship: A stream-based pedestrian fundamental diagram is used that relates density and walking speed in anisotropic flow. Unlike in the previous specification, the walking speed in the direction of major flow may be higher than in the direction of minor flow if densities are high. The proposed model is applied to two different case studies in Berlin and Hong Kong. The explicit

modeling of anisotropy in walking speed significantly improves the ability of the model to reproduce empirically observed travel times.

Chapter 5 applies the modeling framework developed in the previous two chapters to assess the usage and level-of-service in rail access facilities of Lausanne railway station (boxes at the bottom of Fig. 1.1). A detailed discussion of origin-destination demand, network flows, density maps and travel time distributions is provided. Moreover, the modeling framework is embedded in a six-step planning guideline that can be used in the process of designing and optimizing rail access facilities of new train stations, or those that need to be expanded. The chapter is self-sufficient, and accessible to readers without a particular knowledge of mathematics.

Chapter 6 summarizes the contributions of the thesis, provides further practical recommendations, and outlines future research directions.

Chapter 2

Context and case study

2.1 Literature review

Questions related to the usage and level-of-service of rail access facilities increasingly attract the attention of academic research.

In an early study, Daly et al. (1991) investigate the relationship between speed and flow and between flow and travel time in various pedestrian facilities of London's underground system. Lam and Cheung (2000) examine several metro stations in Hong Kong. Differentiating by trip purpose, flow capacities are evaluated and flow-travel time functions are calibrated. Compared to the results from London, users of Hong Kong's mass transit system are found to be better at dealing with high levels of congestion, which is attributed to the smaller physique of Asians and their higher tolerance to invasion of space (Lee and Lam, 2003).

Lam et al. (1999) investigate the train dwelling time and the distribution of pedestrians on platforms in two stations of Hong Kong's Light Rail Transit system. A behavioral analysis reveals that people are less willing to board a train if it is congested, and if the journey to be made is longer. Also focusing on train platforms, Zhang et al. (2008) describe the process of alighting and boarding in metro stations in Beijing. Pettersson (2011) investigates the behavior of pedestrians on train platforms from an architect's perspective. At the example of a Swedish and a Japanese case study, the effect of signposts, availability of seats and entrances on the distribution of pedestrians along the platform is investigated.

Recently, Ganansia et al. (2014) have studied the use of standard CCTV networks for measuring pedestrian flows in train stations. Several case

studies, including a TGV station and two subway stations in France and Italy, are discussed. It is found that data obtained through such a system is in principle useful for a continuous monitoring of the spatio-temporal evolution of pedestrian flows, but also that an a posteriori ‘correction’ is necessary whenever dense crowds need to be accurately measured. Using such camera-based data, Molyneaux et al. (2014) describe the flows on platform access ways caused by alighting train passengers. Similarly, van den Heuvel and Hoogenraad (2014) use automated fare collection (AFC) data to investigate passenger arrival distributions.

Several studies have been dedicated to the understanding of route choice behavior (Seneviratne and Morrall, 1985; Borgers and Timmermans, 1986). For the case of a metro station in Hong Kong, Cheung and Lam (1998) investigate the route choice between escalators and stairways leading to a train platform. A relationship between flow and travel time is first established. This characteristic relationship is then used in a choice model to predict the percentage of escalator-users for ascending and descending directions as a function of prevailing traffic conditions. By ‘shadowing’ passengers, Daamen et al. (2005) collect route choice data in two Dutch train stations. Likewise, a route choice model is estimated, allowing to predict the influence of level changes in walking routes on passenger route choice behavior. Similar studies are provided by Srikuenthiran et al. (2014), Stubenschrott et al. (2014) and Ton (2014), who consider railway stations in Canada, Austria and the Netherlands, respectively.

Lee et al. (2001) provide one of the first model-based studies of pedestrian flows in train stations. For a major station in Hong Kong’s metro system, origin-destination demand and travel times are collected using human observers. From this data, flow-travel time relationships are derived, which are used in a network-based pedestrian flow model. Along the same lines, Daamen (2004) develops a multitude of models for describing the processes of queueing, boarding, alighting, waiting, walking as well as route and activity choice.

Kaakai et al. (2007) develop a related model using a Petri net. They consider both discrete processes such as the arrival and departure of trains, as well as continuous processes such as the ‘fill-up’ of train platforms by pedestrians awaiting a train, or pedestrian flows in walking facilities. The model is applied to a French case study involving a train station with a single platform. At the microscopic level, Xu et al. (2014) develop a model

describing pedestrian behavior in a Chinese metro station. The framework is entirely based on a queueing network, i.e., all processes including entering the train station, passing ticket gates, walking and boarding are represented by queues. The framework is applied to estimate the maximum service rate of a metro station, as well as to determine the optimal inflow rate at the entrance at which this capacity is attained.

There are several more studies of pedestrian flows in train stations that concentrate on specific applications. Most of them pursue an agent-based approach and describe various practical challenges such as the placement of access gates in Lisbon (Hoogendoorn and Daamen, 2004), the re-design of access ways in Bern (Rindsfuser and Klügl, 2007), the evacuation of a metro station in Beijing (Jiang et al., 2009a), the modeling of waiting areas in German train stations (Davidich et al., 2013), the design of a new station in South Africa (Hermant, 2012), or, based on a macroscopic ‘pedestrian transfer chain’, the assessment of an existing station in the Netherlands (Starmans et al., 2014).

As for other transportation modes, assessment schemes for pedestrian facilities exist that allow to quantify the quality and comfort of pedestrian traffic. The corresponding literature is dominated by the seminal contribution by Fruin (1971), who proposes a density- and flow-based classification of level-of-service (LOS) considering six service levels. Density-based LOS indicators are useful both for walking and waiting areas, for which different thresholds apply. Flow-based indicators are used for walkways, escalators or stairways, and consider the specific flow, i.e., the flow per meter of width. Several other assessment schemes have been proposed, typically focusing on the integration of additional factors such as safety, aesthetics and comfort, or taking the opinion of pedestrians into account (Polus et al., 1983; Mōri and Tsukaguchi, 1987; Khisty, 1994). Due to their more difficult use, Fruin’s classical LOS classification schemes have mostly prevailed in practice, even though minor modifications have been made that consider national differences (Highway Capacity Manual, 2000; Brilon, 2001).

A detailed review of various methodologies that are useful for the estimation of pedestrian OD demand in the context of a railway station, including estimators for transit networks, is provided in Chapter 3. Chapter 4 provides a similar review for pedestrian traffic assignment models, particularly focusing on network loading models. In Chapter 5, a brief practical overview is given regarding how LOS assessment schemes can be

used to optimize the design of rail access facilities.

2.2 Pedestrian data

Pedestrian traffic data is essential for the understanding of rail access facilities in several ways, for instance to assess their safety, security, efficiency and attractiveness (Bauer et al., 2009).

Obtaining pedestrian data is generally difficult. First, the placement of sensors is challenging, as pedestrians can explore space freely, and are not confined to lanes. Second, the detection of pedestrians is an intricate task, as they can almost instantaneously stop or accelerate, and often travel in groups. Pedestrians are by nature heterogeneous, and their appearance depends on age, gender, or even trip purpose. Third, pedestrian traffic is highly variable, and sensors are required to capture a large range of traffic levels (U.S. Department of Transportation, 2013). Data availability is thus often limited in terms of its spatial or temporal coverage, or in terms of quality.

In the following, we provide a classification of data sources in five data types, and discuss the importance of each data type for demand estimation and LOS assessment. For a discussion of sensing technologies as well as further practical guidance, we refer to the literature (Turner et al., 2007; Bauer et al., 2009; U.S. Department of Transportation, 2013).

OD flow data: Origin-destination (OD) trip tables represent the number of people traveling between each pair of origin and destination during pre-defined time intervals. The definition of OD areas depends on the layout of a train station, and may include platforms or platform sectors, shops, as well as entrance/exit areas. No distinction between ‘intermediate’ and ‘final’ destinations is made. If a pedestrian visits multiple destinations in a row, instead each intermediate trip is represented by an independent OD pair. A pedestrian may thus be associated with multiple OD trips. These OD trips are counted when the pedestrian leaves the respective origin.

OD flow data are obtained from pedestrian tracking systems, travel surveys, electronic tickets, or passive ICT sensors such as Bluetooth and Wi-Fi scanners (Versichele et al., 2012; Alahi et al., 2013b; Kim et al., 2015). Due to their expensive collection, OD flow data are often not available for

the entire network of interest (Bauer et al., 2009). Moreover, sampling is typically an issue, as in practice only a subset of pedestrians may be successfully detected. This holds in particular for ICT sensors, which capture only pedestrians carrying a corresponding device. Moreover, the temporal resolution is often low, with devices being detected only every couple of minutes (Danalet, 2015).

OD flow data are of particular importance for OD demand estimation, where they help to reduce the underdetermination that results if only indirect indicators of demand, such as link flows, are available (Cascetta et al., 1993). For LOS assessment, OD flows can also be useful if a traffic assignment model is available that allows to estimate LOS indicators.

Link flow data: Pedestrian infrastructures are often represented as a flow network, consisting of nodes and links. Links include in particular walkways or walkway sections, stairways, or escalators. By convention, ‘link flow’ refers to the inflow to a link, i.e., the flow that is measured at the origin of a link. Link flow data may be obtained from turnstiles, camera-based systems, infrared sensors or other detectors, including manual counting (Lee et al., 2001; Ton, 2014; Kim et al., 2015). Compared to OD flow data, the sensor technology for obtaining link flows are relatively mature, and the counting precision is high (U.S. Department of Transportation, 2013).

For OD demand estimation, link flow data represents the most common type of input data (Cascetta and Improta, 2002). The efficient placement of sensors within a network is difficult, and widely discussed in the literature (Gentili and Mirchandani, 2012; Viti et al., 2014).

There are two ways of using link flow data for LOS assessment. Directly, by computing the flow per meter of width, and by comparing that to facility-specific thresholds (Fruin, 1971). For simple geometries, such as straight corridors with a constant width, this may be appropriate. A second way of using link flow data for LOS assessment is by using a traffic assignment model, applying it to the link of interest. The traffic assignment model then predicts densities and velocities, providing indirect information about the expected level of congestion.

Traffic condition data: Traffic condition data include measurements of density, walking speed, or travel times. Such observations are typically

obtained from a pedestrian tracking system, or ICT sensors (Alahi et al., 2013b; Montero et al., 2015).

For the estimation of pedestrian OD demand, traffic condition data can be used as exogenous variables in the estimation process. For instance, Montero et al. (2015) use observed travel times to approximate the travel time distribution within a demand model. Alternatively, they can be used to indirectly validate the OD demand estimates, if the latter are combined with a traffic assignment model (see e.g. Djukic et al., 2015).

Traffic condition data are probably the most relevant source of information for LOS assessment. The most widely used LOS indicators are directly based on density and flow (Fruin, 1971).

Train timetable and ridership data: The train timetable has a significant impact on the usage of pedestrian facilities, both in terms of accumulation and in terms of flows. Fig. 2.1 provides a schematic representation of the most relevant types of flows that are influenced by the train timetable, namely boarding/alighting flows at train doors (solid arrows), as well as exit and access flows on platform access ways (dashed and dotted, respectively). A direct relationship between the train timetable and platform exit flows is established in Chapter 3.

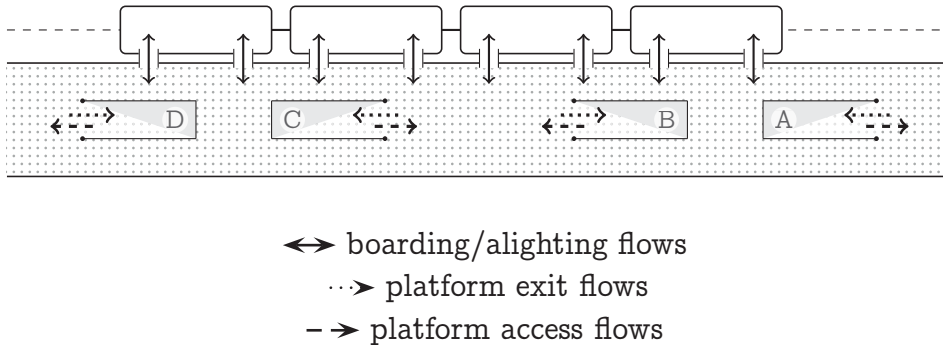


Figure 2.1: Train-induced flows on platforms and platform access ways.

If train delays are to be expected, the actual instead of the scheduled train timetable should be used. It may be obtained by observation, or from corresponding train delay models (Higgins and Kozan, 1998; Goverde, 2007). Particularly railway networks during peak periods or highly-interconnected timetables are prone to delays (Cule et al., 2011).

The number of boarding and alighting passengers per train may be obtained from door sensors, ticket sales, travel surveys, or approximated from the train capacity (Zhang et al., 2008; Kim et al., 2015; Fernández et al., 2015).

For OD demand estimation, the timetable and ridership information can be used to improve the accuracy of the estimate, or to provide a priori estimates when no other data is available. In terms of LOS assessment, the number of boarding and alighting passengers is particularly useful for the dimensioning of platforms, which in practice is typically done using hydrodynamic models (Buchmüller and Weidmann, 2008).

Other demand data: Further information sources, such as sales or survey data, are sometimes available (Seneviratne and Morrall, 1985; Lee et al., 2001). These are typically useful for demand estimation, where they help narrowing the solution space. Video footage or a photographic documentation may be helpful for a qualitative level-of-service assessment (Helbing et al., 2002). Practical knowledge by the station operator regarding pedestrian dynamics, congested areas and the use of infrastructure in general may be a useful source of information as well.

Infrastructure data: Knowledge of the infrastructural layout is a prerequisite for both the estimation of demand and the level-of-service assessment. This typically includes the topology of pedestrian facilities, the location of access doors, ticket machines and shops, as well as the topology of the monitoring system, such as the location of Wi-Fi and Bluetooth access points, cameras, or counting systems.

The choice of sensors depends decisively on the desired information and the available budget. There is no single sensing technique that fits all purposes. Instead, often the simultaneous consideration of multiple data sources yields the most reliable results. For instance, the combination of Wi-Fi traces with a low temporal resolution and a strong sample bias with accurate, but spatially isolated count data may provide a good understanding of pedestrian flows. Further visual sensors may be helpful to assess pedestrian densities, and to quantify the prevailing level-of-service. Chapter 3 presents a framework of how multiple data sources can be combined in a mathematically rigorous way.

The cost of data collection depends on multiple factors, in particular on the already existing infrastructure. For instance, if a dense network of Wi-Fi antennas is already available, it may be relatively cheap to collect Wi-Fi traces. If not, the installation of a power and data network, as well as of the Wi-Fi antennas themselves, may incur a significant cost. For optical sensors, such as tracking or count systems, the lighting conditions, height of the ceiling, requirements for protection from bad weather or vandalism, and many other factors may play a role.

2.3 Lausanne railway station

Throughout this thesis, reference is made to the train station of Lausanne, which we have studied together with the Swiss Federal Railways (SBB) between 2011 and 2015. Lausanne railway station is the largest node in the railway network of Western Switzerland, serving 650 arriving and departing trains on weekdays (Amacker, 2012). The station has reached capacity in the year 2010, and a doubling of passenger demand is expected by 2030. About € 450,000 have been invested in a pedestrian tracking system to monitor and understand pedestrian movements on central walkways, to which this thesis has access. In total, € 1.1 billion is spent between 2010 and 2020 to enlarge the station, preparing it for future growth.

Fig. 2.2 shows a schematic map of the station, encompassing nine railway tracks for passenger traffic (thin dashed lines). At its heart are two pedestrian underpasses (PUs), referred to as PU West and PU East (vertical corridors). Platforms are shown as dotted areas. Solid lines represent the walking network of the pedestrian facilities, and dashed curves represent corresponding network links that cannot be shown in the 2D scheme. OD areas are represented by rectangles. Dark rectangles symbolize entrance/exit areas as well as service points within the train station. Rounded rectangles represent platform OD areas, i.e., platform sectors or entire platforms. Pedestrian count sensors are represented by diamonds. The shaded parts in the two pedestrian underpasses represent areas that are covered by a pedestrian tracking system.

Using the classification presented in the previous section, the following data sources are available:

OD flow data: Subroute flows are available for the two pedestrian under-

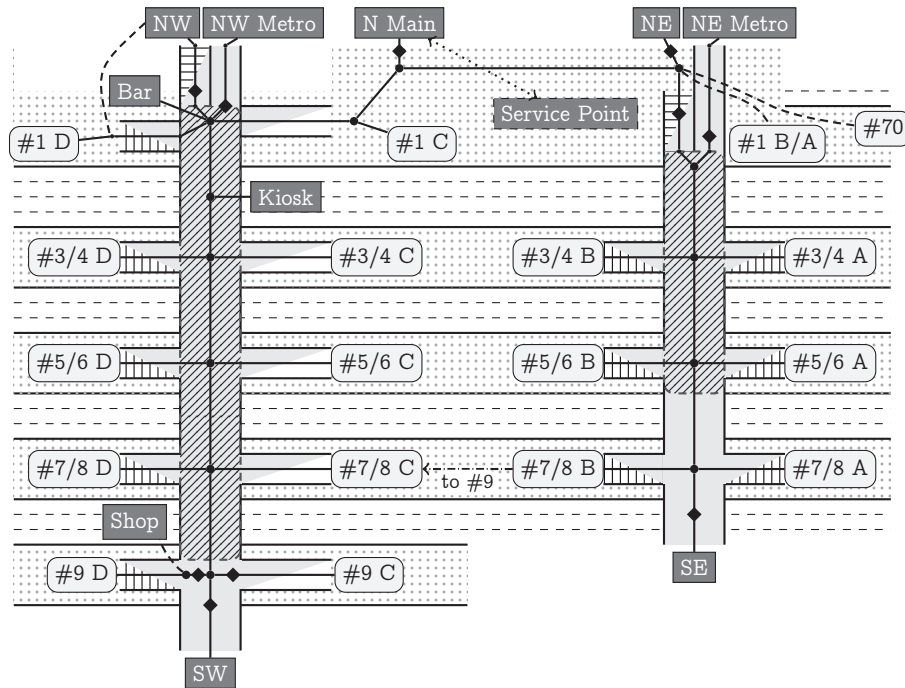


Figure 2.2: Lausanne railway station.

passes, in which a tracking system consisting of 60 sensors is installed. This sensor system allows to simultaneously track the trajectories of pedestrians across space and time. Details of the installation, as well as of the accuracy of observations, are described by Alahi et al. (2013b).

Link flow data: Ten links of the pedestrian walking network, marked by diamonds in Fig. 2.2, are equipped with sensors that provide directed link counts with a resolution of one minute. To account for sensor saturation, observations are post-processed using a quadratic correction function (Ganansia et al., 2014).

Traffic condition data: Pedestrian trajectories obtained from the aforementioned tracking system allow to compute the prevailing speed, density and accumulation in pedestrian underpasses. Accumulation is defined as the number of pedestrians present in an area at a given point in time.

Train timetable and ridership data: The actual arrival and departure

times and the assigned track are known for each train. An average estimate of boarding and alighting volumes is available from ticket sales data, within-train surveys, and infrared-based counts at train doors (Anken et al., 2012). These estimates date back to the year 2010 and are increased by 15% to reach the estimated level of the year 2013, which is considered throughout this thesis (Gendre and Zulauf, 2010). The boarding and alighting volumes are considered as random normal variables with a standard deviation equal to 19.2% of their mean (Molyneaux et al., 2014).

Other demand data: For the sales points located in PU West (see Fig. 2.2), an estimate of the number of customer visits is available.

Infrastructure data: Detailed building plans containing the dimensions of all relevant pedestrian facilities, and the exact location of all parts of the monitoring system are available.

The usage of pedestrian facilities in Lausanne railway station is subject to recurring temporal patterns that are due to differences between weekdays/weekend, the day/night-rhythm, and a cyclic train timetable.

Fig. 2.3a shows the level of demand in the PUs over a typical working week, as measured by the pedestrian tracking system for the period between February 25 and May 19, 2013 (April 1 and 2 are excluded due to a sensor malfunctioning). Standard deviations are around $\pm 15,000$ pedestrians for a typical working day.

The total number of pedestrian visits in the two pedestrian underpasses of Lausanne railway station (PU West and East) is slightly below 120,000 ped/day on weekdays. This is in agreement with numbers reported by SBB, according to which there are in total about 140,000 station users per weekday, of which 98,000 are train users (Amacker, 2012). On Fridays, the station is busier than during the week due to weekly commuters returning to their principal place of residence, as well as due to weekend travelers. These additional passengers are spread around the evening peak period. The pedestrian demand on Saturdays and Sundays on the other hand is significantly lower. The shown pattern is similar to other major train stations in Switzerland, including in particular Basel, Bern and Zürich, which are serving up to four times as many passengers.

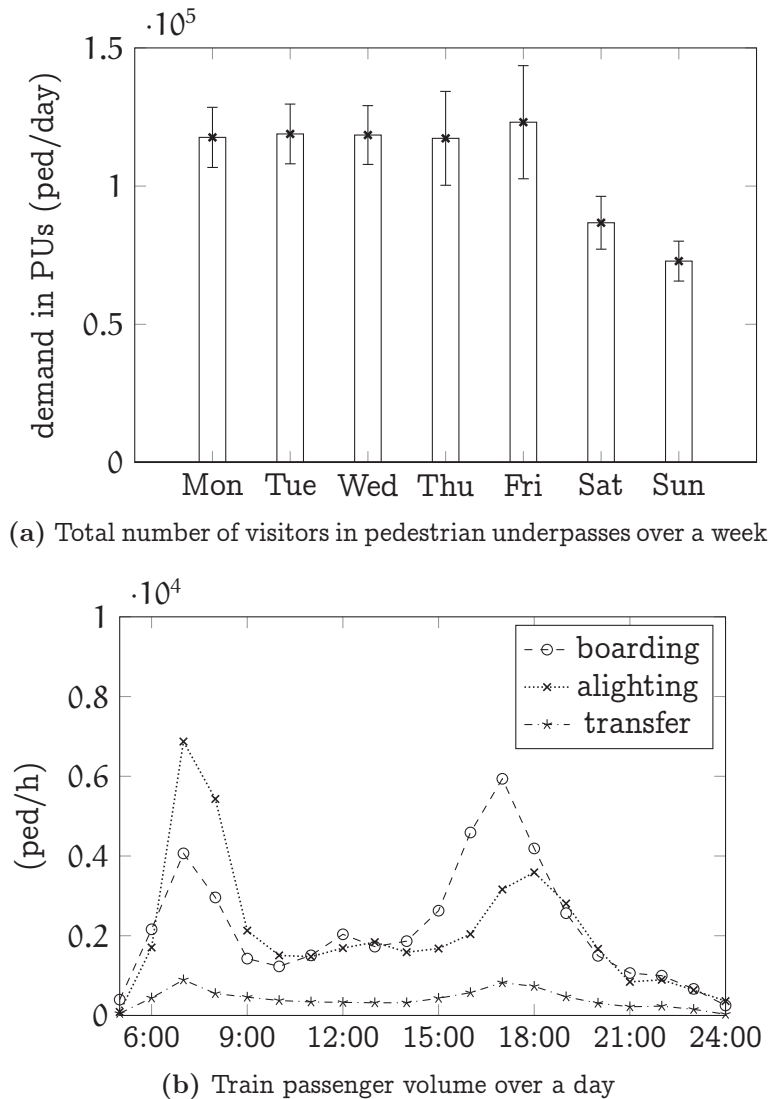


Figure 2.3: Observed demand in Lausanne railway station (year 2013).

Fig. 2.3b shows the evolution of train passengers during the course of a weekday. The shown data is obtained from semi-automatic travel surveys conducted in the year 2010, increased by 15% to approximate the demand in 2013 (Anken et al., 2012). It is distinguished between outgoing passengers (boarding), incoming passengers (alighting), and transfers, i.e., passengers that change train in Lausanne.

Between 7:00 and 8:00, the alighting volume (6,871 ped) is higher than the boarding volume (4,066 ped), whereas in the evening rush hour between

17:00 and 18:00, the number of boardings is higher (3,161 vs. 5,937 ped). According to these results, people come to Lausanne for work and leave the city again in the evening. The morning peak hour is shorter and busier than the evening peak hour, while the percentage of transfer passengers is just below 10% and nearly constant during the day. The bi-modal distribution of train passengers with a distinct peak in the morning and evening is typical for most train stations, with the exception of those that are primarily used for timed events such as concerts, or for touristic purposes.

A further analysis of the morning peak hour shows that the absolute peak over a weekday is reached between 07:35 and 7:50 (AM), when several long distance trains arrive and depart in close succession (Gendre and Zulauf, 2010). At this time of the day, more than 500 incoming users alight during a peak minute, whereas a few minutes later it can be less than a hundred per minute (Alahi et al., 2013a).

In the remainder of the thesis, we consider the time period between 07:30 and 08:00. Data for a set of 10 ‘reference weekdays’ is available, namely for January 22 and 23, February 6, 27 and 28, March 5, as well as April 9, 10, 18 and 30, 2013. These dates represent a set of typical weekdays (Tue, Wed, Thu) without major disruptions in the railway system, for which all of the aforementioned data sources are available.

Fig. 2.4a shows the evolution of the number of tracked pedestrians that enter one of the two pedestrian underpasses for this set of dates. Each day is represented by a separate curve, illustrating the significant day-to-day variability. The shaded area represents the standard deviation band, defined by the area within the mean \pm one standard deviation. As far as the mean is considered, the demand fluctuates between less than 70 and more than 500 ped/min, i.e., by almost an order of magnitude.

For the same period, Fig. 2.4b shows a box plot of the arrival times of the ten trains with the largest alighting volumes, which typically amount to 250 pedestrians or more. Early arrivals lead to a negative delay. It can be seen that delays of more than 3 min are relatively rare in the studied 10-day reference set. Nevertheless, given that only undisrupted days are considered, the day-to-day variability in train arrival times is remarkable. A similar finding holds for the departure time of trains.

Fig. 2.5a shows a scatter plot of accumulation vs. travel time along the main route in PU West, #1C \rightarrow SW. The data points represent 1,745 pedestrians. The accumulation is measured when a person enters PU West.

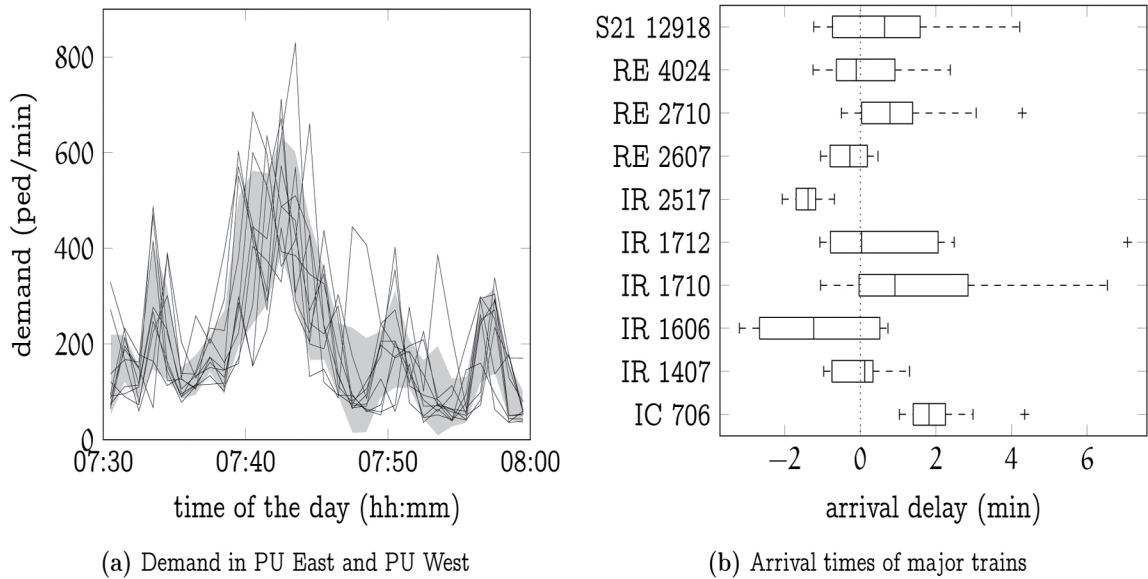
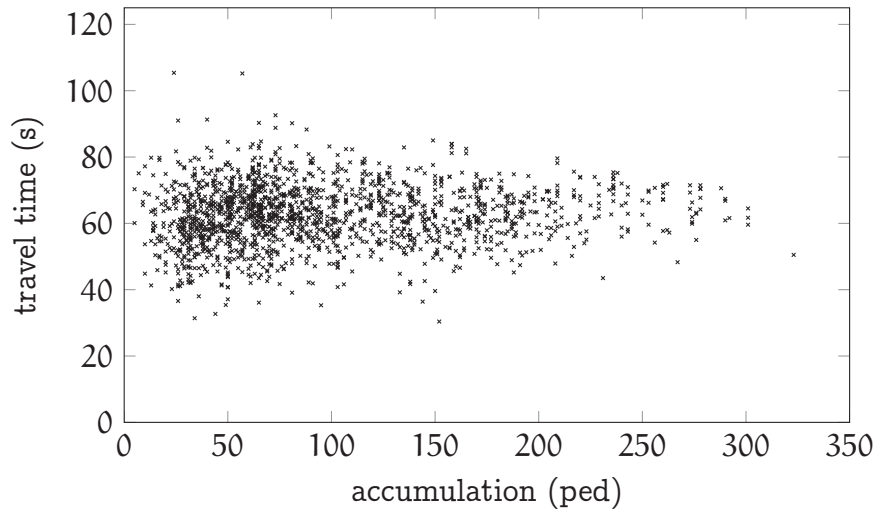


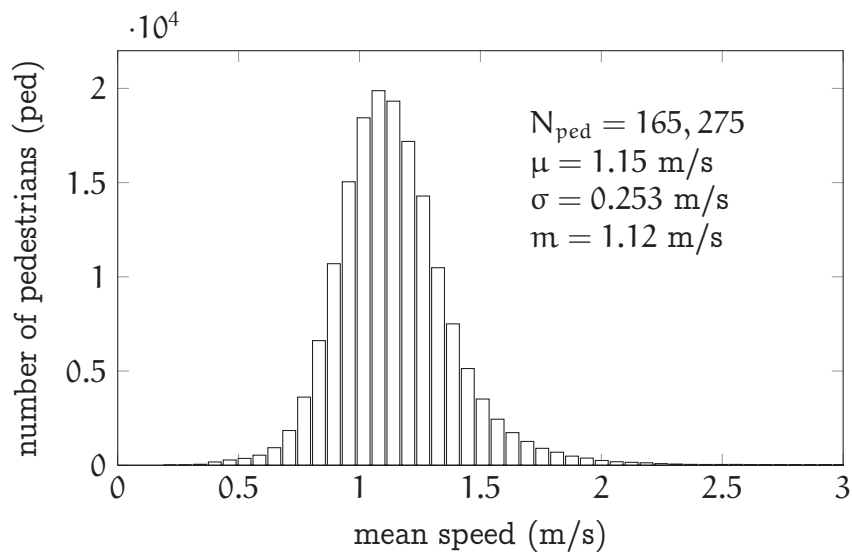
Figure 2.4: Day-to-day variability in the 10-day reference set.

The distribution of travel times is relatively wide, particularly at low values of accumulation. The mean travel times do not depend significantly on the accumulation, as would be the case if the facility were congested. This is an important finding for the demand estimation, where data sources from different locations are combined. In the case of Lausanne railway station, the ‘temporal distance’ between sensors remains approximately constant across time, irrespective of the demand. It is unclear to what extent this finding can be generalized to other train stations. Presumably, it holds for most other train stations with a low to moderate level of congestion. For highly congested train stations, such as they are found in large cities, travel times are likely to depend on the prevailing densities.

Fig. 2.5b shows the walking speed distribution for a total of 165,275 pedestrians. The walking speed is computed from the ratio of traveled distance and travel time. A mean velocity of 1.15 m/s is observed, and the median lies at 1.12 m/s. These values are in good agreement with the literature. For instance, Weidmann (1992) reports for the mean speed a range between 0.99 m/s for tourists, up to 1.45 m/s for business people. The spreading of the walking speed distribution is largely caused by differences in trip purpose, as well as by population heterogeneity in terms of age and gender. Other factors, such as time pressure, whether luggage is carried,



(a) Correlation between accumulation and travel time on route #1C → SW



(b) Walking speed during morning peak hour in pedestrian underpasses

Figure 2.5: Travel times and walking speeds.

or general health may also play a role.

Chapter 3

Demand estimation

3.1 Introduction

Knowledge of pedestrian demand is a prerequisite for the analysis of pedestrian flows in train stations, be it for the design of infrastructure, the optimization of operations such as the train-track assignment, or the real-time management and control of pedestrian flows. Unless a comprehensive pedestrian tracking system is available, pedestrian demand can only be observed indirectly, for instance in the form of flows or densities. The challenge then consists in establishing a relationship between pedestrian demand that is unknown, and demand indicators that can be observed. Especially if different types of observation data are available, this may be an intricate task.

While pedestrian behavior in train stations generally attracts the attention of academic research, methodologies for estimating pedestrian demand are still exceedingly rare. Many studies are solely based on theoretical demand scenarios (Hoogendoorn and Daamen, 2004; Rindsfuser and Klügl, 2007; Davidich et al., 2013). Other studies rely on simple assumptions to estimate demand (Kaakai et al., 2007; van den Heuvel and Hoogenraad, 2014), or consider train stations that serve only a single line (Lee et al., 2001; Xu et al., 2014).

Several approaches to estimate pedestrian demand in train stations are conceivable. Activity-based models, and methodologies focusing on pedestrian origin-destination (OD) demand are among the most promising approaches (see Chapter 1). Estimation methods for OD demand do not require disaggregate data for their estimation, which in practice is rarely

available. Moreover, they are less computationally expensive, making them the primary choice for real-time applications, or for considering large estimation problems. Thus, in the following the problem of estimating pedestrian demand in train stations is considered in terms of OD demand. For further information regarding activity-based approaches, the reader is referred to the literature (Hoogendoorn and Bovy, 2004; Danalet, 2015).

The problem of estimating OD demand has a long history in the context of road networks, for which link flow volumes and other indirect observations of demand are available (van Zuylen and Willumsen, 1980; Cascetta, 1984). Typically, an assignment map is assumed that relates observations to OD volumes, such that the latter can be ‘reverse engineered’. This map may be obtained via a dynamic traffic assignment (DTA) model, which can also be developed in the context of pedestrian flows (see Chapter 4). The problem of pedestrian OD demand estimation in train stations is thus in principle amenable to ‘classical’ estimation techniques.

A key issue in OD demand estimation is the ratio between the number of unknowns and the number of independent observations, yielding an intrinsically underdetermined problem. Various forms of exogenous information, either in the form of a priori knowledge or structural assumptions, are used to lead the calculation to a unique solution.

For static OD estimation, concepts like gravity (Casey, 1955), entropy maximization (Wilson, 1970; Willumsen, 1981) or information minimization (van Zuylen and Willumsen, 1980) have been used in the context of road traffic. In most cases, however, an a priori OD trip table (Cascetta and Nguyen, 1988) is used. Other researchers make specific assumptions on the structure of OD trip tables (Bierlaire and Toint, 1995) or the covariance across measurements (Hazelton, 2003).

For dynamic problems, a common approach is to assume a dynamic process for the evolution of demand, such as an autoregressive process in the deviates from historical estimates (Ashok and Ben-Akiva, 2000; Bierlaire and Crittin, 2004; Zhou and Mahmassani, 2007, again all in the context of vehicular traffic). Recent approaches assume slowly evolving route split fractions in the framework of a ‘quasi-dynamic’ estimator (Marzano et al., 2009; Cascetta et al., 2013), or reduce the dimensionality of the estimation problem by applying principal component analysis (Djukic et al., 2012).

Several researchers consider also the problem of OD demand estima-

tion in transit networks, i.e., that of estimating the station-to-station OD demand in a potentially multimodal transportation network. Early approaches assume a constant average cost along routes (Nguyen et al., 1988), whereas newer studies focus on schedule-based transit network models (Wong and Tong, 1998), of which some additionally consider passenger overload delays (Lam et al., 2003) or data from ICT sensors (Montero et al., 2015). These models can predict the evolution of in- and outflows at stations or the number of passengers in vehicles, but do not provide detailed information on OD demand *within* a train station.

Pedestrian OD demand in train stations is particularly unsteady due to arriving and departing trains that lead to demand ‘micro-patterns’. A manifestation of these demand micro-patterns are the highly variable flows on platform exit ways after train arrivals, or the fluctuating accumulation of prospective train passengers on platforms prior to train departures. The associated rapid and recurrent changes in demand are typical for the environment of train stations, and largely influenced by the train timetable.

Acyclic schedules and unplanned delays make it difficult to use historical OD data, or any other of the aforementioned approaches for dealing with underdetermination in the demand estimation process. This is where we would like to make a contribution. In this chapter, we propose a dedicated methodology for estimating pedestrian OD demand in train stations in general, and we do so by integrating the train timetable and ridership data in particular. The schedule of departing trains is considered in a temporally aggregated way, i.e., the train-track assignment is used to compute cumulative platform departure flows. The train arrival times are considered explicitly.

The next section presents a methodological framework for estimating pedestrian OD demand based on the notion of a train timetable, and an example specification that is applicable to any suitable train station. Section 3.3 then presents a case study based on that specification. Section 3.4 contains concluding remarks.

3.2 Methodological framework

A recapitulation of important variables introduced in this section is provided in Appendix A.

3.2.1 Notation

The time period of interest is divided into a set of discrete intervals \mathcal{T} , where each interval $\tau \in \mathcal{T}$ is of uniform length Δt .

Walkable space is represented by a directed graph $\mathcal{G} = (\mathcal{N}, \mathcal{L})$, where \mathcal{N} is the set of nodes $v \in \mathcal{N}$, and \mathcal{L} the set of directed links $\lambda \in \mathcal{L}$. Certain elements of pedestrian facilities, such as stairs or corridors, translate naturally into links, and others naturally into nodes, like for instance entrance/exit points. For other elements, such as waiting halls or platforms, a decomposition into areas can be made. An area α is associated with a subnetwork $(\mathcal{N}_\alpha, \mathcal{L}_\alpha)$ denoted by \mathcal{G}_α . The set \mathcal{N}_α contains all the nodes corresponding to physical locations in the area, and $\mathcal{L}_\alpha \subset \mathcal{L}$ all links such that their two incident nodes belong to \mathcal{N}_α . Areas are allowed to overlap, and their union is not required to cover the full network.

A network-type representation of space is adequate for demand estimation, where computational efficiency is crucial and the walking behavior of pedestrians is of secondary relevance. For most practical cases, defining a walking network is straightforward, including multi-story buildings. At the traffic assignment level, where a detailed understanding of pedestrian dynamics in terms of the emergence and dissolution of congestion is required, a more detailed space representation may be more appropriate (see Chapter 4).

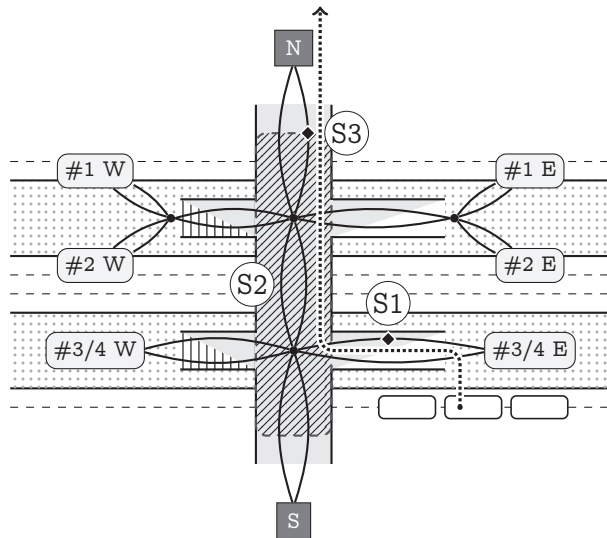


Figure 3.1: Network topology at the example of a simple train station.

Fig. 3.1 illustrates the proposed space representation. Railway tracks are denoted by dashed lines. Levels are bridged by ramps and stairways, which are denoted by standard floor plan symbols. Platform sectors are represented by OD nodes shown as labeled rectangles with rounded corners. They may be associated with one or a pair of railway tracks. Further OD nodes are shown as labeled squares, which include sales or service points, or exit/entrance areas. The pedestrian walking network is represented by solid lines. The dotted path represents a sample pedestrian alighting from a train and leaving the station to the north. Two count sensors, denoted by S1 and S3, are represented by diamonds. S2 denotes an area-based sensor, represented by the shaded area in the center of the figure.

Nodes through which pedestrians enter and leave the pedestrian network are referred to as OD nodes, and their set is denoted by $\mathcal{N}_{\text{OD}} \subset \mathcal{N}$.

We assume that the network is connected, i.e., any two OD nodes are connected by at least one route. A route ρ is a sequence of links connecting two OD nodes, $\rho = (\lambda_1, \lambda_2, \dots)$. A sequence of links that does not connect two OD nodes is called a subroute. The set of routes and subroutes is denoted by \mathcal{R} and \mathcal{R}_{sub} , respectively.

Each pedestrian is associated with a pair of OD nodes, denoted by $\kappa \in \mathcal{K}$ where \mathcal{K} is the set of OD pairs. In principle, it is possible to associate pedestrians with further attributes, such as behavior classes (Wong et al., 2005). The necessary extension is straightforward, and useful if personal attributes such as trip purpose, age or gender are available. In the interest of a more readable notation, in this work a single-class formulation is considered.

The number of travelers associated with OD pair κ that depart during time interval τ is represented by $d_{\kappa, \tau}$. We refer to this variable as demand. Demand is by nature stochastic, i.e., it varies from day to day.

A set of demand indicators is derived from OD demand to facilitate the formulation of the structural and measurement models. These include in particular link flows and area accumulations. Flow is cumulative over a time interval τ . Accumulation is defined as the time-mean average number of users in an area (Eddie, 1963). Table 3.1 provides an overview of these indicators. Further demand indicators are defined in Section 3.2.3 to integrate specific data sources.

A set of trains \mathcal{Z} is considered. For a train $\zeta \in \mathcal{Z}$, t_{ζ}^{arr} and t_{ζ}^{dep} denote the actual arrival and departure time in the train station. They are assumed to follow a known random distribution that may be obtained empirically,

Table 3.1: List of demand and demand indicators. The unit is ‘number of pedestrians per unit of time’, unless stated otherwise.

$\mathbf{d} = [d_{\kappa,\tau}]$	<u>D</u> emand $d_{\kappa,\tau}$ associated with OD pair κ and departure time interval τ , and time-space expanded vector \mathbf{d} of length $ \mathcal{K} \mathcal{T} $.
$\mathbf{f} = [f_{\lambda,\tau}]$	<u>F</u> low $f_{\lambda,\tau}$ entering link λ during time interval τ , and time-space expanded vector \mathbf{f} of length $ \mathcal{L} \mathcal{T} $.
$\mathbf{a} = [a_{\alpha,\tau}]$	Time-mean average <u>a</u> ccumulation $a_{\alpha,\tau}$ on area α during time interval τ , and time-space expanded vector \mathbf{a} of length $ \mathcal{A} \mathcal{T} $.
$\mathbf{e}_{\text{off}} = [e_{\zeta}^{\text{off}}]$, $\mathbf{e}_{\text{on}} = [e_{\zeta}^{\text{on}}]$	Train <u>e</u> xchange volumes associated with alighting, e_{ζ}^{off} , and boarding, e_{ζ}^{on} , of train ζ , and corresponding vectors \mathbf{e}_{off} and \mathbf{e}_{on} of length $ \mathcal{Z} $. The unit is ‘number of pedestrians’.

or computed by any suitable delay model. Each train is associated with an alighting and boarding volume, referred to as train exchange volumes and denoted by e_{ζ}^{off} and e_{ζ}^{on} , respectively. The platform serving train ζ is denoted by π_{ζ} . Each platform $\pi \in \mathcal{P}$, with \mathcal{P} the set of all platforms, is associated with a set of OD nodes, $\mathcal{N}_{\pi}^{\text{OD}} \subset \mathcal{N}_{\text{OD}}$. The set of all platform OD nodes is denoted by $\mathcal{N}_{\mathcal{P}} \subset \mathcal{N}$.

3.2.2 Illustration

The problem of estimating pedestrian OD demand in a train station may be introduced from an intuitive point of view. Consider the pedestrian described in Fig. 3.1 that alights from a train, and crosses the train station to leave it on the northside. Information of that pedestrian is contained in the alighting volume e_{ζ}^{off} of the feeding train ζ , in the flow counts of the sensors S1 and S3 denoted by $f_{S1,\tau'}$ and $f_{S3,\tau''}$, and in the accumulation of the area monitored by sensor S2, $a_{S2,\tau''}$. This information should be used to estimate the OD demand $d_{\#3/4\text{E} \rightarrow \text{N},\tau}$, unless it is spared for its validation.

A critical step in that process is the quantification of the spatio-temporal correlation between sensor and ridership data on one hand side, and the OD demand estimate on the other. If the pedestrian has arrived at the station during time interval τ , he may have been captured by sensor S3 during a later time step $\tau'' > \tau$. Clearly, it would be wrong to assume $\tau = \tau' = \tau'' = \tau'''$ in the above example. Likewise, if the pedestrian can choose among multiple routes, as it may be the case in a more complex network, he may not have been captured by a given sensor at all.

To define the association between train-related information, sensor data and OD demand, in the following a structural model and a measurement model are combined within a demand estimation framework. The idea consists in finding an estimate of OD demand that is in agreement with the train timetable and ridership information, and consistent with the available sensor data.

3.2.3 Data requirements

To distinguish between model estimates and actual observations, the latter are marked by a hat (e.g. \hat{f}). Often, such observations are not available for the complete network, or only for certain time intervals. Vectors containing a reduced set of variables are marked by a prime (e.g. f'), and a reduction matrix Δ is defined that relates each of them to the corresponding full vector (e.g. $f' = \Delta_f f$). This notation is consistent with that proposed by Cascetta et al. (1993) in the context of vehicular traffic.

For the estimation methodology, availability of the actual train timetable, t_ζ^{arr} and t_ζ^{dep} for each train $\zeta \in \mathcal{Z}$, and of the corresponding exchange volumes $\hat{e}_\zeta^{\text{off}}$, $\hat{e}_\zeta^{\text{on}}$ is essential. Moreover, indirect observations of demand, for instance in the form of link flows \hat{f}' or area accumulations \hat{a}' , are required. These observations need to be such that demand micro-patterns of individual trains are captured, i.e., an aggregation in the order of minutes is desirable. Availability of an a priori estimate of demand \hat{d}' is useful to improve the estimation, but not required.

Example specification: To illustrate the demand estimation methodology, a concrete specification is elaborated. For that purpose, several assumptions are made. The general estimation methodology is however independent of these assumptions.

Assumption 1 (Data availability) *Available are (i) the actual train timetable, (ii) train exchange volumes, (iii) partial observations of link flows, and (iv) cumulative origin and destination flows for selected OD nodes (e.g. from sales data). For validation, (v) partial observations of area accumulations, and (vi) flows along selected subroutes are available. No a priori estimate of demand is assumed available.*

To capture the format of these data sources, corresponding demand indicators are defined in Table 3.2. The specification of these demand indicators can be adapted based on the available data. For instance, if Wi-Fi traces are available, partial route flows or route travel times may be defined. The only requirement is that a mathematical relationship between OD demand and these indicators can be established, which is discussed in the following.

Table 3.2: Additional demand indicators.

$\mathbf{f}_{\text{sub}} = [f_{\rho,\tau}^{\text{sub}}]$	Subroute flow $e_{\rho,\tau}^{\text{sub}}$ reaching subroute ρ during time interval τ , and time-space expanded vector \mathbf{f}_{sub} of length $ \mathcal{R}_{\text{sub}} \mathcal{T} $. Its unit is ‘number of pedestrians per unit time’.
$\mathbf{f}_{\text{out,cum}} = [f_{\nu}^{\text{out,cum}}]$	Cumulative origin flow $f_{\nu}^{\text{out,cum}}$ emanating from OD node ν during the time period \mathcal{T} , and vector $\mathbf{f}_{\text{out,cum}}$ of length $ \mathcal{N}_{\text{OD}} $. Its unit is ‘number of pedestrians’.
$\mathbf{f}_{\text{in,cum}} = [f_{\nu}^{\text{in,cum}}]$	Cumulative destination flow $f_{\nu}^{\text{in,cum}}$ reaching OD node ν during time period \mathcal{T} , and vector $\mathbf{f}_{\text{in,cum}}$ of length $ \mathcal{N}_{\text{OD}} $. Its unit is ‘number of pedestrians’.

3.2.4 Structural model

The structural model describes the relationship among the various variables involved in the framework. We consider two parts, namely a pedestrian traffic assignment model, and a schedule-based model that considers the arrivals and departures of trains.

Assignment model

A pre-specified aggregate network supply model, referred to as assignment model, is assumed to exist. It is designed to derive the demand indicators from a given demand, depending on a parameter vector \mathbf{y} . If $\Sigma(\mathbf{d}; \mathbf{y})$ denotes the assignment model, and if $\Sigma_{(\cdot)}$ is its output with respect to demand indicator (\cdot) and $\eta_{(\cdot)}$ the corresponding structural error, the aforementioned link flow and area accumulation vectors may be expressed as

$$\mathbf{f} = \Sigma_{\mathbf{f}}(\mathbf{d}; \mathbf{y}) + \eta_{\mathbf{f}}, \quad (3.1)$$

$$\mathbf{a} = \Sigma_{\mathbf{a}}(\mathbf{d}; \mathbf{y}) + \eta_{\mathbf{a}}. \quad (3.2)$$

In this work, we assume the parameter vector \mathbf{y} to be known a priori, but note that it could also be estimated simultaneously with demand. Such an approach incurs substantial computational cost, and is not commonly pursued in the literature (Cascetta and Imbrota, 2002).

To implement Eq. (3.1) and Eq. (3.2), any suitable supply model may be used. It can be a simple linear mapping, a commercial DTA model such as PTV Viswalk or Legion for Aimsun, or the model proposed in Chapter 4. Essential is that basic measures of pedestrian traffic like flow and density are provided.

Internally, most assignment models perform two steps to obtain an estimate of demand indicators. First, OD demand is mapped to route flows by means of a route choice model. For a given OD pair and known link and route attributes, it identifies the route that a traveler would select. The choice of alternatives, and all attributes are assumed to be known. A large number of route choice models are available for that purpose, both in the context of road traffic (Dial, 1971; Cascetta et al., 1996; Ben-Akiva and Bierlaire, 2003; Frejinger and Bierlaire, 2007), and in that of pedestrian flow (e.g. Hoogendoorn et al., 2014, 2015). Second, a network loading model is used to describe the propagation of pedestrians along the routes. Chapter 4 of this thesis is dedicated to the development of such a loading model. A large number of models is available in the literature as well (e.g. Løvås, 1994; Helbing and Molnár, 1995; Blue and Adler, 2001; Hughes, 2002; Antonini et al., 2006; Hänseler et al., 2014a). To represent heterogeneity among pedestrians, route choice and network loading are usually expressed by means of probability distributions.

Both route choice and network loading are subject to prevailing traffic conditions, and thus mutually dependent. If the dependency on prevailing traffic conditions is neglected, the relationship between demand and derived indicators becomes linear (Cascetta and Imbrota, 2002). This holds true for an uncongested network. Alternatively, if the traffic situation is known a priori through direct measurements, an estimate of the assignment maps may also be obtained without considering the demand (see the aforementioned example by Montero et al., 2015).

If on the other hand a network is congested and link travel times are unknown, a problem of circular dependence arises between the demand estimation and the network supply model. One way of dealing with that is by formulating a bi-level optimization problem that explicitly includes

traffic equilibrium conditions. Among the most popular studies pursuing such an approach in the context of vehicular traffic are those by Fisk (1988), Yang (1995) and Florian and Chen (1995). An alternative way to consider the mutual dependency between the demand and supply model is by using a fixed-point formulation, as done in the same context by Cascetta and Postorino (2001) and Bierlaire and Crittin (2006).

Example specification: An assignment model for pedestrian walking facilities in a train station with a low level of congestion is considered. It consists of two independent models for route choice and network loading. For the sake of simplicity, we consider an assignment that is demand-independent.

Following Dial (1971), we adapt a probabilistic route choice model that is suitable for traffic assignment and behaviorally accurate in the context of pedestrian flows (Bierlaire and Robin, 2009).

Assumption 2 (Route choice) *The route choice decision rule is given by a logit model, where the cost of a route is equal to the sum of link traversal times. The set of routes is finite and known.*

While this specification of the route choice model is mathematically convenient, it has some well-known shortcomings, such as the assumed independence among alternatives. As routes overlap, more advanced models that take into account the correlation among routes may be used instead (in the context of vehicular traffic, see Cascetta et al., 1996; Frejinger and Bierlaire, 2007). Similarly, the choice set usually only includes ‘efficient’ routes that do not backtrack, i.e., routes where every link has its upstream node closer to the origin than the downstream node (Dial, 1971). Under some circumstances, this may represent a questionable restriction, and other choice set generating methods may be more appropriate (see e.g. Ben-Akiva et al., 1984; Frejinger et al., 2009, again in the context of vehicular traffic). In particular, alternative route choice models should be used if pedestrians are not ‘goal-oriented’, as is likely the case when a prospective train user faces a lot of waiting time until departure. The exploration of corresponding models, and their impact on demand estimation, is left for future research.

Following Mustafa and Ashaari (2015), we assume that the walking speed in pedestrian facilities of a train station with a low or

medium level of congestion is normally distributed (LOS E or better, Highway Capacity Manual, 2000, Exhibit 18-3).

Assumption 3 (Network loading) *The propagation of pedestrians along routes is described by a demand-invariant walking speed distribution $f_v(v)$.*

The resulting mathematical specification of the assignment model is provided in Appendix A. The relationship between route choice and network loading is further discussed in Chapter 4, where pedestrian traffic assignment is discussed in detail.

The impact of Assumption 3 on the accuracy of the OD demand estimate is difficult to assess. Even in otherwise uncongested facilities, there may be stairs, escalators or turnstiles where users experience delays. If these delays are significant compared to the temporal resolution of the OD demand estimator, a different specification of the network loading model should be considered.

Schedule-based model

The schedule-based model establishes a relationship between OD demand and train exchange volumes. It is based on the assumption that the alighting volume of trains served by a specific platform is related to the demand emanating from OD nodes representing that platform, and vice versa for boarding volumes.

Pedestrian demand within a train station is associated with alighting volumes by an assignment matrix $\mathbf{H} = [h_{\zeta,(\kappa,\tau)}]$ and a corresponding error ϵ_{off} such that

$$\mathbf{e}_{\text{off}} = \mathbf{H}\mathbf{d} + \epsilon_{\text{off}}. \quad (3.3)$$

The error ϵ_{off} takes into account pedestrians that visit a platform e.g. by mistake, or to accompany a passenger. The entry $h_{\zeta,(\kappa,\tau)}$ represents the proportion of pedestrians associated with OD pair κ and departure time interval τ that have alighted from train ζ . It is high if the time interval τ coincides with the idling time $[t_{\zeta}^{\text{arr}}, t_{\zeta}^{\text{dep}}]$ of train ζ on platform π , and if the origin node v_{κ}^o of OD pair κ is associated with the corresponding platform, i.e., if $v_{\kappa}^o \in \mathcal{N}_{\pi}^{\text{OD}}$. Otherwise, it is zero. Under the basic assumption that

demand is distributed homogeneously within a demand interval, the entries of the assignment matrix \mathbf{H} are given by

$$h_{\zeta,(\kappa,\tau)} = \begin{cases} \left| \left[t_{\zeta}^{\text{arr}}, t_{\zeta}^{\text{dep}} \right] \cap \tau \right| / |\tau| & \text{if } \nu_{\kappa}^{\circ} \in \mathcal{N}_{\pi}^{\text{OD}}, \\ 0 & \text{otherwise,} \end{cases} \quad (3.4)$$

where $|\tau|$ represents the length of time interval τ .

In principle, a similar approach may be used to relate OD demand to boarding volumes. However, it is difficult to find a meaningful specification of the corresponding assignment matrix. Prospective passengers often arrive at the platform long before the scheduled departure, which may be due to constraints imposed by the schedule of tertiary transport modes, or a high risk aversion (van Hagen, 2011). We leave the development of an appropriate arrival process, for instance based on a Poisson distribution, for future research.

For now, boarding volumes may be considered in a temporally aggregated way. We denote by $f_{\pi}^{\text{dep,cum}}$ the cumulative departure flow from platform π during time period \mathcal{T} , given by

$$f_{\pi}^{\text{dep,cum}} = \sum_{\tau \in \mathcal{T}} \sum_{\nu \in \mathcal{N}_{\pi}^{\text{OD}}} \sum_{\kappa \in \mathcal{K}_{\nu}^{\text{dest}}} d_{\kappa,\tau}, \quad (3.5)$$

where the set $\mathcal{K}_{\nu}^{\text{dest}}$ contains all OD pairs with destination ν . The corresponding vector $\mathbf{f}_{\text{dep,cum}} = [f_{\pi}^{\text{dep,cum}}]$ is of length $|\mathcal{P}|$.

If $\boldsymbol{\varepsilon}_{\chi}$ represents a vector containing structural errors, the vector of cumulative platform departure flows can also be expressed by summing over the boarding volumes of the served trains, i.e.,

$$\mathbf{f}_{\text{dep,cum}} = \boldsymbol{\chi}(\mathbf{e}_{\text{on}}) + \boldsymbol{\varepsilon}_{\chi}, \quad (3.6)$$

where $\boldsymbol{\chi} = [\chi_{\pi}]$ is given by

$$\chi_{\pi}(\mathbf{e}_{\text{on}}) = \sum_{\zeta \in \mathcal{Z}_{\pi}} e_{\zeta}^{\text{on}}, \quad (3.7)$$

and where \mathcal{Z}_{π} is the set of trains associated with platform π .

Eq. (3.6) provides no information about the distribution of demand across time. Similarly, Eq. (3.3) may not provide significant temporal information unless the train idling times are of approximately the same length as the discretization time intervals.

Empirical relations between OD demand and exchange volumes may instead be used to obtain such temporal information. This approach is illustrated at the example of ‘train-induced arrival flows’, and further discussed in the specification below.

Let $\mathcal{L}_\pi^{\text{arr}}$ denote the set of links representing the exit ways of platform π , and $\phi_{\lambda,\tau}(\mathbf{e}_{\text{off}}; \mathbf{y})$ a model that predicts the cumulative flow on link $\lambda \in \mathcal{L}_\pi^{\text{arr}}$ during time interval τ based on the arrival times of trains and their alighting volumes. If $\boldsymbol{\varphi}(\mathbf{e}_{\text{off}}; \mathbf{y}) = [\phi_{\lambda,\tau}]$ represents the corresponding time-space expanded vector, it holds that

$$\mathbf{f}_{\text{arr}} = \boldsymbol{\varphi}(\mathbf{e}_{\text{off}}; \mathbf{y}) + \boldsymbol{\varepsilon}_\varphi, \quad (3.8)$$

where $\boldsymbol{\varepsilon}_\varphi$ denotes a structural error, and where the flow vector associated with arrival links is given by

$$\mathbf{f}_{\text{arr}} = \boldsymbol{\Delta}_{\text{arr}} \mathbf{f} \quad (3.9)$$

and where the reduction matrix $\boldsymbol{\Delta}_{\text{arr}}$ is of size $|\mathcal{L}_\pi^{\text{arr}}| |\mathcal{T}| \times |\mathcal{L}| |\mathcal{T}|$.

Eq. (3.8) can be used to complement, or to replace Eq. (3.3). If an accurate empirical model is available, Eq. (3.3) does not provide much additional information, and can be omitted. This is assumed to be the case in the specification below. If on the other hand both Eq. (3.3) and Eq. (3.8) are used, a strong correlation among their error terms is likely to exist and needs to be explicitly considered.

Example specification: Our approach is inspired by Benmoussa et al. (2011) and Lavadinho (2012).

Assumption 4 (Schedule-based model) *Flows on platform exit ways consist of independent ‘arrival flows’ induced by trains served by the corresponding platform. These ‘train-induced arrival flows’ follow a piecewise linear model, characterized by a lagged onset of flow after the train arrival, and a constant flow thereafter until all passengers have left the platform.*

Assumption 4 allows to empirically predict the platform exit flows by decomposing them into independent contributions of trains. Assume that for a train ζ , the arrival flow rate at continuous time t on link $\lambda \in \mathcal{L}_\pi^{\text{arr}}$ is

given by $\tilde{\phi}_{\zeta,\lambda}(\mathbf{t}; e_{\zeta}^{\text{off}}, t_{\zeta}^{\text{arr}}, \mathbf{y})$. The platform exit flow during time interval τ on link $\lambda \in \mathcal{L}_{\pi}^{\text{arr}}$ is then given by

$$\phi_{\lambda,\tau} = \int_{\mathbf{t} \in \tau} \sum_{\zeta \in \mathcal{Z}_{\pi}} \tilde{\phi}_{\zeta,\lambda}(\mathbf{t}; \hat{e}_{\zeta}^{\text{off}}, t_{\zeta}^{\text{arr}}, \mathbf{y}) \, d\mathbf{t}. \quad (3.10)$$

Let $\tilde{f}_{\zeta} = \tilde{f}_{\pi}(e^{\text{off}})$ denote the total exit flow rate associated with platform π if train $\zeta \in \mathcal{Z}_{\pi}$ with alighting volume e_{ζ}^{off} has arrived, and let $\Delta t_{\zeta,\lambda}^{\text{lag}}$ be the lag time representing the delay between the arrival of train ζ and the onset of flow on link $\lambda \in \mathcal{L}_{\pi}^{\text{arr}}$. This lag may be due to the necessary walking to reach the exit ways, or a delay in the opening of train doors after the train has stopped. It may be modeled as a normally distributed random variable, and assumed to depend on the platform only, i.e., $\Delta t_{\zeta,\lambda}^{\text{lag}} = \Delta t_{\pi}^{\text{lag}}$, where $\pi = \pi_{\zeta}$ (Molyneaux et al., 2014).

Assuming that the total exit flow rate of platform π is shared according to platform sector split fractions $r_{\zeta,\lambda}^{\text{sec}}$ with $\sum_{\lambda \in \mathcal{L}_{\pi}^{\text{arr}}} r_{\zeta,\lambda}^{\text{sec}} = 1$, the flow rate on link λ associated with train $\zeta \in \mathcal{Z}_{\pi}$ is given by

$$\tilde{\phi}_{\zeta,\lambda}(\mathbf{t}) = \begin{cases} r_{\zeta,\lambda}^{\text{sec}} \tilde{f}_{\zeta} & \mathbf{t} \in \left(t_{\zeta}^{\text{arr}} + \Delta t_{\zeta,\lambda}^{\text{lag}}, t_{\zeta}^{\text{arr}} + \Delta t_{\zeta,\lambda}^{\text{lag}} + e_{\zeta}^{\text{off}}/\tilde{f}_{\zeta} \right), \\ 0 & \text{otherwise.} \end{cases} \quad (3.11)$$

Fig. 3.2 illustrates the cumulative arrival flow associated with Eq. (3.11). The solid curve illustrates an observation from Lausanne railway station (Molyneaux et al., 2014), and the dash-dotted curve a piecewise linear approximation.

The total platform exit flow rate $\tilde{f}_{\pi}(e^{\text{off}})$ is assumed to depend linearly on the alighting volume e^{off} at low values, and to reach saturation at a platform-specific threshold e_{π}^{crit} . If q_{π} , b_{π} and c_{π} represent shape parameters, the total exit flow rate on platform π is given by the stochastic model

$$\tilde{f}_{\pi}(e^{\text{off}}) = \tilde{f}_{\pi}^{\text{det}}(e^{\text{off}}) + \mathcal{N}(0, q_{\pi}), \quad (3.12)$$

where the deterministic part of the flow rate is specified as

$$\tilde{f}_{\pi}^{\text{det}}(e^{\text{off}}) = \begin{cases} b_{\pi} e^{\text{off}} + c_{\pi} & \text{if } e^{\text{off}} \leq e_{\pi}^{\text{crit}}, \\ b_{\pi} e_{\pi}^{\text{crit}} + c_{\pi} & \text{otherwise.} \end{cases} \quad (3.13)$$

Eq. (3.11) and Eq. (3.12) may be specified based on studies by Weidmann (1992), Buchmüller and Weidmann (2008) and Molyneaux et al. (2014). Alternatively, they can be calibrated on actual data. An example of the latter is provided in Section 3.3.

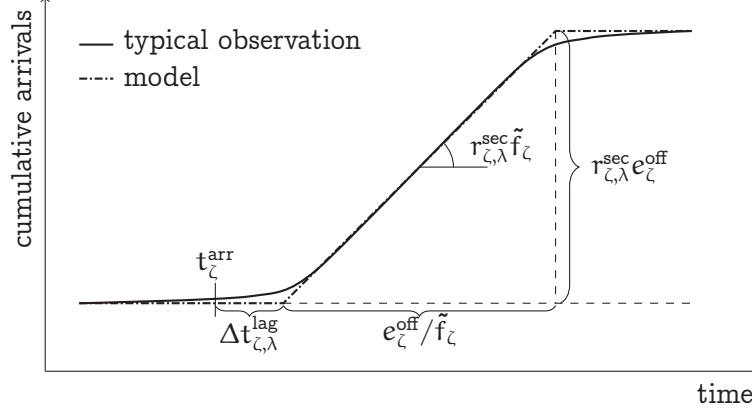


Figure 3.2: Model for train-induced arrival flows.

3.2.5 Measurement model

The measurement model links the structural model to a priori information and measurements, which is required for the estimation of demand, and for validating the obtained results.

For each data source, a random error term takes into account the uncertainty it is afflicted with, and the aforementioned reduction matrices account for the incomplete coverage of the data collection infrastructure, i.e.,

$$\hat{\mathbf{d}}' = \Delta_{\mathbf{d}} \mathbf{d} + \boldsymbol{\omega}'_{\mathbf{d}}, \quad (3.14)$$

$$\hat{\mathbf{f}}' = \Delta_{\mathbf{f}} \mathbf{f} + \boldsymbol{\omega}'_{\mathbf{f}}, \quad (3.15)$$

$$\hat{\mathbf{a}}' = \Delta_{\mathbf{a}} \mathbf{a} + \boldsymbol{\omega}'_{\mathbf{a}}, \quad (3.16)$$

$$\hat{\mathbf{e}}'_{\text{on}} = \Delta_{\text{on}} \mathbf{e}_{\text{on}} + \boldsymbol{\omega}'_{\text{on}}, \quad (3.17)$$

$$\hat{\mathbf{e}}'_{\text{off}} = \Delta_{\text{off}} \mathbf{e}_{\text{off}} + \boldsymbol{\omega}'_{\text{off}}. \quad (3.18)$$

The measurement errors $\boldsymbol{\omega}_{(\cdot)}$ are generally correlated, both across time and space. Temporal correlation occurs if a sensor is malfunctioning, or if it reaches saturation. Spatial correlation is a concern if two sensors capture similar information, for instance if they are placed nearby. For an efficient statistical inference, these effects need to be taken into account by using an appropriate covariance matrix, which is however often difficult to estimate.

Example specification: For the illustration of the model, the estimation problem is reduced to a formulation that is linear in the unknown demand vector.

The cumulative origin and destination flows are obtained by aggregation, i.e.,

$$f_v^{\text{out,cum}} = \sum_{\tau \in \mathcal{T}} \sum_{\kappa \in \mathcal{K}_v^{\text{orig}}} d_{\kappa,\tau}, \quad (3.19)$$

$$f_v^{\text{in,cum}} = \sum_{\tau \in \mathcal{T}} \sum_{\kappa \in \mathcal{K}_v^{\text{dest}}} d_{\kappa,\tau}, \quad (3.20)$$

where v_κ^d is the destination of OD pair κ , and where $\mathcal{K}_v^{\text{orig}}$ and $\mathcal{K}_v^{\text{dest}}$ denote the set of OD pairs which originate and terminate at OD node v , respectively.

Assumption 5 (Measurement model) *The distribution of train exchange volumes is a priori known, and used to pre-compute cumulative platform departure as well as platform arrival flows.*

It is unclear how sensitive the OD demand estimates are to Assumption 5. For regular situations with accurate a priori estimates of train exchange volumes, its impact is probably negligible. In case of a disruption of train operations, however, the assumption would be unlikely to hold.

The measurement model is given by Eq. (3.15), as well as by

$$\hat{f}_{\text{out,cum}}' = \Delta_{\text{out}} f_{\text{out,cum}} + \omega'_{\text{out}}, \quad (3.21)$$

$$\hat{f}_{\text{in,cum}}' = \Delta_{\text{in}} f_{\text{in,cum}} + \omega'_{\text{in}}, \quad (3.22)$$

$$\hat{\phi} = \Delta_{\text{arr}} f + \omega_\phi, \quad (3.23)$$

$$\hat{\chi} = f_{\text{dep,cum}} + \omega_\chi. \quad (3.24)$$

Eq. (3.23) and Eq. (3.24) consider empirical estimates of platform arrival and departure flows, $\hat{\phi}$ and $\hat{\chi}$, which are pre-computed based on the train timetable and a priori known train exchange volumes.

3.2.6 Estimation problem

The estimation problem consists in finding the distribution of the OD demand volumes \mathbf{d}^* such that (i) actual observations of demand indicators are

reproduced at best, (ii) platform arrival and platform departure flows are ‘most consistent’ with empirical predictions based on the train timetable, and (iii) the resulting estimate matches the historical one in case the estimation problem is underdetermined.

In the most general case, these three objectives are captured by a joint distance measure $\text{dist}\langle\cdot\rangle$. A statistically meaningful specification can be found using pure likelihood methods, or within the Bayesian framework, and depends on the assumptions that are made regarding the distribution of the error terms (Hazelton, 2000).

Alternatively, if the cross-correlation across the three objectives is negligible, the joint distance measure can be replaced by three separate terms $\text{dist}_{\text{obs}}\langle\cdot\rangle$, $\text{dist}_{\text{sched}}\langle\cdot\rangle$ and $\text{dist}_{\text{hist}}\langle\cdot\rangle$. The estimation problem reads then as

$$\mathbf{d}_y^* = \arg \min_{\mathbf{d} \geq 0} \text{dist}_{\text{obs}} \left\langle \left(\begin{array}{c} \hat{\mathbf{e}}'_{\text{on}} \\ \hat{\mathbf{e}}'_{\text{off}} \\ \hat{\mathbf{f}}' \\ \hat{\mathbf{a}}' \end{array} \right), \left(\begin{array}{c} \mathbf{e}'_{\text{on}} \\ \mathbf{e}'_{\text{off}} \\ \mathbf{f}' \\ \mathbf{a}' \end{array} \right) \right\rangle + \text{dist}_{\text{sched}} \left\langle \left(\begin{array}{c} \boldsymbol{\varphi}' \\ \boldsymbol{\chi}' \end{array} \right), \left(\begin{array}{c} \mathbf{f}'_{\text{arr}} \\ \mathbf{f}'_{\text{dep,cum}} \end{array} \right) \right\rangle + \text{dist}_{\text{hist}} \langle \hat{\mathbf{d}}', \mathbf{d}' \rangle. \quad (3.25)$$

While the distance measures in Eq. (3.25) are mutually independent, internally they may still consider complex error structures that, for instance in the context of least squares, can be taken into account by inner weights.

When solving Eq. (3.25), it is critical not to rely on point estimates. The demand vector \mathbf{d}^* is generally distributed, and follows a complex distribution that is insufficiently described by a single value such as its mean. The distribution depends both on the variation of input variables, which can be distributed themselves, and on the uncertainty involved in terms of modeling and measurement errors.

To approximate the distribution of \mathbf{d}^* , Monte Carlo sampling may be used. Demand on each day is assumed to represent independent random variables that follow a joint distribution. This is valid as long as seasonal effects are absent and no significant one-off events affect the network.

Example specification: As often done in practice, the correlation between error terms is neglected (Cascetta and Improta, 2002).

Assumption 6 (Error terms) *Each error term $\omega_{(\cdot)}$ follows an independent, univariate normal distribution with zero mean.*

Based on Assumptions 1–6, Eq. (3.25) reduces to a constrained, generalized least squares (GLS) problem both in the context of maximum likelihood and Bayesian estimation (Cascetta et al., 1993). It consists in finding

$$\begin{aligned} \mathbf{d}_y^* = \arg \min_{\mathbf{d} \geq 0} & w_{\text{flow}} \|\widehat{\mathbf{f}}' - \mathbf{f}'\|_2^2 + \\ & w_{\text{out}} \|\widehat{\mathbf{f}}'_{\text{out,cum}} - \mathbf{f}'_{\text{out,cum}}\|_2^2 + w_{\text{in}} \|\widehat{\mathbf{f}}'_{\text{in,cum}} - \mathbf{f}'_{\text{in,cum}}\|_2^2 + \\ & w_{\text{arr}} \|\widehat{\boldsymbol{\varphi}} - \mathbf{f}_{\text{arr}}\|_2^2 + w_{\text{dep}} \|\widehat{\boldsymbol{\chi}} - \mathbf{f}_{\text{dep,cum}}\|_2^2, \end{aligned} \quad (3.26)$$

where the parameters $w_{(\cdot)}$ denote weights whose specification is discussed below.

The first term on the RHS of Eq. (3.26) represents the distance between the observed link flows and those predicted by the model (see Eq. 3.1, 3.15). The terms on the second line consider the distance between model prediction and survey data in terms of cumulative origin and destination flows (Eq. 3.19, 3.21 and Eq. 3.20, 3.22). The two terms on the last line consider the distance to the pre-computed train-induced arrival flows (Eq. 3.8, 3.10, 3.11, 3.23) and the cumulative platform departure flows (Eq. 3.5, 3.6, 3.24).

For optimal statistical efficiency, the weights $w_{(\cdot)}$ are assumed equal to the reciprocal of the variance of the corresponding error term, i.e., $w_{\text{flow}} = 1/\text{Var}(\boldsymbol{\eta}'_f + \boldsymbol{\omega}'_f)$, $w_{\text{out}} = 1/\text{Var}(\boldsymbol{\omega}'_{\text{out}})$, $w_{\text{in}} = 1/\text{Var}(\boldsymbol{\omega}'_{\text{in}})$, $w_{\text{arr}} = 1/\text{Var}(\boldsymbol{\varepsilon}'_{\varphi})$ and $w_{\text{dep}} = 1/\text{Var}(\boldsymbol{\varepsilon}'_{\chi})$. In practice, these variances are unknown, and need to be estimated (Cascetta and Improta, 2002).

An active set method (Lawson and Hanson, 1974; Bierlaire et al., 1991) is used to solve the KKT conditions for the resulting non-negative least squares problem, Eq. (3.26). If several optimal solutions exist, the one with the lowest norm is selected, yielding a solution with maximum entropy (Cascetta et al., 1993).

3.3 Case study

To demonstrate the applicability of the proposed framework, a case study of Lausanne railway station is carried out. All code developed for the implementation, including the assignment model, is freely available (Hänseler and Molyneaux, 2015).

3.3.1 Assessment

To assess the efficiency of the proposed framework, two estimators are compared. A ‘base estimator’, representing a minimum norm solver taking into account link flow data only, and a ‘full estimator’, that additionally considers a ‘static’ and a ‘dynamic’ prior (see Fig. 3.3).

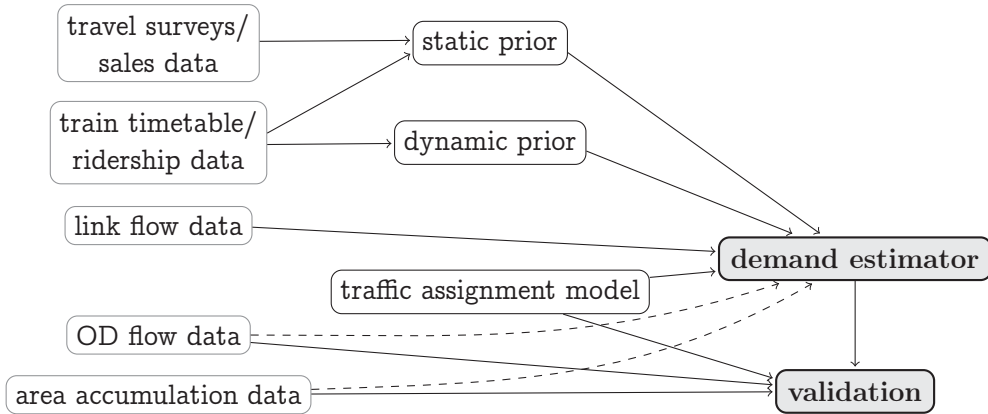


Figure 3.3: Scheme of the specification of the demand estimation framework.

The static prior includes cumulative origin and destination flows obtained from sales and ridership data. The dynamic prior represents train-induced arrival flows that are pre-computed based on the train timetable and ridership data. OD flow data and traffic condition data are used for validation. In a real context, once the specification is successfully validated, these two data sources would also be integrated in the estimation process to improve the quality of the estimate (dashed arrows in Fig. 3.3).

3.3.2 Parametrization

The pedestrian walking network of Lausanne railway station has a unique shortest path between every OD pair. During peak periods, regular commuters constitute the largest user group, which are familiar with the facilities (Lavadinho, 2012; Ton, 2014). Following Lavadinho (2012), they almost exclusively travel along these shortest paths, obviating the need for a route choice model.

To describe the propagation of pedestrians along routes, the walking

speed distribution proposed by Weidmann (1992),

$$v \sim \mathcal{N}(1.34 \text{ m/s}, 0.34 \text{ m/s}), \quad (3.27)$$

is used. It holds for even walking areas; link lengths on inclined areas or stairways need to be adjusted beforehand (Weidmann, 1992). The validity of speed distribution (3.27) has been empirically verified based on the available trajectory recordings, which show no significant signs of demand-supply interaction (see Section 2.3). In principle, the speed distribution observed in the PUs of Lausanne railway station could be used (see Figure 2.5b). However, since no measurements are available for other walkways or other facilities such as stairways, the parametrization proposed by Weidmann (1992) is used.

The schedule-based model is parametrized empirically (Molyneaux et al., 2014). Fig. 3.4 shows the total exit flow rates observed for platform #3/4, as well as the corresponding model fit. At low volumes, the flow rate increases linearly until a threshold is reached, beyond which the flow rate remains constant. The solid curve denotes the predicted flow rate according to Eq. (3.12), and the dashed lines the width of the prediction band in terms of \pm one standard deviation.

Two observations may be made. First, the length of a train, measured in number of passenger cars, n_{car} , does not have a significant influence on the flow rate. This is explicitly pointed out since the train length is shown below to have a considerable influence on the platform sector split fractions $r_{\zeta,\lambda}^{\text{sec}}$. Second, the flow rates are relatively high, such that the duration of flow is typically below one minute (up to an alighting volume of 333 passengers), and never exceeds 2 min.

Based on this specification, Fig. 3.5 shows the predicted exit flow for platform #5/6 on April 10, 2013, as well as the corresponding observation. The prediction is represented by a hexagonal lattice whose shading represents the time-dependent probability of the cumulative arrivals (Fig. 3.5a) and of the arrival flow rate (Fig. 3.5b) to reach a given value represented by the y-axis. These probabilities are obtained from 7500 Monte Carlo samplings of Eq. (3.5), each representing a simulated observation. The scale of the probability density plot is logarithmic and dimensionless. The alighting volumes e_{ζ}^{off} of each train ζ are inferred from the historical ridership data mentioned in Section 2.3. The actual observation is represented by a solid line. A good agreement between observation and prediction is found,

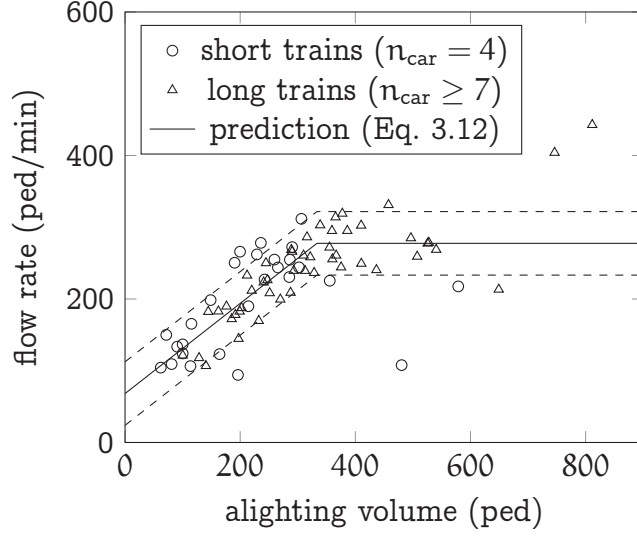


Figure 3.4: Total platform exit flow rate \hat{f} on platform #3/4.

although the standard deviation band is relatively wide. This is due to the high variation in alighting volumes across days.

The split fractions $r_{\zeta,\lambda}^{\text{sec}}$ depend on various factors such as the length of a train, its position along a platform, the distribution of passengers within a train, as well as their immediate next destination. Fig. 3.6 shows measurements from platform #3/4. The results are grouped by train length and ordered by alighting volumes. For short trains with $n_{\text{car}} = 4$, mostly the interior platform sectors B and C are used. This is the case particularly if the alighting volume is low. For larger trains with $n_{\text{car}} \geq 7$, the lateral sectors absorb a larger share, and the influence of the alighting volume is smaller.

In the framework of this study, two different specifications of the platform sector split fractions for short trains ($n_{\text{car}} = 4$) and long trains ($n_{\text{car}} \geq 7$) are considered. For each case, a multivariate normal distribution is developed, from which the train- and link-specific platform sector split fractions $r_{\zeta,\lambda}^{\text{sec}}$ can be drawn (Molyneaux et al., 2014).

The weights of demand indicators in Eq. (3.26) are determined based on the premise that pedestrian trajectory recordings represent the truth. Given the accuracy of the trajectory recordings, and their high spatial and temporal resolution compared to the other data sources, this assumption seems justifiable. It allows to estimate the variance of the errors associated

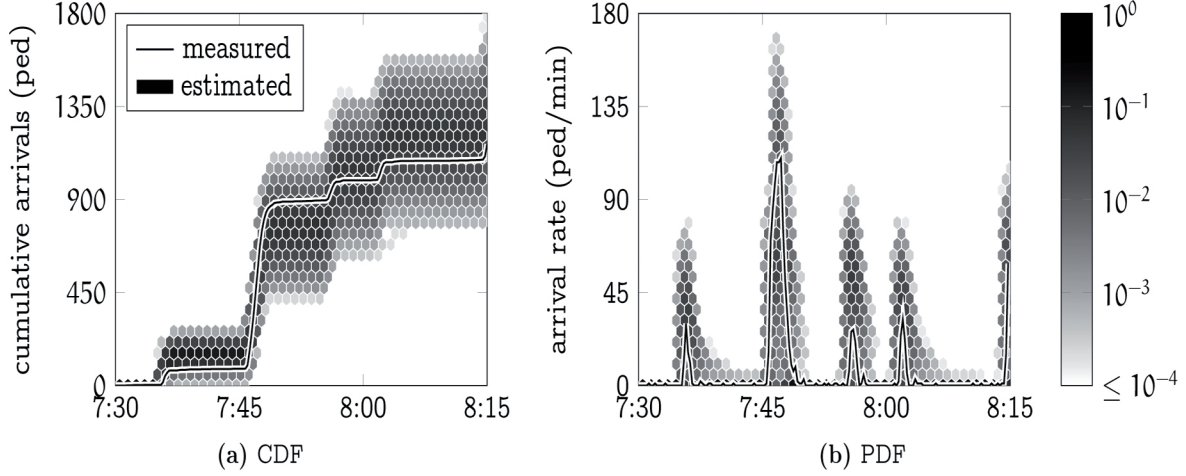


Figure 3.5: Total platform exit flow of platform #5/6 on April 10, 2013.

with the link flow data and the platform exit flows inferred from the train timetable. If, without loss of generality, the weight associated with link flow data is set to one, $w_{\text{flow}} = 1$, a value of $w_{\text{dyn}} = w_{\text{arr}} = 0.69$ results for the weight of the dynamic prior if the reciprocal of the variance of the corresponding error terms is considered. This specification maximizes the statistical efficiency of the estimator, as described in Section 3.2.6.

Regarding the weight of the static prior, $w_{\text{stat}} = w_{\{\text{out},\text{in},\text{dep}\}}$, in the range $10^{-4} \leq w_{\text{stat}} \leq 10^{-1}$ only little variation in the resulting demand estimate is perceivable. For lower values, due to numerical errors, its influence on the model estimate vanishes completely; for values larger than 10^{-1} , its influence grows rapidly. Given the relative inaccuracy of the data sources it contains, the static prior mainly serves to narrow the solution space. Thus, a value of $w_{\text{stat}} = 10^{-1}$ is used.

The resulting size of the estimation problem is given by the number of considered OD pairs, and the number of time intervals. The time discretization is of one minute, which is sufficient to capture demand micro-patterns, and coincides with that of the pedestrian count data, which is updated every 60s. To account for artificial transients during a potential ‘heat-up’ of the estimation, the computations include an additional 7 minutes both at the beginning and the end of the 30-minute analysis period. Therefore, an estimation problem with a total of 16,280 unknowns has to be solved per day. For each day, 24 Monte Carlo samplings of Eq. (3.26) are conducted,

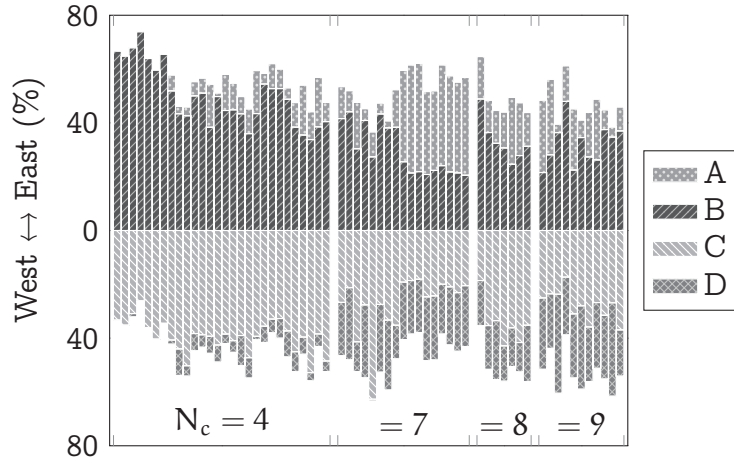


Figure 3.6: Split fractions of arrival flows across sectors on platform #3/4 grouped by train size and ordered by alighting volumes (increasing from left to right).

which is sufficient to generate reproducible and numerically stable results.

3.3.3 Results

The temporal evolution of total demand in PU East and PU West is shown in Fig. 3.7, in which the base and full estimator are compared to actual observations. The expected values and the standard deviation bands are shown. Both estimators are capable of following the overall trend. The base estimator, however, tends to underestimate the peaks, and underestimates the cumulative demand by more than 20%. The full estimate mostly represents an accurate guess of the peak amplitudes, and yields an error of less than 4% for the overall demand. It performs between 40.8% (MAE) and 46.7% (RMSE) better than the base estimator. The estimated day-to-day variability, as represented by the standard deviation band, is comparable to the observed one (see Fig. 2.4a). A similar finding results by investigating the accumulation in PU West and PU East, for which the improvements for MAE and RMSE amount to 49.9% and 40.7%, respectively (no figure shown). The lowest average accumulation of 56.6 pedestrians is reached between 7:59 and 8:00, and the maximum of 261.5 pedestrians between 7:43 and 7:44.

The ability of the two estimators to reproduce platform exit flows can be

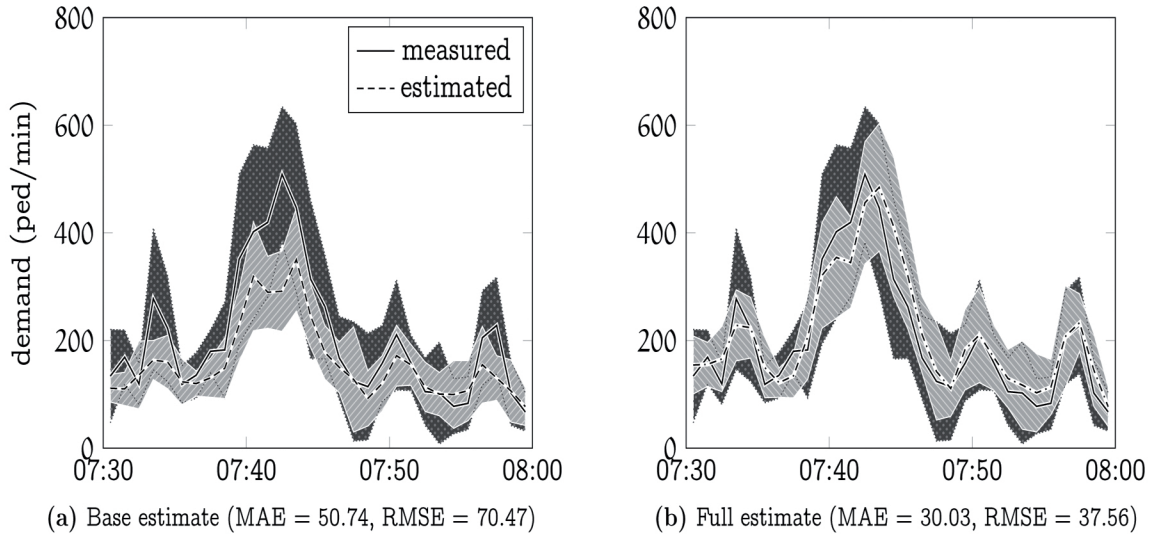


Figure 3.7: Total demand in PU East and PU West. Data: 10-day reference set, 2013 (see Section 2.3).

assessed in Fig. 3.8, showing a scatter plot of observed and estimated flows for platforms #3/4 and #5/6. The accuracy of these estimates is important for the dimensioning of platform access ways. The total platform exit flow is underestimated by the base model by -18.33%, and overestimated by the full model by 6.98%. The improvement in MAE and RMSE amounts to 30.26% and 23.35%, respectively.

Table 3.3 provides the RMSE for subroute flows and area accumulations in PU East and PU West for different estimators. Compared to the base model, in particular the incorporation of the dynamic prior leads to a significant improvement. The consideration of the train timetable increases the prediction quality significantly more than sales data and cumulative platform departure flows. The full model globally performs best, even though the accumulation estimate is slightly worse than in the case with a dynamic, but no static prior. Similar findings result if instead of RMSE another statistical measure, such as MAE, is used.

For further details of this case study, see Chapter 5.

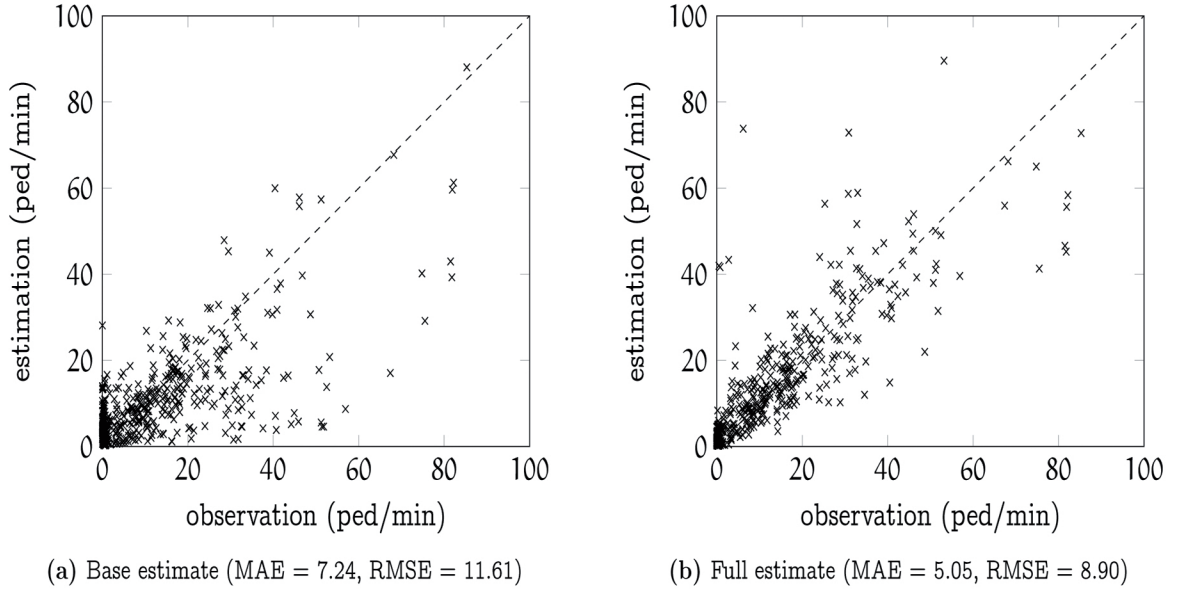


Figure 3.8: Arrival flows at platforms #3/4 and #5/6. Data: 10-day reference set, 2013.

Table 3.3: RMSE for subroute flows and accumulation in PU East and PU West. Data: 10-day reference set, 2013.

	subroute flow	accumulation
Base estimate	3.52 ped/min	58.84 ped
Estimate with static prior (STAT)	+2.43%	-15.03%
Estimate with dynamic prior (DYN)	-15.59%	-41.76%
Full estimate (STAT + DYN)	-31.07%	-40.74%

3.4 Concluding remarks

A framework for the time-dependent estimation of pedestrian origin-destination demand within a train station has been presented. Besides direct and indirect demand indicators such as flow counts or sales data, the train timetable is explicitly taken into account. This is achieved by establishing an empirical relationship between the arrival of a train and the subsequent flow of alighting passengers on platform exit ways. The formulation of the framework is such that it can be applied to various types of train stations and may be used with different data sources.

A case study of the morning peak period in Lausanne railway station has been presented. The obtained results are in good agreement with pedestrian tracking data that has been used for validation. A significant performance gain has been shown to exist when the train timetable is used in the estimation process. Moreover, spatial and temporal fluctuations, both intra- and inter-day, have been investigated and are shown to be important, justifying the use of a fully dynamic and probabilistic framework.

We can think of mainly two ways to extend the proposed framework. An obvious way relates to its application to real-time problems, such as traffic monitoring or crowd control. Another way is to focus on the improvement of the presented model specification. Clearly, the empirical relationship between the train timetable and pedestrian movements can be strengthened, or a demand-dependent network loading model could be integrated. This may be a macroscopic model, or an agent-based microsimulator. Arguably the most pressing issue, however, is the explicit consideration of correlation among measurements, which could significantly improve the statistical inference.

Chapter 4

Traffic assignment

4.1 Introduction

The goal of pedestrian traffic assignment models is to determine pedestrian flows and crowd conditions that result from the mutual interaction among demand and infrastructure. Their input is pedestrian demand, which may for instance be obtained in the form of OD flows from the estimation methodology described in Chapter 3. The outputs include traffic conditions, such as travel times or prevailing walking speeds, or level-of-service indicators such as density.

Traffic assignment models that take OD demand as input typically consist of a route choice model, and of a network loading model. In the context of pedestrian flows, the notion of a ‘route’ is less obvious than for vehicular flows, where the concept of assignment models is inspired from. However, at an aggregate level, pedestrian facilities may be approximated by a network, and the concept of routes is useful to preliminarily assign pedestrians to facilities. To capture pedestrian dynamics within them, most pedestrian network loading models operate at a finer scale. The propagation of pedestrians is typically described along ‘paths’. Such paths may be defined as trajectories in continuous space (e.g. Helbing and Molnár, 1995), sequences of cells (Blue and Adler, 2001), ‘routes’ in a network with a finer discretization (Asano et al., 2007), or described by continuous density distributions (Hughes, 2002).

In terms of route choice, a common behavioral assumption is that pedestrians choose the available route having the least cost between their origin and destination. This cost generally incorporates various factors

such as travel time, physical effort, or comfort. A large number of route choice models have been developed, both in the context of vehicular traffic (Dial, 1971; Cascetta et al., 1996), and in the context of pedestrian flows (Seneviratne and Morrall, 1985; Cheung and Lam, 1998; Hoogendoorn and Bovy, 2004). Pedestrian route choice is particularly complex due to issues entailing scale (e.g. local vs. global route choice), context (travel purpose, age, gender, facility type, weather, culture), its relation with activity scheduling, habit, and other factors. However, data availability is still limited, making research on the topic difficult.

In terms of network loading models, a multitude of suitable approaches have been proposed as well. These range from the well-known social force model (Helbing and Molnár, 1995) to cellular automata (Blue and Adler, 2001), queueing networks (Løvås, 1994), behavioral models (Robin et al., 2009), activity choice models (Hoogendoorn and Bovy, 2004) or continuum models (Hughes, 2002; Hoogendoorn et al., 2014). Despite this wide availability of modeling approaches, a recent review has found that current models are either computationally inefficient, or of questionable accuracy (Duives et al., 2013). To close this gap, either a macroscopic or a microscopic approach may be pursued. For complex settings involving a large number of pedestrians, typically macroscopic models are preferable. Besides computational advantages, they can be readily calibrated on real data, and directly interact with aggregate demand estimation models (see Chapter 3).

In the remainder of this chapter, the focus is on the development of an accurate and computationally efficient network loading model. Accordingly, it is assumed that pedestrian ‘route demand’ is known, i.e., that the OD demand has already been assigned to routes by any of the aforementioned route choice models. Interposing a route choice model between an OD demand estimator and a network loading model is straightforward in a pedestrian context, where route choice is widely assumed to be reactive, i.e., independent of future traffic conditions (Jiang et al., 2009b).

The chapter is structured as follows. Section 4.2 provides an overview of the literature on macroscopic network loading models, and a recapitulation of recent findings from related empirical studies. Based on that review, Section 4.3 presents a novel macroscopic model that is comparably accurate and computationally cheap. Sections 4.4–4.7 present an operational model specification, and discuss several case studies. Section 4.8 contains

concluding remarks.

4.2 Literature review

The following review focuses on macroscopic approaches for the loading of pedestrian networks, and specifically on continuum models and related phenomenological models. For a comprehensive review of pedestrian flow models including microscopic and hybrid models, the reader is referred to Duives et al. (2013).

Continuum models interpret pedestrians as particles of flow that are conserved. They formulate a set of partial differential equations (PDEs) in which walking speed is typically determined by a fundamental diagram relating pedestrian density and speed. Inspired by the kinematic wave theory, it is assumed that the fundamental diagram also holds for non-stationary traffic, implying that pedestrians adapt their speed instantaneously with infinite acceleration.

One of the first continuum models for pedestrian movements has been proposed by Al-Gadhi and Mahmassani (1990), who study circular movements around religious stone monuments during the Hajj, a Muslim pilgrimage to Makkah, Saudi Arabia. Their approach has been generalized by Hughes (2002) in his seminal ‘continuum theory for the flow of pedestrians’. This theory is a two-dimensional extension of the Lighthill–Whitham–Richard (LWR) model that is used to approximate the traffic movement on a uni-directional highway (Lighthill and Whitham, 1955; Richards, 1956). Hughes’ continuum theory allows for multi-commodity flow involving pedestrians with different walking directions and destinations. Several discretization schemes have been proposed to illustrate such flows by means of numerical examples (Xia et al., 2008; Huang et al., 2009; Jiang et al., 2009b). Moreover, Colombo and Rosini (2005) and Goatin et al. (2009) have extended the model to describe ‘overcompression’ during panic, i.e., the increase of pedestrian density beyond the jam density during extreme situations.

Hoogendoorn et al. (2014, 2015) derive a continuum model from a microscopic pedestrian model. As for the previous models, pedestrian flow is assumed in equilibrium by setting all acceleration terms to zero. A closed-form expression for the walking speed is obtained by approximati-

ing the density using a first-order Taylor series expansion. The model is then specified such that a linear and isotropic density-speed relationship results. Several numerical examples are considered using a two-dimensional Godunov scheme (Lebacque, 1996; van Wageningen-Kessels et al., 2015a).

The above models have in common that they express a system of PDEs that are solved numerically by discretization. The resulting solution schemes are similar to a group of models that are referred to as ‘phenomenological’. Phenomenological models may provide a comparable level of detail in terms of spatial and temporal dynamics, but they are not a direct product of the discretization of a system of PDEs. Having said that, they lend many ideas from such discretization schemes, in particular the cell transmission model (CTM, Daganzo, 1994, 1995). Phenomenological models leave more freedom to the modeler and are sometimes more accurate, as the system of PDEs discussed previously do not represent any physical law in the first place. Furthermore, they are typically less costly to apply in practice.

Asano et al. (2007) have been first to propose a generalized CTM to describe pedestrian flows. As used by Daganzo in the context of vehicular traffic, an isotropic trapezoidal fundamental diagram is assumed in their pedestrian cell transmission model. No framework for estimating ‘turning proportions’ is provided. Instead, the fractions of pedestrians associated with each walking direction are exogenously given, and the exact sequence of cells that a pedestrian traverses must be known in advance. This can be a severe constraint for the application of their model in practice.

Extended by a discrete potential field, Guo et al. (2011) present a related framework to study pedestrian route choice behavior and congestion during evacuation. A specification of the exact sequence of cells for pedestrians is no longer required. However, their framework is only capable of dealing with a trapezoidal fundamental diagram, which is shown for the case of uni-directional flow. The use of a more general density-flow relationship, as it may be found in applications different from evacuation, is not possible.

Most of the aforementioned models are difficult to apply to real case studies, be it due to their computational cost (Xia et al., 2008; Huang et al., 2009; Jiang et al., 2009b), or due to their focus on particular geometries or extreme events (Al-Gadhi and Mahmassani, 1990; Asano et al., 2007; Guo et al., 2011). Another limitation of a large majority of macroscopic

pedestrian models is their reliance on isotropic density-speed relationships. Only Al-Gadhi and Mahmassani (1990) and Jiang et al. (2009b) consider a bi-directional fundamental diagram for two specific applications. Yet pedestrian flow is in many cases multi-directional, and in particular under congested conditions, ‘anisotropic’.

Anisotropy is the property of being direction-dependent, here of the walking speed. In anisotropic pedestrian flow, the walking speed at the same point in space may be different depending on the orientation of a pedestrian. This definition is consistent with that used in material science or physics (e.g. Sayir et al., 2008). For an alternative definition of anisotropy in the context of microscopic models, see e.g. Hoogendoorn and Bovy (2002).

Compared to uni-directional flow, Navin and Wheeler (1969) observe in an empirical study that counter-flow reduces walking speed by up to 14.5% in case of a flow ratio of 10%:90%, and by 4% in case of symmetric flow. This is in qualitative agreement with findings by Lam et al. (2002) who report that the maximum reduction in capacity is around 19% for the same 10%:90% split ratio. Further studies of anisotropy have been conducted by Zhang et al. (2012), Zhang and Seyfried (2014) as well as Wong et al. (2010) and Xie and Wong (2015).

In this chapter, we develop a macroscopic pedestrian network loading model that is based on an approximation to the continuum theory for pedestrian flow and a CTM-like discretization scheme. Specifically, we build on the framework for multi-directional flows proposed by Asano et al. (2007) and adapt the concept of cell-specific potentials proposed by Guo et al. (2011). This yields a fast and accurate loading model for pedestrian flow. Moreover, we overcome the assumption of isotropy by relying on a stream-based formulation of a pedestrian fundamental diagram. This allows to realistically describe congested multi-directional flow at the macroscopic level. The resulting model is easily applicable to large and complex real-world applications.

4.3 Model framework

Inspired by the cell transmission model (Daganzo, 1994), we consider a discrete-time discrete-space model where each time interval $\tau \in \mathcal{T}$ is of

uniform length Δt .

As suggested by Løvås (1994), walkable space is represented by a directed graph $\mathcal{G} = (\mathcal{N}, \Lambda)$, where \mathcal{N} represents the set of nodes $v \in \mathcal{N}$, and Λ the set of directed streams $\lambda \in \Lambda$. The topology of the network depends on the specific application, particularly the major prevailing movement directions. Nodes through which pedestrian traffic is discharged and leaves the network are referred to as origin/destination nodes, and their set is denoted by $\mathcal{N}_{\text{OD}} \subseteq \mathcal{N}$. While their typical position is at the border of a walking facility, OD nodes can also be located in the interior if they represent an access way to e.g. an elevator or an escalator. Nodes have no physical length.

A stream λ connects two nodes and has a fixed length $L_\lambda > 0$. It carries pedestrians only in one direction. Streams are obtained by decomposing the generally multi-directional flow. This decomposition depends on the prevalent pedestrian flow, and the geometry of the walking facility. It is assumed that a meaningful decomposition is known a priori. In the literature on empirical flow characterization, several decomposition strategies are discussed (Nikolić and Bierlaire, 2014; Xie and Wong, 2015).

Walkable space is partitioned into a set of areas \mathcal{X} . Every stream λ is associated with an area $\xi \in \mathcal{X}$, defining a space in which it interacts with other streams. The surface size of an area ξ is denoted by A_ξ , which takes into account a potential presence of internal obstacles. Such obstacles include any object that reduces the walkable space, such as a pillar or a trash bin. No prior assumptions about the shape and size of areas are necessary. The set of streams associated with area ξ is denoted by Λ_ξ , with $\Lambda_\xi \subset \Lambda$ and $\Lambda_\xi \cap \Lambda_{\xi'} = \emptyset$ if $\xi \neq \xi'$.

Fig. 4.1 illustrates the proposed space representation at the example of a longitudinal corridor with an orthogonal space discretization. In this illustration, multi-directional flow is decomposed into left-right as well as diagonal movements, resulting in six distinct flow directions. Areas are delimited by solid lines, streams represented by dashed lines, and nodes by circles. Since streams are direction-specific, each dashed line in Fig. 4.1 represents two streams, one in each direction. Pedestrians may cross from one area to another at any position along the joint boundary, and not only through nodes. Likewise, when traversing areas, pedestrians are not confined to the dashed lines, which only represent their direction of flow conceptually. Origin/destination nodes at both ends of the corridor are

represented by the two stars.

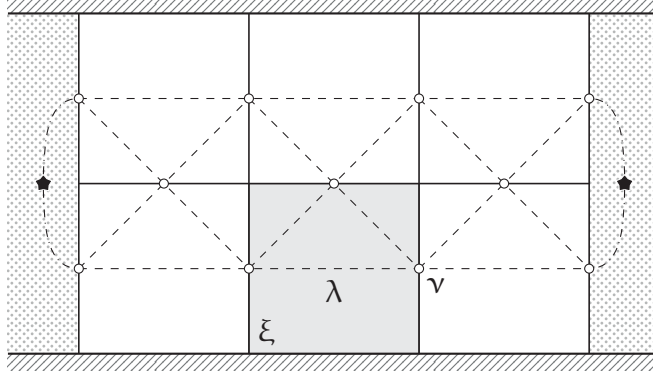


Figure 4.1: Illustration of space representation.

An orthogonal discretization as in Fig. 4.1 represents the most common specification for flow models relying on a fundamental diagram (Treuille et al., 2006; Huang et al., 2009). The size of areas is typically between 1 m² and 10 m². In this range, the model dynamics are found to be approximately scale-invariant. Specifically, we have tested several discretization meshes in that range at the example of the case studies presented later in this chapter, with no significant changes in the resulting model dynamics and calibration parameters. For artificial test scenarios with abrupt changes in demand and density, this result may however not hold. The main alternatives to an orthogonal space discretization are triangular or hexagonal grids (Guo et al., 2011; Chen et al., 2014; van Wageningen-Kessels et al., 2015b). Even irregular discretization geometries may be envisaged if they better fit the infrastructural layout.

A route ρ is defined by a pair of origin and destination nodes (v_o^ρ, v_d^ρ) , $v_o^\rho, v_d^\rho \in \mathcal{N}_{OD}$, and a set of streams Λ_ρ that connect them. The set Λ_ρ may be obtained by selecting streams individually, or by including all streams that are associated with a set of areas. There can be several routes connecting the same pair of OD nodes. Each route starts and ends at an OD node, but cannot contain any OD node in between. The set of all routes is denoted by \mathcal{R} .

Depending on the network \mathcal{G} and the set of streams Λ_ρ , multiple ‘stream sequences’ may connect the origin and destination of a route ρ . Such stream sequences are referred to as paths. To avoid their explicit enumeration, the concept of a path is not explicitly used. Instead, the choice of a path within

a route is considered by means of turning proportions that are computed at every node. They may depend both on the route and the prevailing traffic conditions. Depending on their specification, pedestrians may be distributed across multiple paths within a route, or stick to a single one, for instance the shortest path.

Pedestrians are organized in ‘packets’. A pedestrian packet ℓ is characterized by a route ρ_ℓ , a departure time interval τ_ℓ , and the number of people X_ℓ that it contains. In contrast to the definition of a ‘pedestrian type’ by Hughes (2002), a pedestrian packet is attributed a departure time and a route, instead of only a destination. On the other hand, pedestrian types in Hughes (2002) may differ with respect to their walking characteristics, whereas pedestrian packets as defined in this work may not (for a multi-commodity framework, see e.g. Cooper, 2014).

The set of all packets is denoted by $\mathcal{L} \subset \mathcal{R} \times \mathcal{T}$. The size X_ℓ of each pedestrian packet $\ell \in \mathcal{L}$ is assumed to be known a priori, and the corresponding demand vector is denoted by $\mathbf{X} = [X_\ell]$. Such information can be inferred from a demand estimation framework in combination with a suitable route choice model, as discussed previously.

A conservation principle with respect to the number of pedestrians on each stream is combined with an empirical density-speed relationship for calculating the flows between them. Within a stream, pedestrians are assumed to be homogeneously distributed, and their movements are not modeled explicitly. This concept is similar to that of the cell transmission model (Daganzo, 1994), with the difference that it is formulated at the level of streams instead of areas.

When pedestrian packets are propagated along the streams, they typically split up into fragments. In principle, these fragments can split indefinitely, but they merge again such that there is at most one fragment per packet in a stream. The state of the model at any time interval is described by the distribution of the fragments on the network. The number of pedestrians associated with packet ℓ in stream λ during time interval τ is denoted by $M_{\lambda,\tau}^\ell$ and referred to as the corresponding ‘fragment size’. The sum of all fragments in a stream λ during time interval τ is denoted by $M_{\lambda,\tau}$ and referred to as the stream accumulation. The vector of stream accumulations associated with area ξ and time interval τ is denoted by $\mathbf{M}_{\xi,\tau} = [M_{\lambda,\tau}]$, with $\lambda \in \Lambda_\xi$.

Each stream λ during time interval τ is associated with a walking speed

$v_{\lambda,\tau}$. The velocity vector of area ξ , $\mathbf{v}_{\xi,\tau} = [v_{\lambda,\tau}]$, groups these stream speeds.

For each area ξ and time interval τ , a functional relationship between the stream accumulation and velocity vectors is assumed to exist. This relationship may for instance be a stream-based fundamental diagram. In practice, time-invariant specifications are mostly used due to the difficulty of calibrating time-dependent models.

If v_f represents the ‘global’ free-flow walking speed, the stream velocity vector associated with area ξ during time interval τ is expressed as

$$\mathbf{v}_{\xi,\tau} = v_f \mathbf{F}_{\xi,\tau}(\mathbf{M}_{\xi,\tau}), \quad (4.1)$$

where $\mathbf{F}_{\xi,\tau}(\mathbf{M}_{\xi,\tau})$ represents the corresponding dimensionless density-speed relationship. Eq. (4.1) describes the relationship between the accumulation of each stream in an area, and the corresponding pedestrian stream speeds. Several possible specifications, both isotropic and anisotropic, are provided in Section 4.4.

The assumption of a fundamental diagram implies that pedestrians instantaneously adapt their speed if a change in accumulation occurs. In traffic flow theory, this is characteristic for first-order flow models. For pedestrian models, such an assumption is particularly well suited, since pedestrian can accelerate from standstill to free-flow walking speed almost immediately and vice versa (Weidmann, 1992).

Regarding the functional form of the vectorial density-speed relationship $\mathbf{F}_{\xi,\tau}(\mathbf{M}_{\xi,\tau})$, two assumptions are made. These are inspired by Hughes’ continuum theory for pedestrian flows (Hughes, 2002).

First, it is hypothesized that in an unoccupied area, the walking speed in every stream must be larger than zero, but may not exceed the global free-flow speed. If $F_{\lambda,\tau}$ represents the entry in $\mathbf{F}_{\xi,\tau}$ associated with stream $\lambda \in \Lambda_\xi$, this translates to

$$0 < F_{\lambda,\tau}(\mathbf{0}) \leq 1 \quad \forall \lambda \in \Lambda_\xi, \xi \in \mathcal{X}, \tau \in \mathcal{T}, \quad (4.2)$$

where $\mathbf{0}$ represents the null vector of length $|\Lambda_\xi|$. The walking speed at zero density can be lower than the global free-flow speed, which may be adequate for instance in uneven terrain. It may however not be zero, excluding phenomena like waiting. The resulting formulation therefore represents an exclusive walking model like most macroscopic approaches in the literature.

Second, the fundamental diagram is assumed to be monotonically decreasing, i.e.,

$$\frac{\partial F_{\lambda,\tau}}{\partial M_{\lambda',\tau}} \leq 0 \quad \forall \lambda, \lambda' \in \Lambda_\xi, \xi \in \mathcal{X}, \tau \in \mathcal{T}. \quad (4.3)$$

The assumption of monotonicity is widely accepted under ‘normal’ conditions (Daganzo, 1994; Hughes, 2002).

Some fundamental diagrams specify a jam density k_{jam} , i.e., a density at which all pedestrian movement halts. Equivalently, at the area level, a storage capacity $N_\xi^{\text{jam}} = k_{\text{jam}}A_\xi$ may be considered, representing the maximum number of pedestrians that can be present in an area at any time. In that case, it is further required that

$$F_{\lambda,\tau}(M_{\xi,\tau}) = 0 \quad \text{if } N_{\xi,\tau} = N_\xi^{\text{jam}}, \quad (4.4)$$

where $N_{\xi,\tau} = \sum_{\lambda \in \Lambda_\xi} M_{\lambda,\tau}$ denotes the total accumulation in area ξ during time interval τ .

As discussed by Daganzo (1994), the time discretization has to be such that pedestrians cannot traverse more than one stream in a single time step. In numerical mathematics, this consideration is referred to as the Courant–Friedrichs–Lewy (CFL) condition (Courant et al., 1967). It can be expressed as

$$\Delta t \leq \frac{L_\lambda}{v_f}, \quad \forall \lambda \in \Lambda. \quad (4.5)$$

According to Eq. (4.5), the ratio of the shortest stream length and the free-flow walking speed represents an upper bound for the time discretization. For instance, for the space representation shown in Fig. 4.1, the constraining length is that of the diagonal links, which are shorter than the horizontal ones.

The actual choice of the time step Δt is not critical for the stability of the model, but known to have an influence on numerical dispersion and computational cost (van Wageningen-Kessels et al., 2015a). In practice, it has been observed that such dispersion can even lead to more realistic results (Lebacque, 1996). As such, the time step can be seen as a calibration parameter. In this work, this possibility is not explored, and as in most traffic flow studies, the bound defined in Eq. (4.5) is used to specify the time step, i.e.,

$$\Delta t = \min_{\lambda \in \Lambda} \{L_\lambda / v_f\}. \quad (4.6)$$

Given that pedestrian streams are uni-directional, the associated flow is given by the hydrodynamic theory as the product of speed and density. Specifically, for stream $\lambda \in \Lambda_\xi$ during time interval τ , the flow increment during an infinitesimal time interval dt can be expressed as

$$dQ_{\lambda,\tau} = \frac{M_{\lambda,\tau}}{L_\lambda} v_f F_{\lambda,\tau}(M_{\xi,\tau}) dt. \quad (4.7)$$

Based on Eq. (4.6), and by defining the minimum stream length as $L_{\min} = \min_{\lambda \in \Lambda} L_\lambda$, the cumulative hydrodynamic flow of stream λ during time interval τ is given by

$$\Delta Q_{\lambda,\tau} = \frac{L_{\min}}{L_\lambda} M_{\lambda,\tau} F_{\lambda,\tau}(M_{\xi,\tau}). \quad (4.8)$$

The cumulative hydrodynamic stream flow does not represent an actual flow, but is a characteristic quantity from which further stream properties can be calculated (Daganzo, 1994).

Due to properties (4.2) and (4.3), the function defined in Eq. (4.8) is known to reach a maximum $\Delta Q_{\lambda,\tau}^{\text{crit}}$ at a characteristic accumulation $M_{\lambda,\tau}^{\text{crit}}$, referred to as the critical cumulative hydrodynamic flow and the critical stream accumulation, respectively. For each stream and time interval, the critical accumulation $M_{\lambda,\tau}^{\text{crit}}$ divides the density-flow relationship (Eq. 4.8) into a free-flow and a congested regime. In the free-flow regime, an infinitesimal increase in accumulation leads to an increased cumulative hydrodynamic flow. In the congested regime, inversely an increase in accumulation leads to a decrease in pedestrian flow.

A diminishing flow with increasing density beyond a critical accumulation is a characteristic property of most traffic networks. For multi-directional flow, the main cause is friction between different pedestrian streams that lead to degradation of traffic conditions. In uni-directional flow, a ‘capacity drop’ may result from the faster-is-slower effect due to an increasing ‘pedestrian pressure’ (Helbing, 2001). This is captured by the fundamental diagram, which describes such effects implicitly.

The critical accumulation associated with stream λ during time interval τ is computed by assuming that the accumulation of all other pedestrian streams in the same area, $M'_{\xi,\tau}$ with $\lambda' \in \Lambda_\xi$ and $\lambda' \neq \lambda$, are known, i.e.,

$$M_{\lambda,\tau}^{\text{crit}} = \arg \max_{M \geq 0} MF_{\lambda,\tau}(M; M'_{\xi,\tau}). \quad (4.9)$$

If the critical walking speed of stream λ during time interval τ is given by $v_{\lambda,\tau}^{\text{crit}} = v_f F_{\lambda,\tau}(M_{\lambda,\tau}^{\text{crit}}, M'_{\xi,\tau})$, the critical cumulative hydrodynamic flow of stream λ during time interval τ is given by

$$\Delta Q_{\lambda,\tau}^{\text{crit}} = \frac{L_{\min}}{L_{\lambda}} M_{\lambda,\tau}^{\text{crit}} \frac{v_{\lambda,\tau}^{\text{crit}}}{v_f}. \quad (4.10)$$

The cumulative hydrodynamic flow allows to determine an outflow capacity at the end of a stream, and an inflow capacity at the beginning (Lebacque, 1996). The hydrodynamic outflow capacity can be thought of as the maximum amount of pedestrians that could be sent to a next stream in case of an unlimited supply. It is defined as equal to the cumulative hydrodynamic flow if the stream is in the free-flow regime, and set equal to the critical cumulative hydrodynamic flow if it is in the congested regime. The hydrodynamic outflow capacity of stream λ during time interval τ is thus given by

$$\Delta Q_{\lambda,\tau}^{\text{out}} = \begin{cases} \Delta Q_{\lambda,\tau} & \text{if } M_{\lambda,\tau} \leq M_{\lambda,\tau}^{\text{crit}}, \\ \Delta Q_{\lambda,\tau}^{\text{crit}} & \text{otherwise.} \end{cases} \quad (4.11)$$

Likewise, the hydrodynamic inflow capacity can be considered as the maximum amount of pedestrians that can be received by a stream in case of an infinite traffic demand. It is equal to the critical cumulative hydrodynamic flow if the stream is in the free-flow regime, and set equal to the cumulative hydrodynamic flow otherwise. This is, the cumulative hydrodynamic inflow capacity of stream λ' during time interval τ is given by

$$\Delta Q_{\lambda',\tau}^{\text{in}} = \begin{cases} \Delta Q_{\lambda',\tau}^{\text{crit}} & \text{if } M_{\lambda',\tau} \leq M_{\lambda',\tau}^{\text{crit}}, \\ \Delta Q_{\lambda',\tau} & \text{otherwise.} \end{cases} \quad (4.12)$$

Eq. (4.11) and Eq. (4.12) are as defined in the cell transmission model (Daganzo, 1994).

To propagate pedestrians from one stream to the next, route-specific turning proportions at each node need to be known. They may be exogenous, or computed by an en-route path choice model based on the prevailing pedestrian traffic conditions. Assuming that all pedestrians embarked on a given route have the same walking behavior, the turning proportion corresponding to the stream sequence $\lambda \rightarrow \lambda'$ for the ensemble of people following route ρ that are in stream λ during time interval τ may be denoted by $\delta_{\lambda \rightarrow \lambda',\tau}^{\rho}$. Since pedestrians can only be sent to adjacent streams

that are part of their route, it must hold that

$$\sum_{\lambda' \in \Theta_\lambda^\rho} \delta_{\lambda \rightarrow \lambda', \tau}^\rho = 1, \quad (4.13)$$

where Θ_λ^ρ denotes the set of streams that originate from the end of stream λ and are part of route ρ . Typically, a potential field is assumed to exist from which the turning proportions for local path choice can be inferred (Hughes, 2002; Guo et al., 2011). These turning proportions guide the pedestrians along their route to their desired destination, taking the prevailing pedestrian traffic conditions into account. Depending on their specification, the en-route path choice may resemble a diffusion model, a shortest path model, or a mixture of both. In Section 4.4, a specification is provided that can reproduce such walking behavior.

Following Daganzo (1994, 1995), the cumulative hydrodynamic inflow and outflow capacity are used to define the receiving and sending capacity, respectively. The receiving capacity of stream λ' during time interval τ is equal to the cumulative hydrodynamic inflow capacity

$$R_{\lambda', \tau} = \Delta Q_{\lambda', \tau}^{\text{in}}, \quad (4.14)$$

where a separate variable is defined for notational consistency with the original CTM. Different from the original CTM, the receiving capacity is stream- and not area-specific, and does not take the area storage capacity N_ξ^{jam} into account. Instead, the storage capacity is considered at the area level as described below.

The counterpart of the receiving capacity is the sending capacity. The sending capacity from stream λ to stream $\lambda' \in \Theta_\lambda^\rho$ for pedestrian packet ℓ during time interval τ is given by

$$S_{\lambda \rightarrow \lambda', \tau}^\ell = \delta_{\lambda \rightarrow \lambda', \tau}^{\rho \ell} \min \left\{ M_{\lambda, \tau}^\ell, \frac{M_{\lambda, \tau}^\ell}{M_{\lambda, \tau}} \Delta Q_{\lambda, \tau}^{\text{out}} \right\}. \quad (4.15)$$

The first term in the curly brackets ensures the conservation of pedestrian flow, i.e., not more pedestrians may advance than are actually on the emitting stream. The second term applies when the hydrodynamic outflow capacity does not suffice to advance all pedestrians present on the stream concerned. In that case, a demand-proportional supply distribution scheme is applied to determine the fraction of each pedestrian packet that is part of the sending capacity.

Whenever demand exceeds supply, dispersion occurs, i.e., pedestrian packets split up in several fragments across streams. Generally, dispersion is present on all except the shortest stream, or whenever the prevailing walking speed is lower than the global free-flow walking speed. From a practical view point, dispersion can be seen as mimicking the presence of slow and fast pedestrians. This is an interesting property for traffic assignment, where estimates of walking time distributions are more useful than simple point estimates.

If the sending capacities exceed the available receiving capacity, they can only be accommodated partially. Let the candidate inflow to stream λ' during time interval τ be given by

$$S_{\lambda',\tau} = \sum_{\lambda'' \in \Phi_{\lambda'}^{\rho}} \sum_{\ell \in \mathcal{L}} S_{\lambda'' \rightarrow \lambda',\tau}^{\ell} \quad (4.16)$$

where $\Phi_{\lambda'}^{\rho}$ is the set of streams that terminate at the start node of stream λ' and are part of route ρ .

Taking the constraints at the stream level into account, the candidate transition flow from stream λ to λ' during time interval τ associated with pedestrian packet ℓ is expressed as

$$Y_{\lambda \rightarrow \lambda',\tau}^{\ell} = \begin{cases} S_{\lambda \rightarrow \lambda',\tau}^{\ell} & \text{if } S_{\lambda',\tau} \leq R_{\lambda',\tau}, \\ \zeta_{\lambda \rightarrow \lambda',\tau}^{\ell} R_{\lambda',\tau} & \text{otherwise.} \end{cases} \quad (4.17)$$

If the candidate inflow to stream λ' is inferior or equal to the corresponding receiving capacity, the candidate transition flow is equal to the sending capacity. Otherwise, the flow disperses and a demand-proportional supply distribution scheme is applied (Asano et al., 2007), i.e.,

$$\zeta_{\lambda \rightarrow \lambda',\tau}^{\ell} = \frac{S_{\lambda \rightarrow \lambda',\tau}^{\ell}}{S_{\lambda',\tau}}. \quad (4.18)$$

In principle, specifications different from Eq. (4.18) can be envisaged. A variety of related models have been proposed in the literature dealing with multi-legged junctions in road networks (Daganzo, 1995; Lebacque, 1996; Jin and Zhang, 2003). Most of these approaches are however specific to the case of vehicular traffic (such as strict first-in-first-out, FIFO), and not directly applicable in the context of pedestrian flows.

Finally, besides constraints at the stream level, also a storage constraint at the area level should be considered if a jam density has been defined. Let the candidate inflow to area ξ' during time interval τ be given by

$$Y_{\xi',\tau} = \sum_{\lambda' \in \Lambda_{\xi'}} \sum_{\lambda'' \in \Phi_{\lambda'}} \sum_{\ell \in \mathcal{L}} Y_{\lambda'' \rightarrow \lambda',\tau}^{\ell}. \quad (4.19)$$

The actual transition flow from stream λ to $\lambda' \in \Lambda_{\xi'}$ during time interval τ associated with pedestrian packet ℓ can then be expressed as

$$G_{\lambda \rightarrow \lambda',\tau}^{\ell} = \begin{cases} Y_{\lambda \rightarrow \lambda',\tau}^{\ell} & \text{if } Y_{\xi',\tau} \leq N_{\xi'}^{\text{jam}} - N_{\xi',\tau}, \\ \eta_{\lambda \rightarrow \lambda',\tau}^{\ell} (N_{\xi'}^{\text{jam}} - N_{\xi',\tau}) & \text{otherwise.} \end{cases} \quad (4.20)$$

If the residual storage capacity at the area level is sufficient, all candidate transition flows are accommodated. Otherwise, a demand-proportional supply distribution is applied, i.e.,

$$\eta_{\lambda \rightarrow \lambda',\tau}^{\ell} = \frac{Y_{\lambda \rightarrow \lambda',\tau}^{\ell}}{Y_{\xi',\tau}}. \quad (4.21)$$

If there is no storage capacity at the area level, it holds $N_{\xi'}^{\text{jam}} \rightarrow \infty$, and thus $G_{\lambda \rightarrow \lambda',\tau}^{\ell} \equiv Y_{\lambda \rightarrow \lambda',\tau}^{\ell}$. This is the case for the large class of fundamental diagrams that do not define a jam density (see Nikolić et al., 2015, for an overview).

For streams adjacent to origin/destination nodes, source and sink terms need to be included. The generation term for stream $\lambda : \nu_o^{\lambda} \rightarrow \nu_d^{\lambda}$ during time interval τ associated with pedestrian packet ℓ is expressed as

$$W_{\lambda,\tau}^{\ell} = \begin{cases} X_{\ell} & \text{if } \nu_o^{\lambda} = \nu_o^{\rho_{\ell}}, \tau = \tau_{\ell}, \\ -M_{\lambda,\tau}^{\ell} & \text{if } \nu_d^{\lambda} = \nu_d^{\rho_{\ell}}, \\ 0 & \text{otherwise.} \end{cases} \quad (4.22)$$

Source/sink areas are assumed to have infinite capacity. Newly added pedestrians that are unable to advance to a next stream are retained in their origin area until the pedestrian traffic situation allows them to do so. Pedestrians reaching their destination are immediately cleared out. If an exit capacity needs to be considered, this may be done by interposing an area with a corresponding static capacity.

Once the transition flows and generation terms defined in Eq. (4.20) and Eq. (4.22) are known, a flow balance equation allows to update the

accumulation of each pedestrian packet in every stream using the difference scheme

$$M_{\lambda,\tau+1}^{\ell} = M_{\lambda,\tau}^{\ell} + \sum_{\lambda' \in \Phi_{\lambda}^{\rho_{\ell}}} G_{\lambda' \rightarrow \lambda, \tau}^{\ell} - \sum_{\lambda'' \in \Theta_{\lambda}^{\rho_{\ell}}} G_{\lambda \rightarrow \lambda'', \tau}^{\ell} + W_{\lambda, \tau}^{\ell}. \quad (4.23)$$

If the demand and the initial state of the system, i.e., the fragment size of all pedestrian packets on all streams at $\tau = 0$, are known, the propagation of pedestrian packets along their routes can be computed by sequentially applying Eq. (4.23) to all packets $\ell \in \mathcal{L}$, streams $\lambda \in \Lambda$ and time intervals $\tau \in \mathcal{T}$.

Recursion (4.23) is independent of the processing order within a time interval, i.e., the order in which streams are updated does not have an influence on the dynamics of the model (Daganzo, 1994). Moreover, Eq. (4.23) guarantees the conservation of each packet and thus represents the discrete counterpart of the continuity equation that is used in fluid dynamics.

In summary, the proposed model requires four types of exogenous inputs. These are (i) the route flow demand in the form of the set of pedestrian packets \mathcal{L} , (ii) a network representation in the form of the set of streams Λ and their associated areas \mathcal{X} , (iii) a fundamental diagram, i.e., a possibly anisotropic density-speed relationship, and (iv) an en-route path choice model that provides the turning proportions at nodes. The first may be obtained by a demand estimation model, or by direct observation. The second is given by the infrastructure of interest. The third and fourth input are discussed in the following section.

4.4 Model specification

A specification of the stream-based pedestrian density-speed relationship and the turning proportions is provided in the following. Both iso- and anisotropic density-speed relationships are considered. A Java implementation of the resulting model specification is freely available (Hänseler and Lederrey, 2015).

4.4.1 Density-speed relationships

Isotropic specifications

One of the most widely used isotropic pedestrian density-speed relationships is that of Weidmann (1992), who defines the isotropic walking speed of any stream λ in area ξ as

$$v_\lambda = v_f \left\{ 1 - \exp \left[-\gamma \left(\frac{A_\xi}{N_\xi} - \frac{1}{k_{\text{jam}}} \right) \right] \right\}. \quad (4.24)$$

According to Weidmann (1992), the free-flow walking speed is estimated at $v_f = 1.34 \text{ m/s}$, the shape parameter at $\gamma = 1.913 \text{ m}^{-2}$, and the jam density at $k_{\text{jam}} = 5.4 \text{ m}^{-2}$. Specification (4.24) has been obtained from a literature review, trying to describe different settings using a single relationship. As such, it may not be the most realistic fundamental diagram for any specific flow configuration, but one that is comparably general and applicable in absence of anisotropy.

The critical stream accumulation M_λ^{crit} associated with Eq. (4.24) corresponds to the root finding problem

$$1 - \exp \left[-\gamma \left(\frac{A_\xi}{M_\lambda^{\text{crit}} + N'_{\lambda,\xi}} - \frac{1}{k_{\text{jam}}} \right) \right] \left(1 + \gamma \frac{M_\lambda^{\text{crit}} A_\xi}{(M_\lambda^{\text{crit}} + N'_{\lambda,\xi})^2} \right) = 0, \quad (4.25)$$

where the accumulation of all but the current stream λ in area ξ , $\lambda \in \Lambda_\xi$, is given by

$$N'_{\lambda,\xi} = \sum_{\substack{\lambda' \in \Lambda_\xi \\ \lambda' \neq \lambda}} M_{\lambda'}. \quad (4.26)$$

Eq. (4.25) is obtained by applying Eq. (4.9) to Eq. (4.24), i.e., by setting to zero the first derivative of the hydrodynamic flow with respect to the accumulation of the current stream.

An alternative is Drake's one-dimensional road traffic model (Drake et al., 1967), in which the speed of stream λ is given by

$$v_\lambda = v_f \exp \left(-\vartheta \left(\frac{N_\xi}{A_\xi} \right)^2 \right). \quad (4.27)$$

Based on Eq. (4.9), the critical accumulation of pedestrian stream $\lambda \in \Lambda_\xi$ associated with Eq. (4.27) can be expressed as

$$M_\lambda^{\text{crit}} = -\frac{N'_{\lambda,\xi}}{2} + \sqrt{\left(\frac{N'_{\lambda,\xi}}{2} \right)^2 + \frac{A_\xi^2}{2\vartheta}}. \quad (4.28)$$

As a benchmark for the assessment of fundamental diagrams, a ‘zero-model’ may additionally be considered, where the walking speed is constant over space and time and given by

$$v_\lambda = v_f. \quad (4.29)$$

For this specification, the critical stream accumulation is infinite, i.e., $M_\lambda^{\text{crit}} = \infty$, and no congested traffic regime exists.

Anisotropic specification

To demonstrate the anisotropic features of the model, we propose a stream-based pedestrian fundamental diagram (SbFD). It represents a generalization of the formulation by Wong et al. (2010) to multiple streams that interact in a pair-wise manner as described by Xie and Wong (2015). We however do not directly use Xie and Wong’s approach, as it requires solving a fixed-point problem, for which the existence and uniqueness of a solution are not a priori guaranteed.

Let $\phi_{\lambda,\lambda'}$ denote the intersection angle between streams λ and λ' with $\phi_{\lambda,\lambda'} = 0$ if $\lambda = \lambda'$, and let β and ϑ denote model parameters. We assume that the walking speed of stream $\lambda \in \Lambda_\xi$ is given by

$$v_\lambda = v_f \exp\left(-\vartheta \left(\frac{N_\xi}{A_\xi}\right)^2\right) \prod_{\lambda' \in \Lambda_\xi} \exp\left(-\beta(1 - \cos \phi_{\lambda,\lambda'}) \frac{M_{\lambda'}}{A_\xi}\right). \quad (4.30)$$

The critical stream accumulation associated with Eq. (4.30) is identical to that of Drake’s one-dimensional traffic model, Eq. (4.28), of which it represents an anisotropic generalization.

The first exponential term of Eq. (4.30) considers the isotropic reduction in walking speed induced by the overall accumulation in an area. A large value of ϑ implies a strong reduction in walking speed with increasing accumulation, and vice versa. The second term, i.e., the product of exponentials, represents the combined reduction in walking speed due to ‘friction’ with other pedestrian streams, depending on their density and the intersection angle. Similarly, a large value of β increases the magnitude of these anisotropic conflicting effects. Wong et al. (2010) estimate v_f at 1.034 m/s and ϑ at 0.075 m⁴, and Xie and Wong (2015) at 1.070 m/s and 0.065 m⁴, respectively. For β , no parameter estimates are available in

the literature. If it is set to zero, Drake’s isotropic fundamental diagram results. In Appendix B, some properties of Eq. (4.30) are discussed, and further explanation for the choice of the specification is provided.

For a rectangular space discretization, multi-directional flow is generally decomposed in 12 uni-directional streams connecting each pair of area edges. There are eight distinct directions to cross an area, namely left/right, up/down, and diagonally. In the subsequent case studies, accordingly there are up to eight directions of flow and up to 12 streams per area (see Fig. 4.8b).

We note that other, more advanced anisotropic formulations of pedestrian fundamental diagrams can be envisaged. In multi-directional pedestrian flow, different behavioral regimes are likely to exist. For instance, for the major stream, a leader-follower behavior may be predominant, while for the minor stream, collision avoidance is more important. Both of these mechanisms probably depend differently on the intersection angle. A case distinction for acute, right and obtuse angles may be beneficial. The exploration of such advanced specifications is left for future research.

4.4.2 Turning proportions

It is assumed that a potential field exists from which local turning proportions can be inferred. These turning proportions are traffic-dependent and route-specific (Guo et al., 2011). Each stream λ is assigned a potential $P_{\lambda,\tau}^\rho$ representing a generalized remaining distance along route ρ at traffic conditions as they are prevalent during time interval τ . For any stream λ that is not associated with route ρ , it is set to infinity.

In principle, various specifications including a linear attribution scheme may be used to deduce turning proportions from stream potentials. In the context of discrete choice theory (Ben-Akiva and Lerman, 1985), the potential of a stream may be interpreted as its ‘utility’. Using a logit-type model with weight μ , the turning proportion associated with the stream sequence $\lambda \rightarrow \lambda'$ and route ρ during time interval τ , with $\lambda' \in \Theta_\lambda^\rho$, can then be calculated by

$$\delta_{\lambda \rightarrow \lambda', \tau}^\rho = \frac{\exp(-\mu P_{\lambda', \tau}^\rho)}{\sum_{\lambda'' \in \Theta_\lambda^\rho} \exp(-\mu P_{\lambda'', \tau}^\rho)}. \quad (4.31)$$

Since the calculation of turning proportions only involves potentials of adjacent streams, the choice set does not overlap, and independence among

choice alternatives may be assumed.

Specification (4.31) assumes that pedestrians rely solely on instantaneous information to make their path-choice decisions. No predictive information is available to them, and travel cost to the respective destination is minimized in a reactive manner (Hoogendoorn and Bovy, 2004).

Two specifications of the stream potential are considered in the following. They are not meant to describe pedestrian route choice in all its details. For instance, they do not account for the influence of ambient conditions, signage or other factors like habit, physical effort, or herding. However, they are sufficient to illustrate the behavior and performance of the model, which is the primary aim.

Speed- and shortest path-based potential

Inspired by Hughes (2002) and Guo et al. (2011), we consider a potential that relies on a static floor field G_λ^ρ and a dynamic floor field $H_{\lambda,\tau}$. The route-specific static floor field G_λ^ρ is assumed to represent the remaining distance from stream λ along route ρ , i.e., the minimum walking length from and including stream λ to the end of route ρ (Dijkstra, 1959). By convention, the static floor field decreases along a route and reaches zero at the destination. The dynamic floor field $H_{\lambda,\tau}$ is assumed to be equal to the prevailing normalized walking speed $v_{\lambda,\tau}/v_f$ of stream λ during time interval τ . The rationale behind this choice is that pedestrians are expected to give preference to streams in which they can walk at velocities closer to the free-flow speed, similar to the concept of the desired velocity in the social force model (Helbing and Molnár, 1995).

Based on these floor fields, each stream may be assigned a route-specific, density-dependent potential

$$P_{\lambda,\tau}^\rho = \alpha G_\lambda^\rho - \beta H_{\lambda,\tau}, \quad (4.32)$$

where the parameters $\alpha, \beta \in \mathbb{R}^+$ denote weights that can assume any positive value. Both floor fields as well as the corresponding weights are non-dimensional. A large value of α means that pedestrians follow the shortest path corresponding to their route very closely. Similarly, a high value of β implies that pedestrians prefer less busy streams in which they can walk as fast as possible.

The provided specification considers the two aspects of getting to the destination on an ‘optimal path’ guided by a static floor field, yet avoiding

streams of high density that are penalized by the dynamic floor field. Full visibility with respect to the static floor field, and visibility of only the neighboring streams with respect to the dynamic floor field is assumed. In contrast to Hughes (2002), the aforementioned ‘optimal path’ is considered by the shortest path in space, instead of the shortest path in time. This explicitly allows reproducing queueing behavior, as people associated with the same route ‘pile up’ along a distinct path in case of congestion.

Fastest path-based potential

While Specification (4.32) is flexible due to its independent weighting of remaining distance and speed, in practice identifying these weights may be difficult. Thus, additionally a potential field based on the shortest path in time is considered, which only has a single weight. The potential $P_{\lambda,\tau}^{\rho}$ then represents the remaining walking time from and including stream λ at pedestrian traffic conditions as they are prevalent during time interval τ , i.e., the instantaneous remaining walking time from stream λ along route ρ to its destination.

A strict pursuit of the shortest path implies that pedestrians have no explicit queueing discipline. When passing a congested bottleneck, typically a semi-circle is formed upstream the entrance, instead of an orderly queue.

4.4.3 Calibration

A pseudo maximum likelihood framework is used for the model calibration (Besag, 1975; Gouieroux et al., 1984). The calibration is based on walking times, which are comparatively easy to observe, yield a robust parametrization, and are an important output of a network loading model. Previously, we have also investigated the use of other calibration measures, such as density and local flows, or a combination thereof (Hänseler et al., 2014a). The results have shown that a calibration based on travel times alone yields an accurate parametrization, and greatly simplifies the estimation process as compared to a multi-objective optimization problem. Besides, for some of the case studies analyzed in the following, only demand and walking time data are available anyway.

In the following, it is assumed that for each pedestrian i , the route ρ_i ,

the departure time t_i^{dep} and the walking time tt_i are known by observation without measurement error. The observed walking time tt_i^{obs} of pedestrian i is considered as a draw from a random variable $\mathbb{T}_i^{\text{obs}}$, whose distribution f_i^{obs} is unknown. In practice, knowledge of that distribution is not available, except if the same experiment is run multiple times (Kretz et al., 2006).

Let $f_i^{\text{est}}(tt|\mathbf{X}, \boldsymbol{\theta})$ denote the walking time probability density of pedestrian i that is generated by the model for a demand \mathbf{X} and a set of parameters $\boldsymbol{\theta}$. It is given by the walking time distribution of the corresponding pedestrian packet $\ell(i)$, with $t_i^{\text{dep}} \in \tau_\ell$ and $\rho_i = \rho_\ell$.

The pseudo log-likelihood to reproduce the walking time vector $\mathbf{tt}_{\text{obs}} = [tt_i^{\text{obs}}]$ for a sample of n pedestrians can then be expressed as

$$\tilde{\mathcal{L}}(\mathbf{tt}_{\text{obs}}|\mathbf{X}, \boldsymbol{\theta}) = \sum_{i=1}^n \log (f_i^{\text{est}}(tt_i^{\text{obs}}|\mathbf{X}, \boldsymbol{\theta})). \quad (4.33)$$

The objective of the calibration is to find a parametrization $\boldsymbol{\theta}$ such that the pseudo likelihood of reproducing the observed walking times is maximized, i.e.,

$$\hat{\boldsymbol{\theta}} = \arg \max \tilde{\mathcal{L}}(\mathbf{tt}_{\text{obs}}|\mathbf{X}, \boldsymbol{\theta}). \quad (4.34)$$

Eq. (4.34) is referred to as the pseudo maximum likelihood estimator. It differs from the actual maximum likelihood estimator in that any correlation between measurements is neglected. There are generally two sources of correlation, namely serial and spatial. Serial correlation is mostly an issue if multiple measurements of the same pedestrian are considered. This is not the case here, since only one walking time estimate per person is available. Spatial correlation occurs if observations are dependent across pedestrians. Such clustering is indeed present in that several pedestrians may be associated with the same pedestrian packet, and thus be described by the same estimated walking time distribution. This leads to an artificial weighting of these distribution terms, which the pseudo likelihood does not account for.

With decreasing packet sizes, the clustering effect vanishes. By changing the space discretization, the time discretization changes through Eq. (4.6), and indirectly the packet sizes can be influenced. In the case studies described in the next section, the discretization is such that a large majority of packets contain at most two or three pedestrians, and are of similar size. We have tested different discretizations and found only a very small influence

on the estimates (Lederrey, 2015). At least if packets are small, the role of spatial correlation seems to be negligible, and the maximization of the pseudo likelihood defined in Eq. (4.33) provides a consistent estimate of the parameters. If large packets are present, other estimation techniques such as indirect inference may be more appropriate (Gourieroux et al., 1993).

Even if it is unbiased, the pseudo likelihood estimator is less efficient than the actual maximum likelihood estimator. Standard techniques for statistical inference need in principle to be adapted for use in a pseudo likelihood setting. Specifically, the Cramér-Rao bound is generally not reached, and the standard likelihood-ratio test does not apply, as the asymptotic distribution of the differences in pseudo log-likelihoods is not χ^2 -distributed (Dodge, 2006). Following Hoogendoorn and Daamen (2007), and taking into account the negligible role of clustering in the considered case studies, we still provide standard variance estimates. We note however that their significance in a pseudo likelihood framework is limited, and refer to the literature for generalized approaches that should be used if pedestrian packets are large (Bai, 1999; Moreira, 2003). To assess the goodness-of-fit of a specification, the Akaike information criterion (AIC) based on the pseudo likelihood is reported. We have also computed the Bayesian information criterion (BIC), and found that it agrees with the AIC on the preferred model for each of the studied cases.

To solve Eq. (4.34), any globally convergent optimization method such as simulated annealing or trust-region methods may be used (Kirkpatrick et al., 1983; Powell, 2009).

4.5 Isotropic case studies

Two isotropic case studies are investigated, one involving multi-directional flows at low density studied at the example of Lausanne railway station, and one considering a uni-directional bottleneck experiment conducted in the Netherlands. As model specification, the density-speed relationship proposed by Weidmann (1992), Eq. (4.24), in combination with the speed- and shortest path-based en-route path choice model, Eq. (4.32), is used. The aim of these case studies is to establish the validity of the proposed macroscopic model as such. In the next section, by means of two anisotropic case studies, the performance of the various model specifications is inves-

tigated and compared.

In the following analysis, a calibration routine different from that described in Section 4.4.3 has been used. Instead of relying on a likelihood framework, a least squares approach based on mean walking times has been used, which is computationally less efficient and statistically less rigorous. Having said this, no significant difference between the two calibration methods is expected, which is why no re-calibration using likelihood estimation has been performed. The reader interested in further details is referred to the original publication (Hänseler et al., 2014a).

The performance of the isotropic specification is evaluated with respect to predictions of walking times and density levels. The obtained results are compared with the ground truth that is available from tracking data. Moreover, for the case study of Lausanne railway station, the model is additionally compared to Viswalk (PTV, 2013, Version 5.40) that implements the social force model (SFM; Helbing and Molnár, 1995), representing the current state-of-the-art in microscopic modeling of walking behavior.

4.5.1 Lausanne railway station

The investigated site in Lausanne railway station comprises the pedestrian underpass West (PU West) with an area of approximately 685 m² (Fig. 4.2).

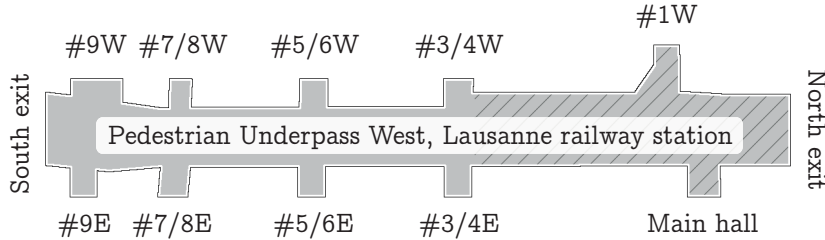


Figure 4.2: PU West of Lausanne railway station.

PU West is discretized into 93 square areas with an edge length of $\Delta L = 2.7$ m. A potential influence of the space discretization on model dynamics has been investigated, but has been found negligible as long as the size of areas remains in the same order of magnitude.

For the calibration of the model, the north side of PU West (shaded area in Fig. 4.2) is considered. Pedestrian tracking data collected in the time period between 07:32 and 07:57 on April 9, 10, 18 and 30, 2013 is available. A further data set, collected on January 22 of the same year, is considered

for validation. While for the calibration only the North part of PU West is considered, for the validation the complete pedestrian underpass is analyzed. The validation concentrates on the peak period between 7:40 and 7:45, representing the busiest time interval of the day. Table 4.1 shows the obtained parameter estimates. These are in agreement with values reported by Weidmann (1992), particularly as far as the shape parameter ($\gamma = 1.95 \text{ m}^{-2}$ vs. 1.913 m^{-2}) and the jam density ($k_{\text{jam}} = 5.88 \text{ m}^{-2}$ vs. 5.4 m^{-2}) are concerned. The free-flow speed is slightly lower ($v_f = 1.22 \text{ m/s}$ vs. 1.34 m/s), but the difference amounts to less than 10%. The resulting parametrization of the weights of the en-route path choice model is discussed in Section 4.7.

Table 4.1: Calibration of isotropic case studies.

	v_f [m/s]	γ [m^{-2}]	k_c [m^{-2}]	α [-]	β [-]
Weidmann (1992)	1.34	1.913	5.4	–	–
Lausanne railway station	1.22	1.95	5.88	2.08	2.55
Dutch bottleneck experiment	1.76	1.77	5.47	4.50	0.05

For the comparison with the social force model, default parameters of Viswalk are used, which are based on a calibration performed by Johansson et al. (2007). Pedestrian demand is aggregated in 60-second periods for Viswalk due to the lack of a suitable mechanism for using a disaggregate origin-destination demand table as input. To account for stochasticity, five simulation runs are performed and averaged. More runs are not necessary, since only aggregated output is reported, which shows little fluctuation across runs. For both the proposed macroscopic model and the microscopic social force model, the time period between 07:37 and 07:47 is computed, but only results for the period between 07:40 and 07:45 are reported in order to remove a bias of an initially empty system.

Fig. 4.3 provides a comparison of route-specific walking times with a temporal aggregation of 60 s. The resulting mean values are shown in a histogram with a bin size of 5 s. The proposed model overestimates the occurrence of long walking times, but otherwise shows a reasonable agreement with trajectory data. The social force model seems to overestimate small walking times and to underestimate the most frequently observed walking times in the range between 35 and 55 s. Overall, the agreement

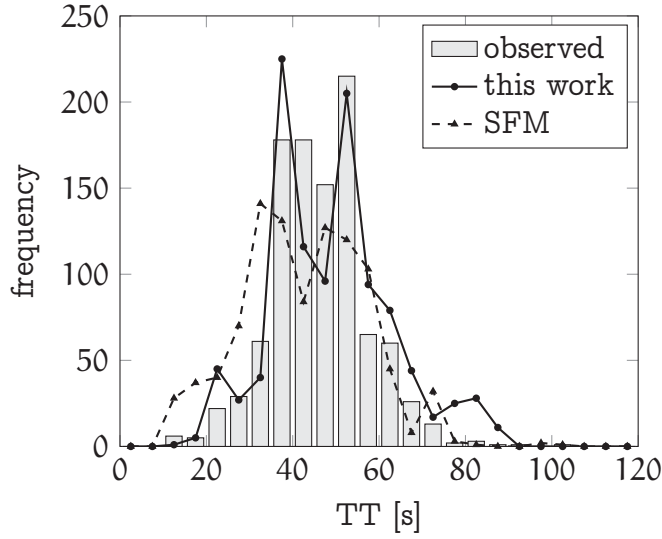


Figure 4.3: Walking time distribution for PU West.

between the proposed model and trajectory data is better than for the social force model if the L^2 -norm is considered (114.4 vs. 181.6 s). Fig. 5.7 in Section 5 additionally provides a comparison of walking times with a finer discretization, underlining the good agreement between measurement and model. In that section, also the ability of the proposed model to reproduce density maps is investigated, concluding that the predictive power in terms of densities is also satisfactory (see Hänseler et al., 2014a, for a comparison to the social force model).

Another way of illustrating the model accuracy is by means of a scatter plot of walking times. Fig. 4.4 shows observed versus predicted walking times in PU West, again aggregated by routes and 60 s-intervals.

A majority of the walking time-pairs come to lie close to the 45° best-fit line (dashed curve in Fig. 4.4). Specifically, for 74% of all observations, the relative error amounts to less than 25%. For around 15% of all observations, the proposed model underestimates the walking time by more than 25% (see observations in the lower right half of Fig. 4.4). A reason for this discrepancy is non-walking behavior of pedestrians, such as waiting or purchasing a ticket. These activities are not considered by the pedestrian walking model. Similarly, the proposed model fails at predicting very short walking times corresponding to average velocities that are higher than the free-flow speed.

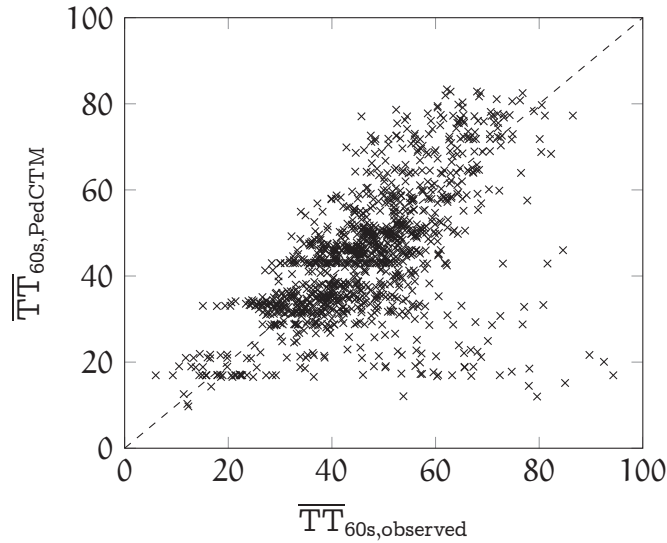


Figure 4.4: Walking time scatter plot for PU West (60 s aggregation; RMSE = 13.37, MAPE = 19.03%).

4.5.2 Bottleneck experiment

To assess the ability of the model to predict traffic-dependent variations in walking times, a congested, uni-directional scenario is considered. Daamen and Hoogendoorn (2003) have performed various controlled walking experiments, including a bottleneck experiment in which saturated flow conditions are reached. Their test site consists of a 10 m long corridor with a width of 4 m, that is reduced to 1 m after a length of 5 m. Fig. 4.5 depicts the studied layout, in which pedestrians are walking from left to right, i.e., from the wide side of the corridor to the small side.

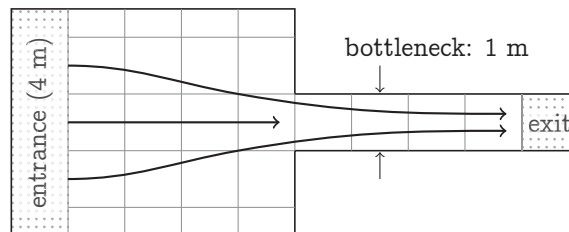


Figure 4.5: Experimental set-up used by Daamen and Hoogendoorn (2003) to study the pedestrian flow through a bottleneck.

During the course of the experiment, which takes about 15 min, the in-

flow is successively increased until a highly congested situation is reached, and then again decreased. A total of about 80 pedestrians of both genders and different age are available for the experiment. Due to its long duration, pedestrians re-enter the corridor multiple times, following a frequency determined by a pedestrian traffic light. For a detailed description of the case study, the reader is referred to Daamen and Hoogendoorn (2003).

Upstream of the bottleneck, the formation of a funnel is reported, i.e., pedestrians anticipate the narrowing of the corridor as indicated by the sample trajectories in Fig. 4.5. This stands in contrast to some studies in which the formation of a half-circle around the bottleneck entrance is found (Helbing et al., 2001), or the full width of the corridor is used (Tajima et al., 2001). This anticipatory behavior may be due to the character of the experiment. The repeated crossing of the same corridor leads to a high familiarization with the setting, and presumably to a joint optimization of the flow.

For the proposed macroscopic model, the walkable space is discretized into square areas with a length of $\Delta L = 1$ m. In the wide part of the corridor, on each side four half areas are present (Fig. 4.5). Due to the symmetry of the layout, these eight half-areas may be considered as four communicating square areas, i.e., the half-areas are pair-wise merged such that in each case one regular area results that is connected to all their joint neighbors.

For the calibration, only trajectory recordings from the first half of the experiment are used, keeping the remaining ones for validation. The obtained parameter set is shown in Table 4.1. While the shape parameter ($\gamma = 1.77 \text{ m}^{-2}$) and the jam density ($k_{\text{jam}} = 5.47 \text{ m}^{-2}$) are again close to the values of Weidmann (1992), the estimate of free-flow speed ($v_f = 1.76 \text{ m/s}$) is significantly higher. Fig. 4.6 shows the corresponding walking time scatter plot, where a temporal aggregation of $\Delta t = L/v_f = 0.57$ s is used (aggregation by pedestrian packets). Data points used for calibration and validation are shown separately.

A variation in walking time by a factor of 5, from 5 s to 25 s, is discernible. Since there is only a single route, this variation is solely caused by changing traffic conditions. For a large majority of data points, the proposed model is capable of reproducing traffic-induced delays in walking times relatively well. The relative error is smaller than 25% in 75% of all cases. For some pedestrian packets, the walking time is overestimated (up-

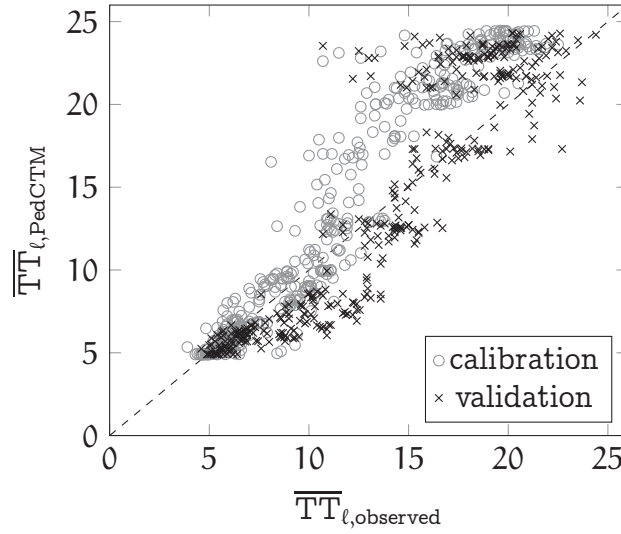


Figure 4.6: Walking time scatter plot for the Dutch bottleneck experiment (aggregation: $\Delta t = 0.57$ s; $\text{RMSE}_{\text{valid}} = 3.15$, $\text{MAPE}_{\text{valid}} = 17.67\%$).

per left half of the plane). This may represent people that are particularly good at avoiding the queue, e.g. by joining it laterally at the tip and thus by overtaking other pedestrians.

4.6 Anisotropic case studies

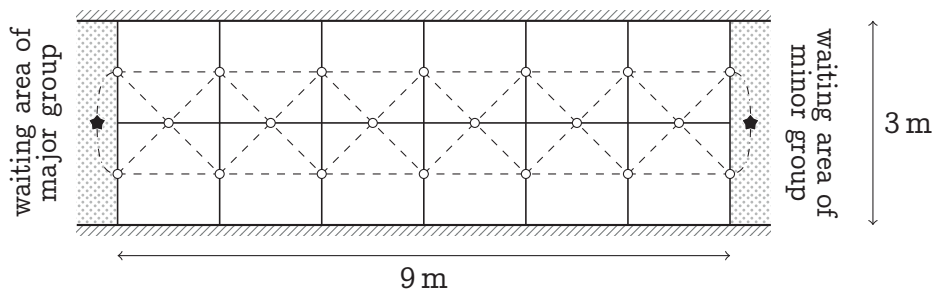
To study the model behavior in case of anisotropy, two multi-directional, congested case studies are considered. One is based on a set of pedestrian counter-flow experiments conducted in Hong Kong, China, and one on a pedestrian cross-flow experiment in Berlin, Germany. The first is particularly useful in that it explores a large range of pedestrian traffic conditions, and the second in that it considers the walking behavior of a typical student population in their daily environment. The focus here is on the performance of the various density-speed relationships, which is investigated in combination with the fastest path-based floor field, representing the simpler of the two specifications for the computation of the turning proportions.

4.6.1 Counter-flow experiments

Wong et al. (2010) provide a set of 89 controlled experiments in which two pedestrian groups of varying size intersect at different angles. These experiments were carried out in a sports hall in Hong Kong, and video footage is available. Among the set of experiments, those with high densities and an intersection angle of 180° yield the highest level of anisotropy (Wong et al., 2010). Table 4.2 provides a list of the corresponding experiments, and Fig. 4.7 describes the 3 m wide and 9 m long walking corridor for the controlled experiments.



(a) Sample image extracted from experiment #85



(b) Walkway configuration

Figure 4.7: Experimental setup of counter-flow experiments (Wong et al., 2010).

Each experiment is conducted once and lasts about 1 min. Pedestrians associated with the major group wear blue hats, and those associated with the minor group wear green hats. Due to a flat viewing angle and high density, no automatic data processing is feasible. Instead, we have manually extracted the departure and walking time of each pedestrian in the six experiments of interest. The ratio of the pedestrian group sizes varies from approximately 10:0, 9:1, 8:2, 7:3, 6:4 to 5:5, of which the first and last experiment yield isotropic flows.

Table 4.2: Observed walking speeds in counter-flow experiments.

Exp.	major group		minor group	
#84	87 ped	1.08 ± 0.15 m/s	–	–
#85	79	1.19 ± 0.13	9 ped	0.80 ± 0.14 m/s
#86	68	0.90 ± 0.10	18	0.74 ± 0.15
#87	61	0.82 ± 0.06	26	0.67 ± 0.10
#88	53	0.83 ± 0.09	30	0.79 ± 0.15
#89	44	0.79 ± 0.10	44	0.79 ± 0.18

To evaluate the proposed model specifications, they are calibrated on two experiments, and cross-validated on the remaining ones. We have tested different compositions and sizes of the training and validation sets, but the results do not change significantly. Importantly, the training set should contain experiments with anisotropic walking behavior. In the following, experiments #85 and #87 are used for calibration, and experiments #84, 86, 88 and 89 for validation. Table 4.3 shows the obtained parameter values and the corresponding AIC values for four different density-speed relationships. The number of observations available for each experiment corresponds to the number of pedestrians involved, and is indicated in brackets. The number of estimation parameters is two, three, four and four for the Zero-, Drake-, Weidmann and SbFD-model, respectively.

Table 4.3: Results of calibration and validation on counter-flow experiments.

	Zero-Model	Drake	SbFD	Weidmann
$AIC_{85,87}^{\text{calib}}$ (175 obs.)	837.7	754.0	704.5	729.4
v_f [m/s]	1.166 ± 0.001	1.170 ± 0.001	1.115 ± 0.000	1.169 ± 0.001
μ [-]	1.43 ± 0.06	12.15 ± 0.29	10.18 ± 2.02	14.84 ± 0.30
ϑ [m ⁴]		0.078 ± 0.000	0.001 ± 0.004	
β [m ²]			0.210 ± 0.005	
γ [m ⁻²]				4.92 ± 0.20
k_{jam} [m ⁻²]				6.58 ± 0.46
AIC_{84}^{valid} (87 obs.)	355.2	338.4	311.4	348.2
AIC_{86}^{valid} (86 obs.)	381.7	371.3	355.3	401.4
AIC_{88}^{valid} (83 obs.)	400.3	384.6	364.0	435.3
AIC_{89}^{valid} (88 obs.)	458.2	408.8	396.8	454.6

The stream-based pedestrian fundamental diagram (SbFD) reaches a better AIC value than the two other fundamental diagrams (Weidmann, Drake), both as far as the training set and the validation experiments are concerned. Interestingly, this not only holds for the anisotropic experiments (#86, #88), but also for the uni-directional pedestrian flow experiment (#84) and that with equal flow shares (#89). A look at the mean walking times for the major and minor pedestrian groups in each experiment corroborates that finding (see Table 4.4). The SbFD-model is able to estimate walking times that are closer to the ones observed, in particular for the minor group. This can also be seen from the significant reduction in the squared error reported at the bottom of Table 4.4.

Table 4.4: Walking times for counter-flow validation experiments.

Exp.	Groups	tt _{obs} [s]	tt _{zero} [s]	tt _{Drake} [s]	tt _{SbFD} [s]	tt _{Weidmann} [s]
#84	87 / 0	8.5 / -	9.5 / -	9.1 / -	8.1 / -	8.3 / -
#86	68 / 18	10.1 / 12.7	9.5 / 9.5	10.0 / 10.8	9.4 / 12.5	8.8 / 9.5
#88	53 / 31	10.9 / 11.8	9.5 / 9.5	10.0 / 10.6	10.3 / 11.7	8.9 / 9.2
#89	44 / 44	11.8 / 11.6	9.5 / 9.5	11.6 / 11.4	11.7 / 11.6	9.7 / 9.9
L ² -error (weighted, [s])			21.4 / 23.4	9.0 / 10.5	7.9 / 0.7	22.3 / 23.3

In Table 4.3, the obtained estimates for the free-flow walking speed vary between 1.115 m/s and 1.170 m/s with generally small errors. For the same parameter, Wong et al. (2010) report a value of 1.034 m/s, which is slightly lower. With the exception of the result for the zero-model ($\mu = 1.43$), the values obtained for the path choice parameter μ lie in the range between 10 and 15, which is relatively high as a comparison to the second case study will show. A high value implies that pedestrians tend to stick to the fastest path, which in an experiment like this is expected. A low value on the other hand leads to dispersion, which explains the low estimate obtained by the zero-model. Dispersion is the only way for the zero-model to reproduce a distribution of walking times for a given route, since it does not take into account any density-speed interaction.

The remaining parameters shown in Table 4.3 are in line with the literature, too. For the Drake-model, the obtained value of ϑ (0.078 m⁴) is in good agreement with previous estimates by Wong et al. (2010) and Xie and Wong (2015), reporting 0.075 m⁴ and 0.065 m⁴, respectively. The

same parameter estimate for SbFD is significantly lower ($\vartheta = 0.001 \text{ m}^4$) since a significant reduction in walking speed at high densities is explained by the friction with opposing pedestrian streams instead. This effect is quantified by the parameter β , for which no comparison to the literature exists. Regarding the Weidmann-specification, the values obtained for the jam density and shape parameter, $k_{\text{jam}} = 6.58 \text{ m}^{-2}$ and $\gamma = 4.92 \text{ m}^{-2}$, are high compared to a European context, for which values of $k_{\text{jam}} = 5.4 \text{ m}^{-2}$ and $\gamma = 1.913 \text{ m}^{-2}$ are reported (Weidmann, 1992). In the Hong Kong experiment, pedestrians are apparently particularly tolerant towards high densities, reducing their walking speed less with increasing density. This is in line with observations from the video footage, and with observations from previous researchers investigating differences in fundamental diagrams across countries (Chattaraj et al., 2009).

4.6.2 Cross-flow experiment

Plaue et al. (2014) present a multi-directional pedestrian flow experiment conducted in the entrance hall of a university building at TU Berlin, Germany. Unlike in the previous example, pedestrians are not confined to a pre-defined corridor, and not ‘conditioned’ from foregoing experiments. The observed population consists primarily of students, of which many carry backpacks, musical instruments, or wear heavy winter clothing. The setting is video-recorded using three networked cameras, and trajectories of pedestrians are extracted using a semi-automatic photogrammetric method.

In total, 142 pedestrians traverse the hall from left to right, and 83 pedestrians from top to bottom (see Fig. 4.8). They intersect at an angle of roughly 90° in a region of about 25 m^2 . According to Plaue et al. (2014), the maximum density amounts to 5 ped/m^2 and the duration of the experiment is 69 s. Fig. 4.8 shows a sample image of the experimental environment, as well as of the modeling configuration of the walking area concerned. As can be seen from Fig. 4.8b, the various entrance and exit zones are modeled by six origin/destination nodes. Local obstacles, namely the two supporting columns, are considered by an according reduction of the surface size of the affected areas.

The various model parameters are calibrated on the full data set (see Table 4.5). The number of observations corresponds to 225 measurements of walking times. Considering the decrease in the AIC value as compared to

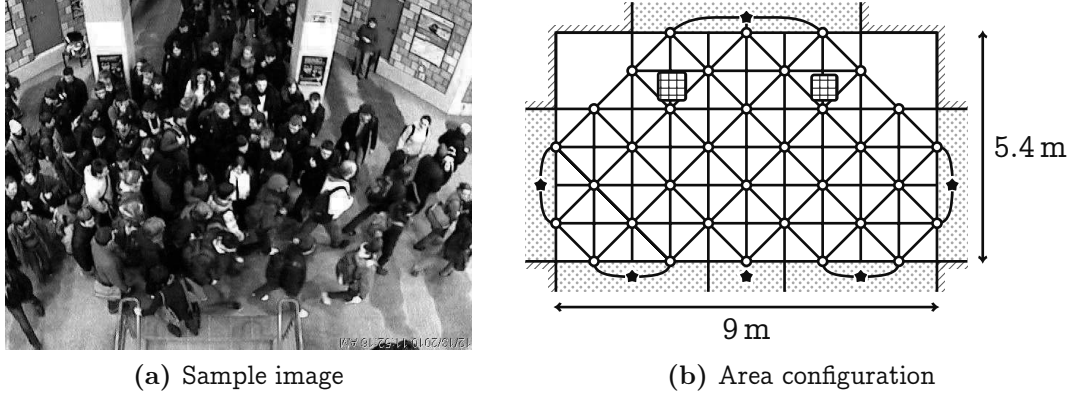


Figure 4.8: Setting of cross-flow experiment at TU Berlin (Plaue et al., 2014).

the zero-model, all ‘non-trivial’ fundamental diagrams represent improvements, with the anisotropic SbFD having the lowest AIC value overall.

Table 4.5: Results of calibration on cross-flow experiment.

	Zero-Model	Drake	SbFD	Weidmann
AIC	1160.0	1101.0	1062.6	1098.8
v_f [m/s]	1.307 ± 0.005	1.308 ± 0.001	1.308 ± 0.006	1.332 ± 0.002
μ [-]	1.16 ± 0.03	1.39 ± 0.02	2.64 ± 0.41	2.05 ± 0.20
ϑ [m ⁴]		0.139 ± 0.004	0.143 ± 0.004	
β [m ²]			0.300 ± 0.008	
γ [m ⁻²]				1.76 ± 0.15
k_{jam} [m ⁻²]				5.99 ± 0.61

The parameter estimates shown in Table 4.5 are in agreement with intuitive expectations. The free-flow walking speeds are estimated between 1.307 m/s and 1.332 m/s, which is similar to previous studies from Europe (e.g. 1.34 m/s according to Weidmann, 1992). The path choice parameter lies in the range between 1.16 and 2.64, which is significantly lower than that in the Hong Kong experiments. Pedestrians seem more willing to deviate from the fastest path, for instance to avoid zones of high density. The entrance hall at TU Berlin leaves more room for such deviations than the narrow corridor used in the Hong Kong experiments. The values obtained for the remaining parameters are comparable to the ones found in the pre-

vious case study. The sensitivity to density is however larger, as can be seen from the higher values of ϑ and β , as well as the lower values of γ and k_{jam} . Besides differences in the experimental conditions, this is likely due to the larger physique of Europeans and their lower tolerance to invasion of space (Lam et al., 2002).

Of all parameters, the path choice parameter μ has the largest relative standard deviation from the mean, referred to as the coefficient of variation (CoV). For SbFD, the CoV of μ corresponds to 15.6%. In turn, the relative standard deviation of the free-flow walking speed v_f is the lowest with a CoV of 0.5%. This is in agreement with our experience, according to which identifying the optimal value of v_f is relatively easy, whereas the calibration of μ takes more computational time.

As for the isotropic case studies, walking time estimates are considered. Fig. 4.9 provides a scatter plot, comparing the observed walking time of pedestrian i , tt_i^{obs} , to the estimated walking time distribution of the corresponding pedestrian packet $\ell(i)$, as approximated by the mean $\overline{tt}_{\ell(i)}^{\text{est}}$ (denoted by circles) and the standard deviation (error bars). For visual guidance, a 45°-reference line (dashed), as well as two isolines (dotted) representing a deviation of $\Delta t = \pm 5$ s are shown. In the figure captions, the squared error is given for each specification.

As expected, the zero-model (Fig. 4.9a) cannot reproduce the full range of observed walking times, as they are simply proportional to the walked path lengths. This can be seen by the horizontal ‘stripes’ that appear in the scatter plot. Similarly, the Drake-specification (Fig. 4.9b) predicts walking times that are confined to a relatively narrow band that does not represent the bandwidth observed in reality. The Weidmann-specification (Fig. 4.9c) is able to reproduce the full width, but with such significant scattering that no improvement in the squared error as compared to the Drake-model is achieved. The SbFD-specification (Fig. 4.9d) finally is able to reproduce the observed width, and the squared error is significantly reduced. The spreading is narrower than that for Weidmann, and the estimated walking time distributions come to lie closer to the 45°-reference line. Nevertheless, the remaining scatter is still substantial. The observed stochasticity is likely due to individual differences in walking behavior in presence of congestion, ranging from a pro-active ‘sneaking through’ to a more passive ‘waiting for a gap’, which may cause a large prediction uncertainty.

In relation to these scatter plots, Table 4.6 summarizes both the ob-

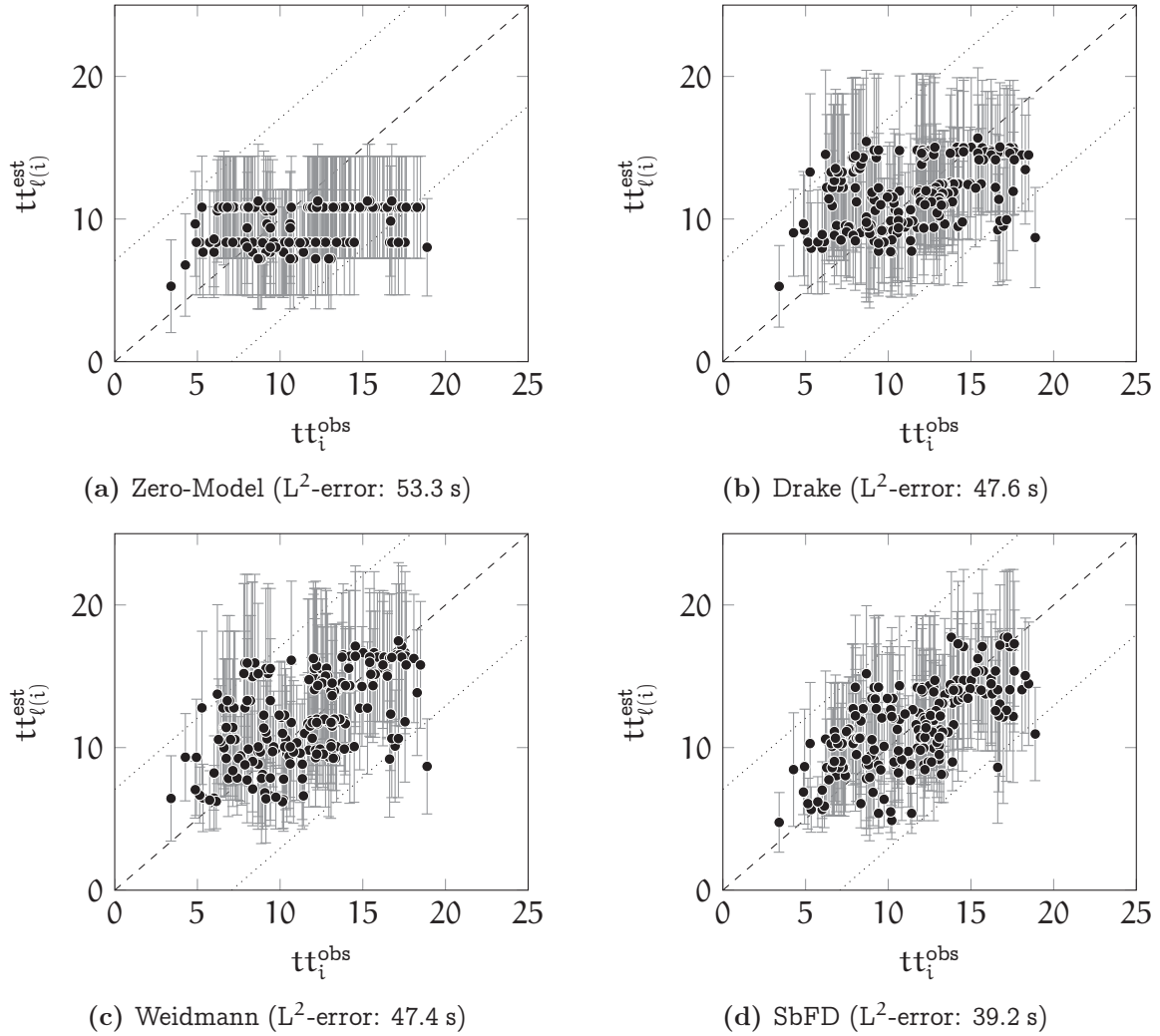


Figure 4.9: Scatter plot of walking times for Berlin case study.

served and estimated aggregate walking times for the two most frequently used routes. Route ‘W \rightarrow E’ (left to right) carries the major pedestrian flow, and has a length of 9 m. Route ‘N \rightarrow SE/SW’ (top to lateral nodes at the bottom) carries the minor pedestrian flow, and is approximately 7 m long. The observed average walking speed of the major stream amounts to 0.72 m/s (= 9 m/12.4 s), whereas for the minor stream a walking speed of 0.66 m/s (= 7 m/10.6 s) is observed, i.e., anisotropy is clearly present. This anisotropy is not reproduced by neither the Drake- nor the Weidmann-based specification, which both overestimate the walking time of the major

stream, and underestimate the walking time of the minor stream. The stream-based fundamental diagram (SbFD), however, yields walking time estimates with errors of 1.8% and 2.2% only. This shows that the explicit consideration of anisotropy for estimating the walking times is not only highly beneficial at the disaggregate, but also at the aggregate level.

Table 4.6: Aggregate route walking times for Berlin case study.

	n_{ped}	tt_{obs} [s]	tt_{Zero} [s]	tt_{Weidmann} [s]	tt_{Drake} [s]	tt_{SbFD} [s]
W → E (9 m)	118	12.4 (base)	10.8 (-12.7%)	14.0 (+12.6%)	13.3 (+7.2%)	12.6 (+1.8%)
N → SE/SW (7 m)	46	10.6 (base)	8.4 (-21.3%)	9.9 (-6.8%)	10.0 (-6.2%)	10.9 (+2.2%)

4.7 Discussion

The obtained parameter sets are generally consistent across the investigated case studies, or the differences well understood. In terms of the density-speed relationships, the highest free-flow speed of 1.76 m/s is obtained for the bottleneck flow experiment, whereas the lowest estimate of approximately 1.12 m/s results for the counter-flow experiments from Hong Kong. The estimates for Lausanne railway station (1.22 m/s) and the Berlin cross-flow experiment (1.31 m/s) are in between. This discrepancy is due to differences in the experimental conditions, as well as differences in the physique of participants. Specifically, the high value obtained for the Dutch bottleneck experiment may be due to the distinct start signal in the form of a traffic light that likely provokes a fast motion, whereas the relatively low speeds measured in Hong Kong may be due to a smaller average body size. In return, the sensitivity of walking speed with respect to density is relatively small in Hong Kong as compared to Berlin, which can be explained by differences in personal space (Lam et al., 2002; Chattaraj et al., 2009).

As far as the jam density in Weidmann's fundamental diagram is concerned (5.4 ped/m² according to Weidmann, 1992), some differences can be observed as well. The values estimated for the European case studies fall in the range between 5.47 ped/m² (Dutch bottleneck experiment) and 5.99 ped/m² (Berlin cross-flow experiment), with a value of 5.86 ped/m² obtained for Lausanne railway station. The jam density obtained for the Hong Kong counter-flow experiments amounts to 6.58 ped/m², which is sig-

nificantly higher. Cultural differences, as well as a lower average body size, seem again the most probable causes.

In terms of the parametrization of the en-route path choice model, differences between the iso- and anisotropic case studies are difficult to assess due to the varying specification of the floor field. However, remarkable differences within each pair of experiments exist. With respect to the anisotropic experiments, it has already been noted that the participants of the Hong Kong counter-flow experiment show a distinct shortest path-behavior, which is not the case for the Berlin experiment. Related to the isotropic experiments, Fig. 4.10 shows the quasi-stationary density distribution obtained for an artificial bottleneck experiment that is useful to illustrate the differences in the specification.

The shown corridor has a length of 22 areas and a width of 6 areas, which at the bottleneck is reduced to two areas. During 100 time steps, the corridor is loaded with a continuous inflow that corresponds to the amount of pedestrians that can be contained by an area at jam density, $\chi = A_\xi k_{\text{jam}}$. The shown density maps correspond to the time step $\tau = 200$, i.e., they are taken 100 time steps after the continuous inflow has stopped. At this stage, pedestrians gradually propagate downstream, but the dynamics of the model are relatively slow.

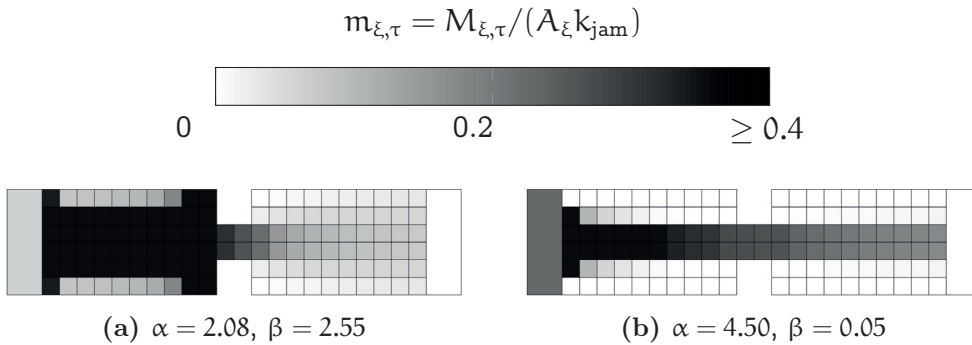


Figure 4.10: Flow patterns in a corridor with bottleneck.

Fig. 4.10a shows the density distribution that is obtained for the Lausanne parametrization. Pedestrians take both the distance to destination and local traffic conditions into account for local path choice. Upstream of the bottleneck, all space is occupied. People act as if they were impatient to pass the bottleneck, which is why a broad zone of high density builds up in front of the bottleneck. At time step $\tau = 200$, 47.9% of all

pedestrians have arrived at the destination. Fig. 4.10b shows the density distribution that results if the weights of the floor field are replaced by those obtained from the Dutch bottleneck experiment. Pedestrians walk along paths that ‘anticipate’ the bottleneck. Only a fraction of space is occupied, mostly along the shortest path. Slightly more pedestrians than in the previous case have reached the destination at $\tau = 200$, namely 48.6%. This is the result of a high queueing discipline that manifests itself in the form of a funnel. While the predicted behavior in the two cases is fundamentally different, it is in good agreement with the respective observations (Daamen and Hoogendoorn, 2003; Lavadinho, 2012). The resulting density distribution of two further cases, namely for a strict shortest path and a Brownian diffusion case, may be found in the literature (Hänseler et al., 2014a).

The successful calibration of both the fundamental diagrams and the en-route path choice model is particularly encouraging since only the pedestrian demand and walking times are required, while typically their estimation necessitates measurements of density and speed. For the calibration of multi-directional fundamental diagrams, usually even trajectory data is required, which is expensive to collect.

Besides the parameters, also the model outputs, in particular walking times, are in agreement with empirical observations. While the ‘goodness’ of this agreement is hard to define, the comparison with the social force model done at the example of Lausanne railway station shows that the accuracy of the proposed model is equal if not superior in the case considered. With respect to the anisotropic extension of the model, the investigated values of walking times and AIC consistently favor the stream-based formulation of the pedestrian fundamental diagram, suggesting that this approach significantly improves the quality of the model.

A further strength of the proposed model is its computational performance. On a standard desktop machine, the anisotropic pedestrian flows occurring in the Berlin case study can be computed for a given parameter set in about one second, which is almost 100 times faster than real-time. In contrast, commercial microscopic simulators operate typically at the speed of real-time only.

Besides its accuracy and computational efficiency, a further advantage of the proposed model is its relative ease of calibration, and the physical interpretation of parameters it allows for. In particular, this facilitates the trans-

ferability of parameters from one case study to another. If the proposed model is to be used for practical applications based on the parametrization obtained in this thesis, we suggest to use the specification obtained from the Lausanne case study, representing a real-world example. The resulting isotropic fundamental diagram is shown in Fig. 5.5b in Chapter 5. In case multi-directional flows at high density are present, anisotropy is likely to occur, and instead the parametrization obtained from the Berlin case study may be used. The corresponding specification of the stream-based pedestrian fundamental diagram is illustrated by Fig. 4.11.

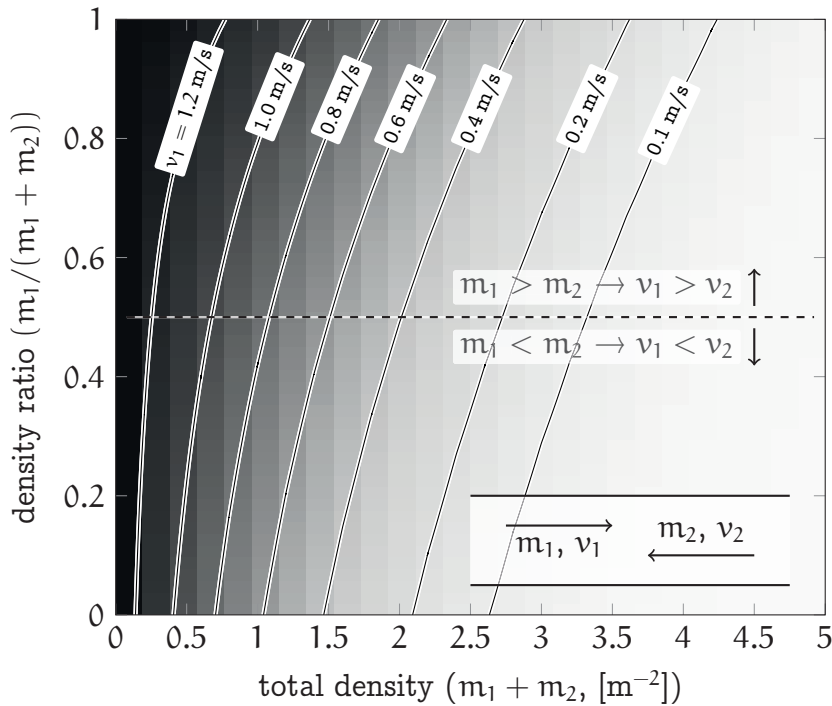


Figure 4.11: Walking speed for bi-directional flow (SbFD, Berlin data).

The contour plot in Fig. 4.11 shows the expected walking speeds in a counter-flow scenario for various total densities (represented by the x -axis), and different density ratios (y -axis). Due to the symmetry of the problem, only the speed of one stream is shown. At low densities, the difference in speed between the two opposing streams is relatively small, independently of the density ratio. The prevalent speeds are close to the free-flow speed. At high total densities (≥ 1.5 ped/m²), the prevalent speed of the major stream can be several times higher than that of the minor stream, and

speeds are in general lower.

A limitation of the model is due to its exclusive consideration of macroscopic walking, ignoring other activities such as waiting or phenomena involving social interaction between individuals. For instance, group walking patterns are known to significantly influence crowd dynamics (Moussaïd et al., 2010). Similarly, non-walking facility elements such as turnstiles or stairs cannot be described by the model.

A further criticism may relate to the fact that phenomena of self-organization have not been reproduced by the proposed model specification. The spontaneous formation of lanes in counter-flow, or of stripes in cross-flow is indeed well known, both empirically (Helbing et al., 2001) and from modeling (Helbing and Molnár, 1995; Treuille et al., 2006; Hoogendoorn et al., 2014). The question of whether macroscopic models should be able to reproduce such patterns is however debatable. First, it may be argued that empirically calibrated fundamental diagrams already capture the influence of self-organization implicitly (Zhang et al., 2012). Second, most macroscopic models are deterministic, whereas self-organized flow patterns emerge spontaneously, and can hardly be predicted. For instance, even for homogenous counter-flow in a simple corridor, the configuration and position of lanes change over time, such that on average no lanes may be discernible. Not predicting any spontaneous patterns of self-organization, and accounting for their impact on flow implicitly, may thus be preferable in a deterministic modeling context.

Overall, the proposed model seems highly useful for the planning and design of congested walking facilities. Typically, the assessment of pedestrian infrastructures is based on aggregate quantities such as density and specific flow (Fruin, 1971; Highway Capacity Manual, 2000). This information is readily available from the model, allowing a quantitative prediction of the expected level-of-service in pedestrian facilities (see Chapter 5). Due to the performance of the model, a large number of infrastructure configurations and complex walking networks can be evaluated in little time. Even an automated optimization may be considered, using for instance an evolutionary framework to ‘streamline’ the design of a facility (Helbing et al., 2002). Besides, an application of the model within a DTA-framework or for OD demand estimation seems interesting for further study, as it is one of very few models that allow to generate reproducible and accurate walking time distributions in a single run and at low cost (Seer et al., 2008;

Hänseler et al., 2015).

4.8 Concluding remarks

A dynamic network loading model for multi-directional and time-varying pedestrian flows has been developed. By combining it with any suitable route choice model from the literature, a powerful and computationally efficient pedestrian traffic assignment model can be obtained.

Besides the development of an accurate macroscopic pedestrian flow model as such, an important novelty lies in the explicit consideration of anisotropy, which is achieved by using a stream-based fundamental diagram for pedestrian traffic.

To assess the performance of the pedestrian network loading model, several model specifications have been considered, and are evaluated at the example of four real case studies, each elucidating different aspects of the model. A detailed analysis shows that the proposed model is able to compute walking time distributions and density maps that are in good agreement with observed data. Moreover, the consideration of a stream-based pedestrian fundamental diagram has been shown to significantly improve the accuracy of the proposed model as far as anisotropic flows are concerned.

Chapter 5

Application and practical guidance

5.1 Introduction

In the following, the practical applicability of the previously developed modeling framework is investigated. In particular, at the example of Lausanne railway station, the estimation of demand and level-of-service are discussed. The objective of this chapter is to provide guidance on the practical use of the framework for the organization, planning and design of train stations. To reach readers that are not familiar with the previous chapters, the main modeling ideas are first recapitulated in a qualitative way.

The chapter is structured as follows. In Section 5.2, the estimation of pedestrian origin-destination demand is discussed, allowing to quantify the current usage of pedestrian infrastructures in Lausanne railway station. Section 5.3 considers the estimation of traffic conditions, which allows for the assessment of the current level-of-service (LOS) in the same station. Section 5.4 provides practical guidance for the use of these modeling tools in the dimensioning of rail access facilities in general, covering all stages of the planning process from the definition of the traffic concept of a train station, via the prediction of demand and level-of-service, to the verification of the dimensioning. Section 5.5 contains concluding remarks.

5.2 Estimation of origin-destination demand

To obtain a comprehensive understanding of the usage of rail access facilities, several data sources have to be ‘combined’. An estimate of OD demand is to be found that, when applied to the pedestrian network of a train station, is most consistent with the corresponding train timetable, historical surveys, and all other data sources that are available (Cascetta and Improta, 2002). In the case of Lausanne railway station, all the data sources described in Section 2.3 are used with the exception of pedestrian trajectory data, which is considered for validation only.

To take the train timetable into account, we concentrate on platform exit flows that are caused by alighting passengers of arriving trains. These are known to cause demand ‘micro-peaks’ that are critical for the dimensioning of rail access facilities (Hermant, 2012). Fig. 5.1 illustrates the typical pattern of platform exit flows (solid line), as well as a corresponding piecewise linear model that is derived from it (dash-dotted).

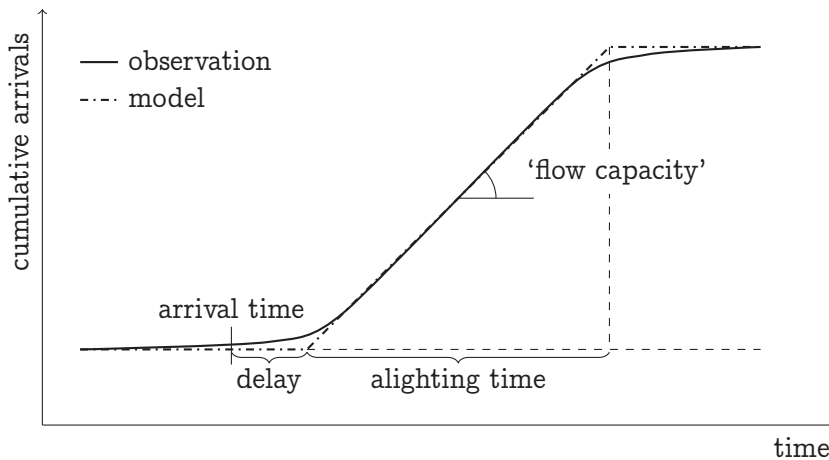


Figure 5.1: Flow of alighting passengers on platform exit ways.

After the arrival of a train, a certain time elapses until the first pedestrians reach the platform exit ways. This may be due to the necessary walking to reach the exit ways, or a delay in the opening of doors after the train has stopped. Subsequently, a constant flow is established, whose magnitude is limited by the capacity of the exit ways. This assumption is based on empirical observations, showing that the exit ways typically

represent the bottleneck in that situation (Benmoussa et al., 2011). Depending on the number of available exit ways, which often is determined by the position and length of a train, the magnitude of the flow may be different. Once all alighting passengers have left the access ways, the flow reaches again zero.

Due to various random effects, such as natural fluctuations in the ridership of a train, its position along a platform, or the distribution of passengers within a train, the parameters of the piece-wise linear model are stochastic variables. The prediction of the model is then also stochastic, and may be represented by a probability band. An example of such a prediction band is shown in Fig. 3.5 in Chapter 3, where a good agreement between prediction and observation is found.

If an appropriate specification of its parameters is available, this model can be applied to estimate the arrival flows on any platform. In the case of Lausanne railway station, such a parametrization is available, and train-induced exit flows can be predicted for all platforms (Molyneaux et al., 2014). These flows are used in the OD demand estimation framework, together with the available pedestrian counts and sales data. To associate the different information sources over space and time, a Normal walking speed distribution is assumed. The specifications for even walkways, inclined areas and stairways proposed by Weidmann (1992) are used.

The OD demand is jointly estimated for the 10-day reference set described in Section 2.3. The accuracy of the resulting estimates is discussed in Chapter 3. By comparing observations and estimates of the demand in the PUs, it is shown that despite the strong and rapid fluctuations, the measured mean lies within the prediction band throughout the considered time horizon. In particular, the differences between the prediction and measurement for individual days are found to be smaller than the day-to-day variability observed in measurements of tracking data. Thus, at least for dimensioning purposes, the estimate of total demand can be considered accurate. Similar findings hold for the estimation of accumulation or OD flows. In all cases, the integration of the train timetable is essential to reach such accuracy.

In Fig. 5.2, the estimated evolution of the total demand is provided, showing the mean and the standard deviation band. Both the within-day and the day-to-day variation (as indicated by the width of the deviation band) are significant. The average cumulative demand over the

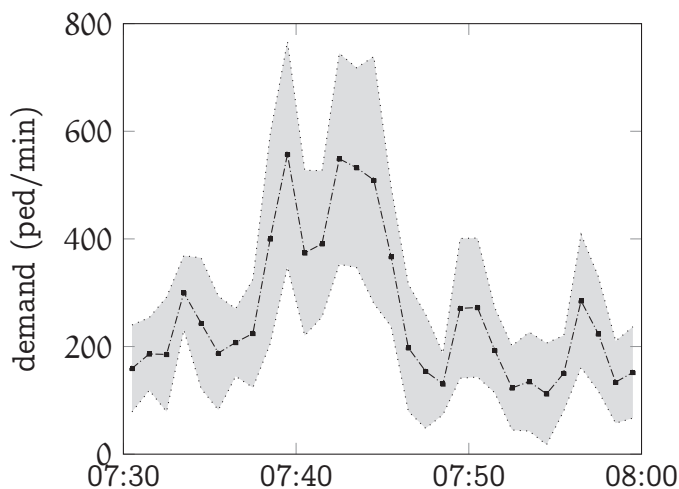


Figure 5.2: Estimated total demand during morning peak hour.

studied 30-min period amounts to 7,906 ped, representing about 8% of the daily station throughput (Amacker, 2012). The highest average demand is found between 7:39 and 7:40, where the overall demand rate amounts to 557.3 ped/min. A quarter of an hour later, between 7:54 and 7:55, the mean demand reaches a minimum of 112.0 ped/min. Within only a couple of minutes, the average demand thus varies by almost a factor of 5. Such a periodical concentration is characteristic for the Swiss railway network that aims at bundling train arrivals and departures in order to minimize the waiting time of transfer passengers (SBB-Infrastruktur, 2013).

To consider the spatial distribution of demand, the latter may be aggregated over time. Fig. 5.3 shows a ‘Circos’ diagram of the average pedestrian OD demand (Krzywinski et al., 2009). Origin/destination areas are grouped into ten centroids, representing the train platforms #1, #3/4, #5/6, #7/8, #9 and #70, the entrances North and South, the passageway to the metro, and a collection of shops. Light gray strips represent pedestrian flows emanating from train platforms, medium gray those originating at the entrance ways North and South as well as at the interface to the metro station, and dark gray strips pedestrian demand emanating from one of the sales points.

Circos diagrams have originally been developed for studying genomes (Krzywinski et al., 2009), but turn out to be a powerful instrument for conveying the spatial structure of pedestrian OD demand to practitioners and

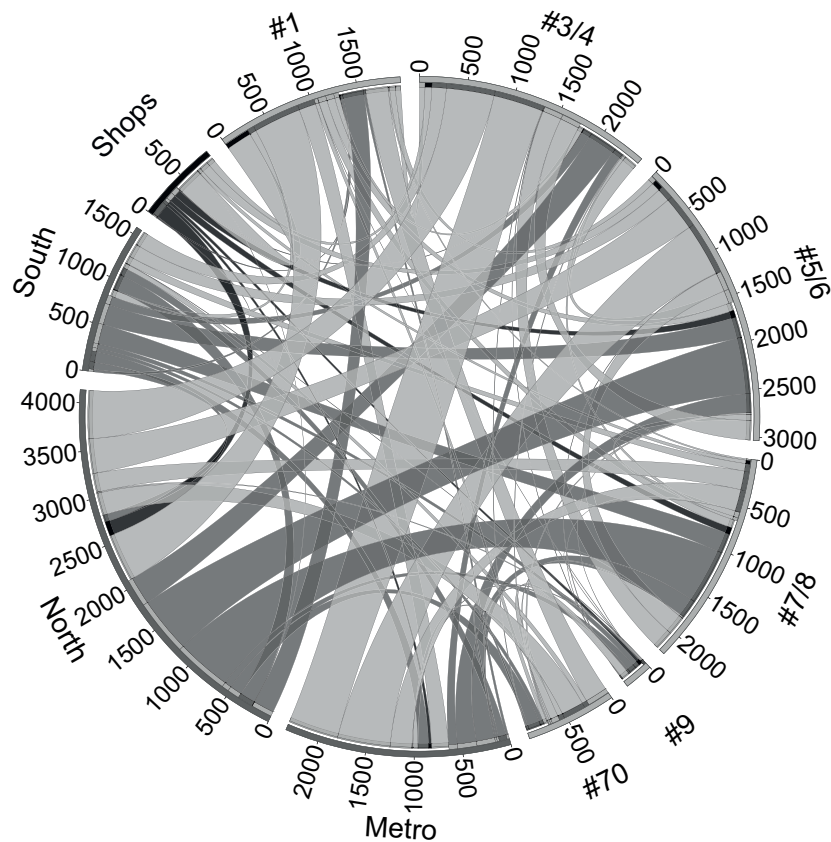


Figure 5.3: Pedestrian OD demand between 07:30 and 08:00. The origin of strips are color-coded as train platforms (light gray), city/metro/bus (medium gray) and shops (dark gray).

authorities. They provide quantitative information of flow between any two centroids, which usually is difficult to represent in a single diagram. Moreover, the share of different user classes can be immediately perceived based on the different shadings. During the considered time period, 44.1% of all station visitors represent inbound passengers, 31.2% represent outbound passengers, 16.4% are transfer passengers, and the remaining pedestrians represent local users. These figures are different for each train station, and change between the morning, evening and off-peak periods.

A further way of visualizing demand is by means of network flows. Fig. 5.4 shows a map of the estimated minute-by-minute link flows for the time period between 7:40 and 7:48 on April 30, 2013. Here, the demand estimate of a specific day is chosen, as it allows to visualize the demand

peaks caused by individual train arrivals and departures. The shading of links represents the cumulative link flow over a minute in both directions. The diameter of nodes represents the minute-by-minute origin flow.

Between 7:40 and 7:41, the arrival of IR 1712 from Sion at 7:38:57 is discernible by the origin flow it creates on platform #5/6. In the time period considered, this train is among those with the highest alighting volumes. During 7:41 and 7:42, the arrival of IR 1606 from Neuchâtel on track #4 can be seen by the trace it leaves in the pedestrian flow map. Within less than a minute, IR 1710, IC 706 and IR 1407 arrive on platform #7 at 7:42:24, platform #5 at 7:42:59, and on platform #3 at 7:43:18, respectively. Especially the former two represent major lines (from Brig and Zürich), causing large pedestrian movements. Their impact is visible in Fig. 5.4d and 5.4e. After the last arrival of a train, IR 2517 from Geneva arriving on platform #1 at 7:44:37, pedestrian flows decay, as can be seen from Fig. 5.4g and 5.4h.

5.3 Level-of-service assessment

Despite its rich content of information, origin-destination demand reveals little about expected traffic conditions. To assess the level-of-service, the interaction between infrastructural supply and demand needs to be taken into account.

For that purpose, the pedestrian traffic assignment model described in Chapter 4 is useful. It is applied in the following to investigate density levels in PU West, representing the busiest area in Lausanne railway station (see Fig. 5.4). The aggregate nature of the model allows for a quick implementation, as well as for an accurate calibration and physical interpretation of the obtained parameterization. These properties are useful for the presented level-of-service analysis, but become essential for planning, design or crowd management applications, where a fast and accurate modeling of pedestrian dynamics is key.

To obtain traffic conditions from the estimated OD demand, two steps are necessary. First, a route choice model is required to assign OD demand to route flows by specifying route split fractions. In PU West, only a single route exists between each OD pair, and computing these fractions is trivial. Second, a network loading model is needed to describe the propagation of

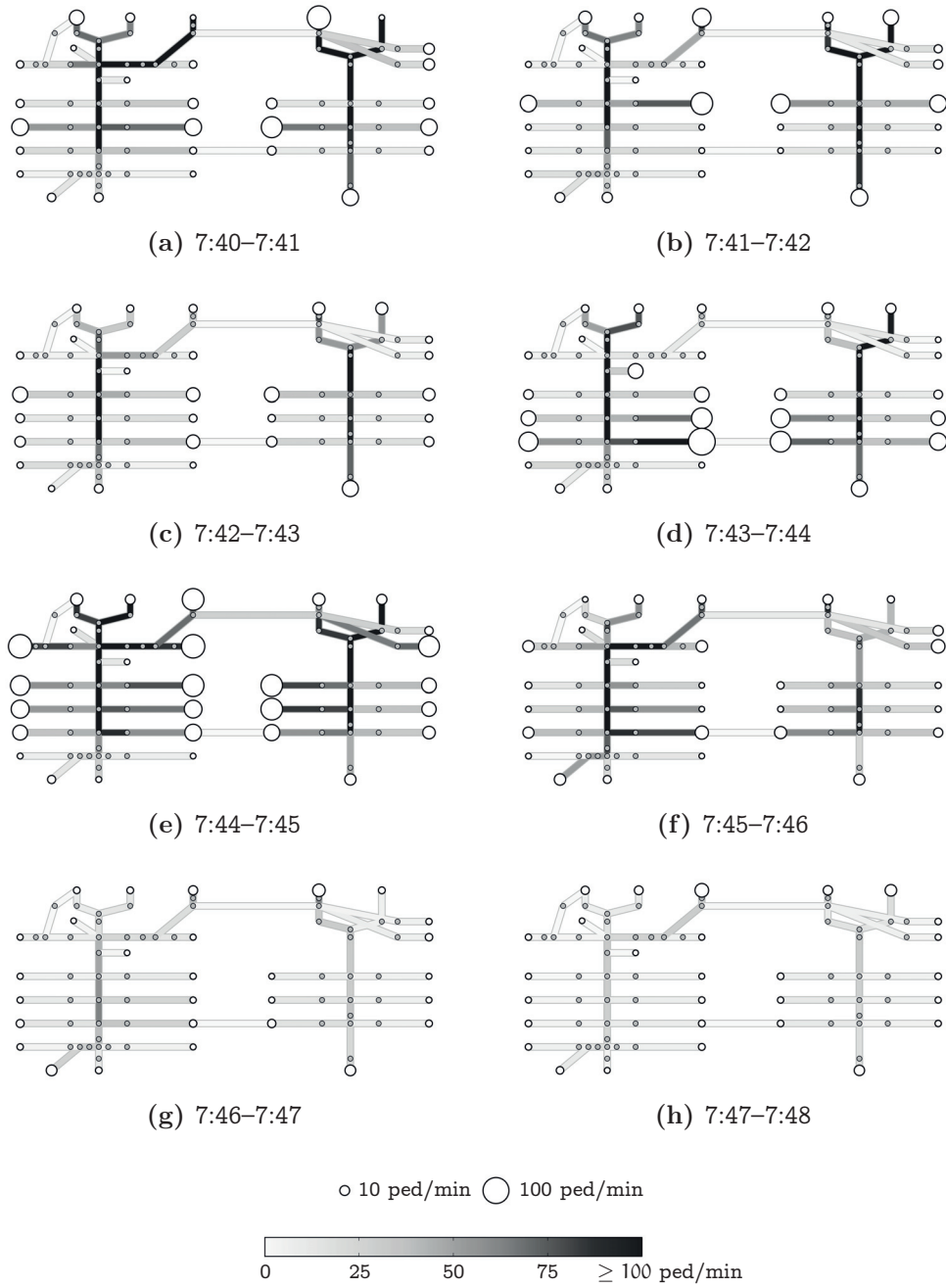


Figure 5.4: Pedestrian flow map between 07:40 and 07:48 on April 30, 2013.

pedestrians along these routes at the aggregate level.

To that end, walkable space is partitioned into a set of areas as illustrated in Fig. 5.5a, where they are delimited by dotted lines. The shape and size of areas can be chosen freely. Typically, areas of approximately 10 m^2 are used (Asano et al., 2007; Guo et al., 2011). A route is given by an origin and a destination, and a subset of areas (illustrated by shaded areas). The choice of the actual sequence of areas within a route is up to the loading model. It is described at the aggregate level by means of turning proportions. These are such that pedestrians gradually approach their destination, avoiding areas of high density.

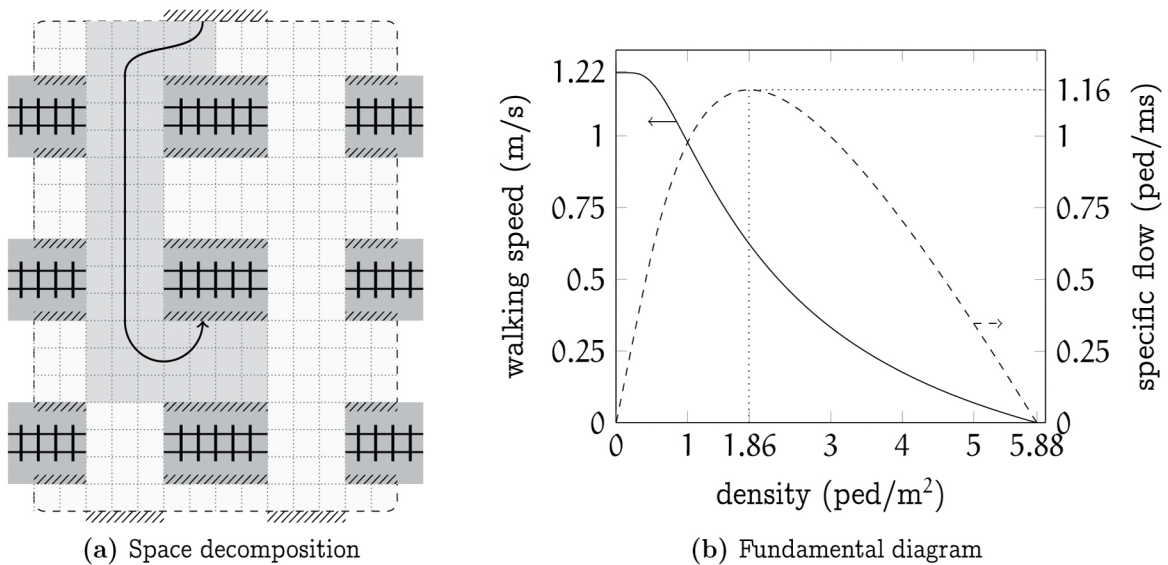


Figure 5.5: Network loading model.

A pedestrian fundamental diagram governs the propagation of pedestrians across areas. Fig. 5.5b shows the used density-speed relationship (solid curve), as well as the corresponding density-flow relationship that results in case of uni-directional motion (dashed curve). Due to the relatively low level of density in Lausanne railway station, an isotropic specification is sufficient. Its functional form is as proposed by Weidmann (1992), and the parametrization is obtained from a calibration on trajectory data collected in Lausanne railway station in April 2013 (see Table 4.1 for the results of the calibration, as well as for a discussion of the corresponding parametrization).

As can be seen from the density-flow relationship, the domain is split

into a free-flow and a congested regime, with the transition at a density of 1.86 ped/m^2 . An increase in density in the free-flow regime leads to an increase in flow, whereas in the congested regime the opposite occurs. Such a behavior is typical for transportation networks, and applies both to vehicles and pedestrians (see e.g. Geroliminis and Daganzo, 2008). In practice, the exact density at which the transition occurs may vary, particularly depending on the prevailing flow pattern. For instance, in multi-directional flow, congested traffic conditions are typically reached at lower densities than in uni-directional flow (see Chapter 4). The reported value of 1.86 ped/m^2 is thus of indicative value only.

For each area at given time intervals, the density is calculated, and based on the fundamental diagram, the corresponding flow is computed. The density in areas can be directly used to assess the perceived comfort and performance of a facility. The Highway Capacity Manual (HCM, Highway Capacity Manual, 2000) distinguishes six levels of service, ranging from LOS A (below 0.18 ped/m^2 , most favorable) to LOS F (above 1.33 ped/m^2 , least favorable).

Fig. 5.6 shows the resulting level-of-service maps for January 22, 2013. For each time period of one minute, the model estimates and the corresponding measurement from pedestrian tracking data are shown.

Visually, the proposed traffic assignment model is able to reproduce the trend of the actual measurements. In the first time interval, the density maps show a high level-of-service, which is then reduced during the following minutes, before it improves again in the last interval. There are certain differences, for instance regarding the concentration of pedestrians along the centerline of the corridor, which is less distinct in the model prediction than in the measurement. An analysis of several days shows that these differences between model prediction and measurement are relatively small compared to the day-to-day variation. For the purposes considered in this work, i.e., for an assessment of the level-of-service that is sufficient for dimensioning, the estimates are considered accurate. Moreover, a comparison to the social force model, which is the state-of-the-art in microscopic pedestrian flow modeling, shows that the performance of the proposed macroscopic model is equivalent or superior in the considered case study (Hänseler et al., 2014a).

The highest pedestrian densities are observed between 7:41 and 7:43, when various trains arrive. The level-of-service lies in the range between A

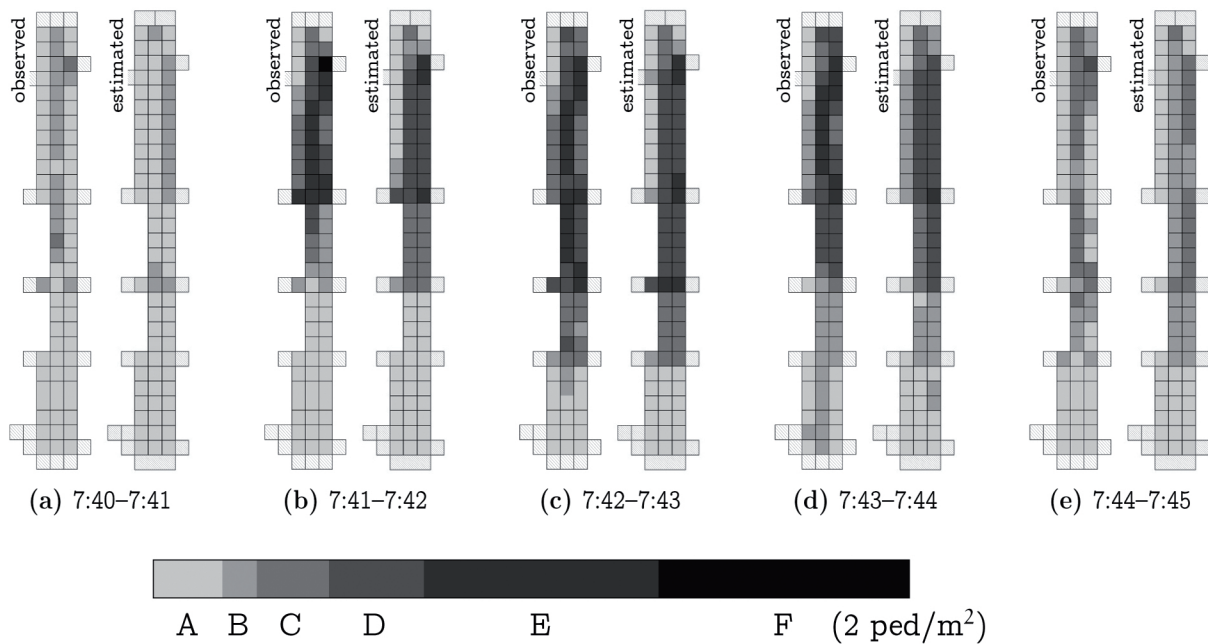


Figure 5.6: Level-of-service in PU West on January 22, 2013.

and E, i.e., densities are generally below 1.33 ped/m². As is discussed in Section 5.4, according to Swiss standards LOS E should only be tolerated in bottlenecks, and not be present on wide walkways as in the case of PU West. The capacity of PU West is thus insufficient not only for the future, but already for the current demand.

To assess the required transfer times between connecting trains, walking times are of interest. Fig. 5.7 shows the walking time distribution in PU West as estimated by the traffic assignment model, and as observed in the trajectory data. A good qualitative agreement is found. Further analysis shows that this also holds for route-specific predictions of walking times, and in case of congestion (Chapter 4).

The area-based pedestrian traffic assignment model can thus be used to accurately predict the level-of-service in walking facilities of a train station. As before, no tracking data is necessary, of which only an independent data set has been used for calibration. Even if the model is calibrated solely based on values from the literature, its predictive quality is still good. This is due to the fact that the obtained parametrization is very similar to those of other researchers (see e.g. Weidmann, 1992).

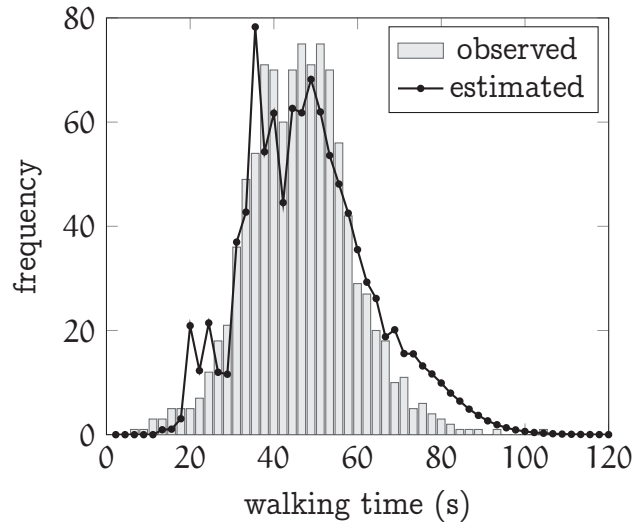


Figure 5.7: Walking time distribution for PU West ($\Delta t = 2.22$ s).

5.4 Planning guidelines

In practice, the estimation of the current demand and level-of-service may be of interest, but typically does not represent the primary objective. More relevant is the consideration of future scenarios, which allow the assessment and optimization of construction plans, and thus the dimensioning of infrastructure facilities.

The configuration and dimensioning of pedestrian facilities in train stations is traditionally based on planning scenarios, such as ‘passengers on platform awaiting boarding’, ‘flow of alighting passengers on platform exit ways’, or ‘transfer flows on pedestrian walkways’ (Hoogendoorn and Daamen, 2004; Buchmüller and Weidmann, 2008; Zhang et al., 2008). In structural engineering, such scenarios are referred to as ‘load cases’. An infrastructure is checked for serviceability against all the load cases it is likely to experience during its lifetime. In the context of rail access facilities, the load cases typically consider the arrival or departure of one or a few reference trains, and the resulting pedestrian OD demand is estimated using rules of thumb. The dimensioning is then done manually and separately for each facility element, such as stairways, ramps, walkways or platforms.

By using a computational framework to estimate demand and level-of-service, the planning process of rail access facilities can be enhanced. First,

due to the explicit integration of the train timetable, the use of individual load cases becomes obsolete. Second, the various facility elements can be dimensioned jointly, which allows to investigate their mutual influence on each other.

Based on our experience from Lausanne railway station, we suggest in the following a six-step process that is useful for the planning and dimensioning of pedestrian facilities in train stations, be it existing ones, or new stations. The approach is based on guidelines by Buchmüller and Weidmann (2008). The differences consist in (i) the direct consideration of the usage of a train station based on the timetable instead of indirectly through load cases, (ii) the use of a computer-based OD demand estimation framework instead of manual estimation techniques, and (iii) the use of a pedestrian traffic assignment model that allows to simultaneously dimension multiple facility elements. For each of the six steps, a short illustration at the example of Lausanne railway station is provided. The process may be iterative.

I. Traffic concept of train station. In a first step, the planning horizon is to be determined, as well as the corresponding operational concept for the expected peak periods. This includes the train timetable or line frequency, as well as the capacity and type of rolling stock. In Swiss train stations, typically the morning peak period on working days is critical, and in rare cases the evening peak hour. In particular cases, such as in touristic areas or for stations close to stadiums, certain periods on weekends or after mass events may be decisive for the dimensioning.

In a second step, a preliminary prediction of pedestrian OD demand can be made. This typically requires an analysis of the status quo, which serves to calibrate the demand estimator (see Chapter 3 and Section 5.2). Unless sufficient information is available, a data collection campaign may be required, involving for instance manual travel surveys, or the installation of flow sensors.

In the case of the on-going expansion of Lausanne railway station, the planning horizon is the year 2030, for which detailed information of the train timetable and rolling stock is available. The demand is ‘expected to double for interregional trains, and to triple for regional trains’ (Caillaud, 2011). To better understand the usage of the train station, a pedestrian tracking system has been installed. An exploratory data analysis, discussed

in Section 2.3, shows that the critical period occurs indeed in the morning.

II. Functional requirements. The desired level-of-service needs to be specified, for instance for walkways, stairways, platforms or waiting areas. Typically, one of the standard LOS schemes is used, which rely on density or specific flow. In accordance with Swiss and US-norms (Weidmann, 1992; Highway Capacity Manual, 2000), it is typically required that LOS B or better be maintained for intervals of several minutes. During short intervals of up to a minute, LOS D is accepted. At bottlenecks, locally LOS E is still tolerated. Separate standards may apply under particular circumstances, such as after mass events. Maximal walking times can also be set, either based on a preliminary timetable that requires certain transfer times, or based on considerations related to comfort. The particular needs of disabled train users need to be taken into account, in accordance with the local legislation.

The placement of service and sales points needs to be discussed. Access to such facilities may increase the comfort and well-being of train station users, but at the same time compromise pedestrian traffic. The effect of the latter should be taken explicitly into account in the dimensioning of pedestrian facilities, both as far as available space is used and additional demand is induced. Generally, the more important a service, the higher its priority in the allocation of space should be, however without violating the pre-defined LOS standards.

In the case of Lausanne, maximum acceptable service levels are defined for platforms, ramps, stairways and horizontal walkways. The density-based LOS schemes specified in the Highway Capacity Manual (2000) are used, with the thresholds as mentioned above (generally LOS B or better, for short intervals LOS D, LOS E exceptionally at bottlenecks). For the placement of sales and service points, the status quo is preserved.

III. Topology of pedestrian facilities. The network of pedestrian facilities is to be developed. This process takes into account (i) the surroundings of the train station, and in particular factors such as the connection to the local transportation system, the local network of walkways, points of attraction in the vicinity of the station, and workplace locations; (ii) existing buildings that are to be preserved, such as historical station halls or facilities that do not require a structural extension; and (iii) the track topology,

which is either the existing one, or imposed by the design of the future rail network.

Subsequently, the type of facility elements and the connection between them can be specified. For vertical level changes, a choice between stairways, ramps, escalators, and elevators exists. Further facility elements that need to be specified include horizontal walkways, waiting areas and platforms. For each element, its position and characteristic dimensions (such as the length for walkways) are to be determined.

Once the topology of pedestrian facilities is specified accordingly, a preliminary assessment of walking distances may be made, verifying that the required transfer times are met. This should include the specific needs of people with reduced mobility. Generally, the topology should allow for short and direct connections between facilities.

For the planned extension of Lausanne railway station, the topology of pedestrian facilities is changed in that it incorporates a newly-built metro station for local transit, it directly connects to a museum complex to the northwest of the station, and in that it features three instead of two transversal pedestrian underpasses.

IV. Demand Prediction. An estimate of pedestrian demand is required. Using the framework discussed in Section 5.2, it can be obtained based on the traffic concept of the train station and the topology of pedestrian facilities. In the estimation process, the impact of congestion on demand is usually neglected. In principle, it would be possible to take that influence into account. However, it requires a joint application of the demand estimator and the traffic assignment model, as well as a detailed layout of facility elements, which is not available at this point. It would thus require a merging of demand estimation and dimensioning (see step V. below), which is cumbersome and rarely done in practice.

In the case of Lausanne, the influence of congestion is neglected in the estimation of demand. To obtain a prediction for the year 2030, the planned instead of the current timetable is used, and the ridership is increased based on available forecasts.

V. Dimensioning. Based on the network topology, a detailed dimensioning of facility elements is to be made. In this process, a traffic assignment model as described in Section 5.3 is useful. It quantitatively predicts the

level-of-service that results for a given demand estimate as a function of the facility layout.

Thanks to a joint consideration of pedestrian facilities, a consistent layout is reached in which the dimensions are balanced across elements. This is crucial for instance for cross-sections of adjacent facilities, such as the width of walkways and stairways. In a second step, the placement of travel services and furniture, such as ticket machines, information panels, benches or mobile sales points can be considered. As a general rule, these should not obstruct the main paths that connect facility elements.

In certain areas of railway stations that are only lightly loaded, a dimensioning based on the resulting level-of-service may be inappropriate. Instead, standard values for cross-sections should be used. Corresponding specifications are often provided by national authorities that seek a minimum degree of comfort (Buchmüller and Weidmann, 2008).

In the case of Lausanne railway station, the development of the network topology and the dimensioning has been a highly iterative process. Several times, the number of pedestrian underpasses has been changed from two to three and vice versa. In the beginning, our mandate consisted mainly in determining an appropriate width of these transversal underpasses. However, it turned out that the main bottleneck is rather the *connection* between these transversal underpasses and lateral platform access ways. By ‘smoothing’ a previously rectangular layout, the level-of-service can be increased more significantly than by simply enlarging the width of pedestrian underpasses. This finding was only possible due to the joint consideration of the underpasses and their platform access ramps, and due to a realistic estimation of demand that yields multi-directional flow. In the literature, a similar example of smoothing a rectangular bottleneck is discussed by Helbing et al. (2001), who use an evolutionary algorithm to improve the design of pedestrian facility elements.

VI. Verification. Evidence is to be provided that the dimensioning fulfills the specified functional requirements, including the desired level-of-service. Due to legal requirements, such a verification typically needs to be done manually. Significant differences in national legislations exist in how such a verification is performed.

In the case of Lausanne railway station, we have provided recommendations regarding the dimensioning of the main walking facilities. However,

we have not been involved in the finalization of the layout, nor in its legal verification.

5.5 Concluding remarks

The framework for assessing the usage and level-of-service of rail access facilities developed in the preceding chapters has been discussed at the example of Lausanne railway station. Specifically, the methodology for estimating pedestrian origin-destination demand from Chapter 3, and the traffic assignment model for estimating the resulting level-of-service from Chapter 4 have been illustrated. The complete modeling framework is freely available (Hänseler et al., 2014b; Hänseler and Molyneaux, 2015).

The results from the case study have shown that dynamic OD demand, level-of-service maps and travel time distributions can be accurately predicted. Required in that process are in particular the train timetable and ridership information.

The modeling framework has been embedded in a six-step planning process that is useful for practitioners and researchers confronted with the task of designing rail access facilities for a new train station to build, or an existing one to expand.

Besides planning applications, the framework can be used to develop practical and policy recommendations for station design, route signage, or even timetabling and train-track allocation. Its most natural application, however, would be for crowd management, for which its aggregate nature, accuracy and computational efficiency make it highly suitable.

Chapter 6

Concluding remarks

6.1 Main findings

A powerful framework for supporting the organization, planning, design and operation of rail access facilities has been presented. It provides a detailed, quantitative understanding of pedestrian flows in train stations, as well as valuable insights for the improvement of pedestrian comfort and safety. For instance, it can predict if safety or throughput issues occur, or be used as a basis for the development of real-time crowd management systems.

While the modeling framework has been developed with rail access facilities in mind, with little effort it may be adapted to other pedestrian facilities such as metro stations, airports, shopping malls, museums, or urban walking areas. The underlying modeling principles, demand estimation and traffic assignment, remain directly applicable.

All research objectives formulated in the introductory chapter have been accomplished. The individual contributions of each chapter are listed in the following.

Chapter 2 introduces a case study of Lausanne railway station, for which a rich data set consisting of pedestrian trajectories, flow counts, train delay data and ridership information has been collected.

An explorative data analysis reveals a demand pattern that is strongly influenced by the train timetable, with distinct peaks during morning and evening rush hours. The day-to-day variability is significant.

The case study is particularly interesting in that it represents a ‘typ-

ical' European train station with around 140,000 daily visitors, and in that several unique data sets are available for the same site.

Chapter 3 presents a framework for estimating pedestrian origin-destination demand in rail access facilities, taking various types of data sources into account.

The framework captures within-day variation in demand, and natural day-to-day fluctuations. Boarding and alighting volumes, as well as train arrival times, are explicitly considered in the estimation process.

Besides the novel field of application, the consideration of the train timetable represents a major contribution of the approach, which is shown to yield a significant improvement in the estimation quality.

Chapter 4 proposes a pedestrian traffic assignment model, and in particular a network loading model for large, congested walking facilities.

The loading model builds on the continuum theory for pedestrian flow (Hughes, 2002), and relies on a stream-based fundamental diagram to reproduce multi-directional flow at high density.

Its applicability to anisotropic flow, a rigorous calibration on real data, and a consistently high performance across several case studies, are among the major contributions of the model.

Chapter 5 applies the developed modeling framework to study the usage and level-of-service of rail access facilities in Lausanne railway station.

The resulting OD demand, density maps and travel time distributions are presented, and the practical applicability of the framework is discussed and demonstrated.

Based on the experience gained, practical guidance for the model-based planning and design of further rail access facilities is provided, representing the main contribution of the chapter.

6.2 Practical recommendations

The proposed modeling framework considers both the problem of demand estimation and traffic assignment in rail access facilities, allowing for a comprehensive understanding of pedestrian flows in train stations. Detailed

practical guidance has been provided for its use in the planning and design of train stations (see Chapter 5). In the following, further recommendations are provided that result from the experience gained in this thesis (see also Helbing et al., 2005; Hoogendoorn, 2015).

The reason for a pedestrian facility to provide a poor level-of-service is often rooted in one or a few facility elements. This may be a narrow access door, stairway, or a congested walkway. Often such performance bottlenecks can be eliminated at comparatively little cost, yielding a significant gain in capacity and performance. It is thus worthwhile to start the analysis of a pedestrian facility by focusing on potential bottlenecks, instead of planning new facilities from scratch.

In multi-directional walking facilities, a separation of lanes may reduce the friction among pedestrians, and contribute to more fluid traffic. This can be achieved by the installation of columns along the centerline of a corridor, or of a free-standing handrail on a stairway. As a consequence, bi-directional flow is divided into separate uni-directional streams, with a corresponding gain in efficiency (see Chapter 4). This measure is systematically applied in the metro stations of Hong Kong's mass transit system, where bi-directional walking facilities and a high traffic load are common.

Another recommendation regards the infrastructural optimization of orifices, such as narrow passageways. Often, a streamlining of the entrance to such bottlenecks allows to reduce turbulence, increasing capacity and saving space without the need to remove the orifice as such (see Chapter 5). In some situations, also the placement of an artificial obstacle upstream the bottleneck, such as a pillar, may yield an improvement by reducing the 'pedestrian pressure' (Helbing et al., 2002).

Beyond infrastructural measures, changes in the operation of pedestrian facilities can yield significant improvements as well. A key principle in crowd management is the pursuit of 'free-flow conditions', i.e., of subcritical pedestrian densities. Under such conditions, the performance of pedestrian facilities is high, whereas under congested conditions, the flow performance drops significantly.

Free-flow conditions may be reached in various ways. The simplest way is by limiting the inflow to a congested facility, for instance by installing access gates. The desired flow rate may be estimated using the traffic assignment model presented in this work. An alternative consists in improving the 'load balancing', by distributing pedestrian demand according

to the capacity of facility elements. This may be done by means of route guidance or information provision. In the context of a train station, also the train timetable, train-track assignment, and train stopping positions may be used to yield a balanced use of pedestrian facilities.

6.3 Future research directions

This thesis has been motivated by the general need to better understand and manage pedestrian flows in public spaces. In that respect, the achievements discussed so far represent only a first step in a broader research agenda. Further research may be organized along the three main dimensions considered previously in this thesis: Models, data and applications.

Models: In terms of demand estimation, a major limitation of the proposed approach lies in the assumed independence between OD trips. In a train station, many pedestrians visit multiple destinations, such as ‘train station hall’, ‘ticket office’ and ‘train platform’. A traditional origin-destination representation of demand does not allow to correctly capture the sequence of these destinations. To account for that, OD trips may be generalized as activity chains, such as ‘enter train station’ → ‘buy ticket’ → ‘board train’. The resulting OD demand is then derived from the prior decision to perform these activities, and the correlation among related OD trips is explicitly considered (Danalet, 2015). Such an activity-based representation of demand may be obtained at the aggregate level, associating several pedestrians with a single activity chain, or at the disaggregate level, where every pedestrian is explicitly represented and may be associated with individual physical and behavioral characteristics. While an activity-based approach is desirable to improve the demand estimation in train stations, for other public spaces, it may be a necessity. For instance, in the case of an airport, a large majority of pedestrians follow complex multi-destination paths of the form ‘check-in’ → ‘baggage drop’ → ‘security’ → . . . → ‘boarding’. Such activity chains cannot be realistically represented by means of OD demand alone.

In terms of traffic assignment, an obvious limitation of the proposed approach consists in the exclusive consideration of walking areas. In many pedestrian facilities such as station halls, check-in areas or shopping malls,

the main activity consists in waiting, queueing or shopping, but not in walking. A straightforward extension of the corresponding network loading model would consist in introducing the concept of desired speed, which may attain zero when pedestrians are not meant to move (Helbing and Molnár, 1995). For microscopic models, extensions of walking models that consider waiting behavior have already been considered, but are generally difficult to calibrate (Davidich et al., 2013). The development of more versatile pedestrian traffic assignment models, both at the aggregate and the disaggregate level, thus represents an interesting subject for future research.

The interaction between demand estimation and traffic assignment models represents another important, but so far largely neglected aspect in the modeling of pedestrian flows. Demand estimation and traffic assignment models are based on fundamentally different assumptions, and ensuring consistency among them is crucial. It is trivial for applications with a negligible interaction between pedestrian demand and infrastructural supply, as in the case of Lausanne railway station. The two models are then independent. For congested spaces, on the other hand, it is complex. In the context of vehicular traffic, various approaches have been developed to deal with this complexity, such as ‘fixed-point’ formulations (Bottom, 2000; Cascetta and Postorino, 2001). Ensuring consistency between demand and supply also in the context of congested pedestrian flows seems of high scientific interest (Rabasco, 2014; Rojas-Lombarte, 2014).

Data: Generally, there is still a lack of pedestrian data from real sites. The available data is often limited in terms of the range of traffic conditions it captures, in terms of its spatial and temporal coverage, or in terms of its quality. For instance, the data collected in Lausanne railway station shows only weak features of demand-supply interaction, pedestrian counts and trajectories are only recorded in main areas, and no socioeconomic information is available.

Data obtained with new collection techniques, such as automated fare collection data in transportation hubs, or Wi-Fi and Bluetooth traces from accordingly equipped facilities, are expected to significantly improve our understanding of pedestrian dynamics in public spaces. Besides collecting more and better data in general, it is of particular importance to obtain real data from pedestrian facilities with high densities. These include for instance congested metro stations or densely populated urban areas. In

such spaces, data collection is generally difficult due to infrastructural, operational and legal restrictions, such as a lack of space for the placement of sensors, a lack of reliable measurement techniques, or privacy concerns.

Additionally, establishing real-time data collection systems represents an interesting endeavor for future research. Availability of such systems would allow exploring aspects such as the real-time monitoring and control of pedestrian flows, and in the long term, it would likely help improving the efficiency, safety and comfort of pedestrian spaces.

Applications: The modeling framework presented in this thesis can be directly applied to the planning and dimensioning of rail access facilities. Applications regarding the operational optimization of rail access facilities, such as of the train-track assignment in the context of pedestrian flows, may be directly derived from it.

Applications involving a direct management of pedestrians, commonly referred to as ‘crowd management systems’, can also be envisaged. Similar to dynamic traffic management systems (DTMS) that have gained tremendous popularity in the context of road networks, crowd management systems enable a ‘smarter’ use of infrastructures by coordinating pedestrian trips. The cost of such ‘intelligent’ approaches is often significantly lower than that of traditional solutions that focus on an increase in static capacity alone. Their field of application includes besides train stations and airports also sport stadiums, music halls, or other facilities that host a large number of people.

In a first step, *passive* crowd management systems may be developed, focusing on the monitoring of pedestrian flows. These are useful to understand the current state of a pedestrian network in terms of demand, densities, walking speeds or level-of-service. They may also be used for short-term prediction, serving as decision-aid tools that help anticipating and preventing dangerous crowd conditions. An important prerequisite for their use is a surveillance system composed of powerful data collection techniques, as in the case of Lausanne railway station. In the ‘era of big data’, such systems are expected to become increasingly available.

In a second step, *active* crowd management systems can be developed. Pedestrian flows may for instance be controlled by a dynamic route guidance system that stimulates the use of access ways and platform areas that are less congested (Pettersson, 2011). The inflow to already congested fa-

cilities may even be directly limited by constraining the flow at entrance gates (Xu et al., 2014). Both can be useful to avoid the overloading of facilities, which, as in vehicular networks, is known to sharply reduce their performance.

In the long term, such crowd management systems are expected to improve pedestrian facilities in particular by reducing congestion and by increasing their reliability. This thesis contributes significantly to their development by providing two essential components, namely a demand estimation and a pedestrian traffic assignment model. At the same time, it opens up completely new research dimensions, which quickly go beyond classical engineering. For instance, if system-wide travel times are rigorously minimized, crowd management systems are likely to favor some pedestrians over others. If this should be ‘allowed’, and to what extent that would be ‘fair’ or ‘reasonable’, are interesting and delicate questions. The path to successful and widely accepted crowd management systems will without any doubt be difficult, but also highly rewarding and beneficial for the safety and welfare of pedestrians in public spaces.

A. Demand estimation

Notation

Table 1: List of recurrent variables.

$\tau \in \mathcal{T}, \Delta t$	time
$\mathcal{G} = (\mathcal{N}, \mathcal{L}), \mathcal{N}_{\text{OD}} \subset \mathcal{N}$	graph, OD nodes
$v \in \mathcal{N}, \lambda \in \mathcal{L}, \alpha \in \mathcal{A}$	node, link, area
$\rho = (\lambda_1, \lambda_2, \dots), \rho \in \mathcal{R}$	route
$\kappa \in \mathcal{K}$	OD pair
$\zeta \in \mathcal{Z}, t_{\zeta}^{\text{arr}}, t_{\zeta}^{\text{dep}}$	train, arrival and departure time
$\pi \in \mathcal{P}$	platform
$\mathbf{d} = [d_{\kappa, \tau}]$	demand
$\mathbf{f} = [f_{\lambda, \tau}]$	flow
$\mathbf{a} = [a_{\alpha, \tau}]$	accumulation
$\mathbf{e}_{\text{on}} = [e_{\zeta}^{\text{on}}], \mathbf{e}_{\text{off}} = [e_{\zeta}^{\text{off}}]$	exchange volumes
Δ	reduction matrix
$\Sigma(\mathbf{d}; \mathbf{y})$	assignment model
\mathbf{y}	parameter vector
$\chi = [\chi_p], \boldsymbol{\varphi} = [\phi_{\lambda, \tau}]$	schedule-based estimates
$\eta, \varepsilon, \omega$	errors
$r_{\zeta, \lambda}^{\text{sec}}$	platform sector split ratio
w	estimation weight

Assignment model for walking facilities

This section outlines an assignment model for walking facilities in an uncongested train station. In accordance with Assumptions 2 and 3 in Sec-

tion 3.2.4, the prevailing traffic conditions are demand-independent.

Route choice: The outcome of the route choice model is represented by a route choice matrix $\mathbf{R}(\mathbf{y}) = [r_{(\rho,\tau'),(\kappa,\tau)}]$ of size $|\mathcal{R}||\mathcal{T}| \times |\mathcal{K}||\mathcal{T}|$. An element $r_{(\rho,\tau'),(\kappa,\tau)}(\mathbf{y})$ denotes the probability that a pedestrian associated with OD pair κ and departure time interval τ chooses route ρ during time interval τ' . Route choice is instantaneous such that $r_{(\rho,\tau'),(\kappa,\tau)} = 0$ if $\tau \neq \tau'$.

The time to traverse link λ during time interval τ is denoted by $\Delta t_{\lambda,\tau}^{\text{trav}}(\mathbf{y})$. The travel time on route ρ during time interval τ is given by

$$U_{\rho,\tau}(\mathbf{y}) = V_{\rho,\tau} + \psi, \quad (1)$$

where $\psi \sim \text{EV}(0, \vartheta)$ with ϑ a calibration parameter contained in \mathbf{y} , and where the sum of link travel times is given by

$$V_{\rho,\tau}(\mathbf{y}) = \sum_{\lambda \in \rho} \Delta t_{\lambda,\tau}^{\text{trav}}. \quad (2)$$

For OD pair κ , the likelihood that a user chooses route $\rho \in \mathcal{R}_\kappa$ is given by

$$r_{(\rho,\tau),(\kappa,\tau)}(\mathbf{y}) = \frac{\exp(-\vartheta V_{\rho,\tau})}{\sum_{\rho' \in \mathcal{R}_\kappa} \exp(-\vartheta V_{\rho',\tau})}. \quad (3)$$

Network loading: The network loading model defines mappings from route flows to link flows and area accumulations. Table 2 defines the corresponding assignment matrices.

Table 2: List of considered network loading maps.

$\mathbf{B} = [b_{(\lambda,\tau'),(\rho,\tau)}]$	The link flow assignment matrix $\mathbf{B}(\mathbf{y})$ is of size $ \mathcal{L} \mathcal{T} \times \mathcal{R} \mathcal{T} $. The entry $b_{(\lambda,\tau'),(\rho,\tau)}(\mathbf{y})$ represents the probability that a pedestrian associated with route ρ and departure time interval τ reaches link λ during time interval τ' .
$\mathbf{C} = [c_{(\alpha,\tau'),(\rho,\tau)}]$	The area accumulation assignment matrix $\mathbf{C}(\mathbf{y})$ is of size $ \mathcal{A} \mathcal{T} \times \mathcal{R} \mathcal{T} $. The entry $c_{(\alpha,\tau'),(\rho,\tau)}(\mathbf{y})$ denotes the expected contribution of a pedestrian associated with route ρ and departure time interval τ to the accumulation of area α during time interval τ' .

Based on these definitions, we may write

$$\Sigma_f(\mathbf{d}; \mathbf{y}) = \mathbf{B}(\mathbf{y})\mathbf{R}(\mathbf{y})\mathbf{d}, \quad (4)$$

and

$$\Sigma_a(\mathbf{d}; \mathbf{y}) = \mathbf{C}(\mathbf{y})\mathbf{R}(\mathbf{y})\mathbf{d}, \quad (5)$$

respectively.

Let the distance along a route ρ up to the beginning of link λ be denoted by ℓ_ρ^λ . Furthermore, let the departure times of pedestrians within a time interval be distributed uniformly, i.e., the distribution of continuous departure time t for any route during a time interval τ is given by

$$h_\tau(t) = \begin{cases} \frac{1}{\Delta t} & \text{if } t \in \tau, \\ 0 & \text{otherwise.} \end{cases} \quad (6)$$

Assuming that each pedestrian is walking at a constant speed, the probability for a person on route ρ that departs during time interval τ to arrive on link λ during time interval τ' is given by

$$\begin{aligned} b_{(\lambda, \tau'), (\rho, \tau)} &= \Pr(t \in \tau, t' \in \tau' | \rho, \lambda) \\ &= \Pr\left(t \in \tau, v \in \left[\frac{\ell_\rho^\lambda}{t_{\tau'}^+ - t}, \frac{\ell_\rho^\lambda}{t_{\tau'}^- - t}\right]\right), \end{aligned} \quad (7)$$

where $t_{\tau'}^-$ and $t_{\tau'}^+$ represent the bounds of time interval τ' , and where t and t' represent the continuous departure and arrival time, respectively. For the most common case that $\ell_\rho^\lambda > 0$ and $\tau' > \tau$, we obtain

$$\begin{aligned} b_{(\lambda, \tau'), (\rho, \tau)} &= \int_{t=t_{\tau'}^-}^{t_{\tau'}^+} \int_{v=\ell_\rho^\lambda/(t_{\tau'}^+ - t)}^{\ell_\rho^\lambda/(t_{\tau'}^- - t)} f_v(v) g_\tau(t) \, dv \, dt \\ &= \frac{1}{\Delta t} \int_{t=t_{\tau'}^-}^{t_{\tau'}^+} F_v\left(\frac{\ell_\rho^\lambda}{t_{\tau'}^- - t}\right) - F_v\left(\frac{\ell_\rho^\lambda}{t_{\tau'}^+ - t}\right) \, dt, \end{aligned} \quad (8)$$

where $F_v(v)$ denotes the cumulative distribution function corresponding to $f_v(v)$. Similarly, if $\ell_\rho^\lambda > 0$ and $\tau = \tau'$, we obtain

$$\begin{aligned} b_{(\lambda, \tau), (\rho, \tau)} &= 1 - \Pr(t \in \tau, t' \notin \tau | \rho, \lambda) \\ &= 1 - \Pr\left(t \in \tau, v \in \left[0, \frac{\ell_\rho^\lambda}{t_{\tau}^+ - t}\right]\right) \\ &= 1 - \frac{1}{\Delta t} \int_{t=t_{\tau}^-}^{t_{\tau}^+} F_v\left(\frac{\ell_\rho^\lambda}{t_{\tau}^+ - t}\right) - F_v(0) \, dt. \end{aligned} \quad (9)$$

Thus, the probability that a user associated with route ρ and departure time interval τ reaches link λ during time interval τ' is given by

$$b_{(\lambda,\tau'),(\rho,\tau)} = \begin{cases} 0 & \text{if } \ell_\rho^\lambda = 0, \tau < \tau', \\ 1 & \text{if } \ell_\rho^\lambda = 0, \tau = \tau', \\ \text{Eq. (8)} & \text{if } \ell_\rho^\lambda > 0, \tau < \tau', \\ \text{Eq. (9)} & \text{if } \ell_\rho^\lambda > 0, \tau = \tau'. \end{cases} \quad (10)$$

The assignment fraction for area accumulations can be derived accordingly. Let us consider an area α , and let us assume that each route enters and leaves area α at most once. Let v be the constant, individual speed of a person traveling along route ρ , $\ell_{\text{in}}^{\rho,\alpha}$ the distance along the route ρ to the entrance of area α and $\ell_{\text{out}}^{\rho,\alpha}$ the corresponding distance to its exit. Consequently, $t_{\text{in}} = \ell_{\text{in}}^{\rho,\alpha}/v$ is the time after departure at which a person with speed v enters area α and $t_{\text{out}} = \ell_{\text{out}}^{\rho,\alpha}/v$ the corresponding time at which it is exited. If a route ρ does not cross area α , then $\ell_{\text{in}}^{\rho,\alpha} = \infty$. If we consider a time interval $[t^-, t^+]$ after departure, the expected sojourn time for this person with constant speed v inside the area α within the interval is given by

$$\sigma(v, \ell_{\text{in}}^{\rho,\alpha}, \ell_{\text{out}}^{\rho,\alpha}, t^-, t^+) = \begin{cases} t^+ - \ell_{\text{in}}^{\rho,\alpha}/v & \text{if } t^- \leq \ell_{\text{in}}^{\rho,\alpha}/v \leq t^+ \leq \ell_{\text{out}}^{\rho,\alpha}/v, \\ \ell_{\text{out}}^{\rho,\alpha}/v - t^- & \text{if } \ell_{\text{in}}^{\rho,\alpha}/v \leq t^- \leq \ell_{\text{out}}^{\rho,\alpha}/v \leq t^+, \\ t^+ - t^- & \text{if } \ell_{\text{in}}^{\rho,\alpha}/v \leq t^- \leq t^+ \leq \ell_{\text{out}}^{\rho,\alpha}/v, \\ (\ell_{\text{out}}^{\rho,\alpha} - \ell_{\text{in}}^{\rho,\alpha})/v & \text{if } t^- \leq \ell_{\text{in}}^{\rho,\alpha}/v \leq \ell_{\text{out}}^{\rho,\alpha}/v \leq t^+, \\ 0 & \text{otherwise.} \end{cases} \quad (11)$$

In Eq. (11), the first line corresponds to the case where a person reaches the area within the time interval, but does not exit it. The second line is the inverse case. The third line represents the case where a person stays within the area during the full time period. Finally, the fourth line represents the case where a pedestrian enters and leaves the area during the period of interest, and the fifth case the situation where a pedestrian is not present in area α during the time interval at all.

Using Eq. (11), the expected contribution of a pedestrian traveling along route ρ with departure time interval τ to the accumulation of area α during

time interval τ' is given by

$$\begin{aligned} c_{(\alpha,\tau'),(\rho,\tau)} &= \int_{t=t_{\tau}^-}^{t_{\tau}^+} \int_{v=0}^{\infty} \frac{\sigma(v, \ell_{\text{in}}^{\rho,\alpha}, \ell_{\text{out}}^{\rho,\alpha}, t_{\tau'}^- - t, t_{\tau'}^+ - t)}{\Delta t} f_v(v) h_{\tau}(t) \, dv \, dt \\ &= \frac{1}{\Delta t^2} \int_{v=0}^{\infty} f_v(v) \int_{t=t_{\tau}^-}^{t_{\tau}^+} \sigma(v, \ell_{\text{in}}^{\rho,\alpha}, \ell_{\text{out}}^{\rho,\alpha}, t_{\tau'}^- - t, t_{\tau'}^+ - t) \, dt \, dv. \end{aligned} \quad (12)$$

For an efficient implementation, we note that the assignment fractions (10) and (12) are time-invariant, i.e., for $\Delta\tau = \tau' - \tau$ it holds that

$$b_{(\lambda,\tau'),(\rho,\tau)} = b_{(\lambda,\Delta\tau),(\rho,0)} \quad \text{and} \quad c_{(\alpha,\tau'),(\rho,\tau)} = c_{(\alpha,\Delta\tau),(\rho,0)}. \quad (13)$$

To further reduce the cost involved in computing Eq. (10) and Eq. (12), a maximum travel time Π_{max} is defined. If $\Delta\tau \geq \Pi_{\text{max}}$, it is assumed that $b_{(\lambda,\Delta\tau),(\rho,0)} = 0 \, \forall \lambda, \rho$ and $c_{(\alpha,\Delta\tau),(\rho,0)} = 0 \, \forall \alpha, \rho$. The threshold Π_{max} is chosen such that the error incurred by this numerical approximation is negligible.

B. Traffic assignment

Stream-based fundamental diagram

The stream-based fundamental diagram ‘SbFD’, defined by Eq. (4.30), belongs to a class of density-speed relationships for which the walking speed of pedestrian stream λ can be expressed as

$$v_\lambda = v_f R_\xi^{\text{iso}} \prod_{\lambda' \in \Lambda} \exp(-\gamma_{\lambda, \lambda'} k_{\lambda'}). \quad (14)$$

In Eq. (14), the variable v_f denotes the free-flow walking speed, $R_\xi^{\text{iso}} \in [0, 1]$ an isotropic reduction factor, $\gamma_{\lambda, \lambda'}$ a parameter describing the friction of stream λ' on stream λ , and $k_{\lambda'}$ the density of stream λ' (defined as $M_{\lambda'}/A_{\xi'}$ in the loading model, where $A_{\xi'}$ is the size of area ξ' with $\lambda' \in \Lambda_{\xi'}$).

The isotropic reduction factor $R_\xi^{\text{iso}}(k_\xi)$ is a function of the area density $k_\xi = \sum_{\lambda \in \Lambda} k_\lambda$. In agreement with the monotonicity assumption stated in Eq. (4.3), it is required that

$$\frac{\partial R_\xi^{\text{iso}}}{\partial k_\xi} \leq 0. \quad (15)$$

The parameter $\gamma_{\lambda, \lambda'}$ is assumed to be independent of the densities of streams λ and λ' , as well as independent of the properties of any other stream. Typically, $\gamma_{\lambda, \lambda'}$ is a function of the intersection angle $\varphi_{\lambda, \lambda'}$ between streams λ and λ' . It is assumed that the pair-wise friction between parallel streams is zero, i.e.,

$$\gamma_{\lambda, \lambda'} = 0 \text{ if } \varphi_{\lambda, \lambda'} = 0. \quad (16)$$

Stream-based fundamental diagrams that can be expressed in the form of Eq. (14) and fulfill Eq. (16) are ‘self-consistent’. This property is illustrated at an example. Consider a stream configuration as shown in Fig. B.1a, where streams A, B' and B'' with $k_A, k_{B'}, k_{B''} \neq 0$ interact. In the

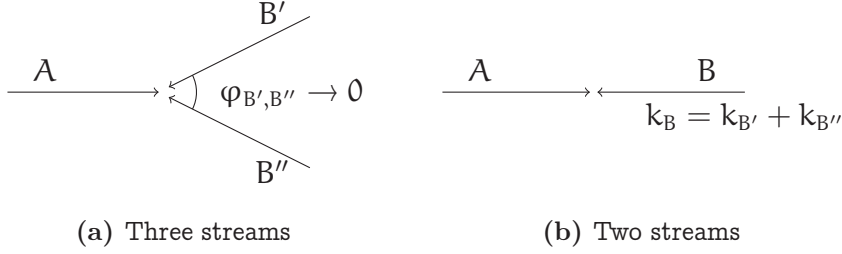


Figure B.1: Illustration of self-consistency.

limit case $\varphi_{B',B''} \rightarrow 0$, the resulting speeds are equivalent to those obtained for the configuration shown in Fig. B.1b, where the streams B' and B'' are ‘merged’ to a single stream B such that $k_B = k_{B'} + k_{B''}$. This can be verified by computing the resulting stream speeds for both configurations. Assuming that $\varphi_{B',B''} = 0$ and $\varphi_{A,B} = \varphi_{A,B'}$, one obtains for stream A

$$v_f R_\xi^{\text{iso}} \exp(-\gamma_{A,B'} k_{B'}) \exp(-\gamma_{A,B''} k_{B''}) = v_f R_\xi^{\text{iso}} \exp(-\gamma_{A,B} k_B), \quad (17)$$

where the LHS corresponds to Fig. B.1a, and the RHS to Fig. B.1b. Eq. (17) holds true since $\gamma_{A,B} = \gamma_{A,B'} = \gamma_{A,B''}$ and $k_B = k_{B'} + k_{B''}$. For stream B, one obtains

$$v_f R_\xi^{\text{iso}} \exp(-\gamma_{B',A} k_A) \exp(-\gamma_{B'',A} k_{B''}) = v_f R_\xi^{\text{iso}} \exp(-\gamma_{B,A} k_A), \quad (18)$$

which holds true since $\gamma_{B,A} = \gamma_{B',A}$ and $\gamma_{B'',A} = 0$.

The self-consistency of fundamental diagrams associated with Eq. (14) is notably due to the exponential form of the product terms, the linearity of the exponent $(-\gamma_{\lambda,\lambda'} k_{\lambda'})$ in $k_{\lambda'}$, its independence from any other stream densities, and due to the assumed absence of inner friction as expressed by Eq. (16). Self-consistency is desirable for theoretical reasons, but also to avoid a recalibration of the model in case parallel streams are merged (see Fig. B.1). Particular emphasis is given to that property as already in the Berlin case study multiple parallel streams are present (see diagonal streams in Fig. 4.8b). If only a small number of streams with distinct angles are considered, self-consistency may be less relevant. For instance, the specifications provided by Wong et al. (2010) and Xie and Wong (2015) cannot be cast in the form of Eq. (14).

The SbFD defined in Eq. (4.30) results from Eq. (14) by setting $R_\xi^{\text{iso}} = \exp(-\partial k_\xi^2)$ as well as $\gamma_{\lambda,\lambda'} = \beta(1 - \cos(\varphi_{\lambda,\lambda'}))$. We have tested several

specifications of the isotropic reduction term R_{ξ}^{iso} , including those proposed by Tregenza (1976) and Weidmann (1992), as well as a linear specification (Older, 1968; Navin and Wheeler, 1969). This set of specifications is motivated by the findings of Nikolić et al. (2015). An analysis based on the case studies discussed in Section 4.6 shows that the Drake-model performs best (Fonseca, 2015). This is in line with the results by Wong et al. (2010) and Xie and Wong (2015), who also use the Drake-model to specify the isotropic reduction term.

Likewise, we have examined several specifications of the parameter $\gamma_{\lambda,\lambda'}$ that describes the dependency of the pair-wise stream friction on the intersection angle $\varphi_{\lambda,\lambda'}$. A comparison with a linear and a piecewise linear model shows that the chosen trigonometric specification yields the best performance, at least as far as the AIC and BIC are concerned. The specification $\gamma_{\lambda,\lambda'} = \beta(1 - \cos(\varphi_{\lambda,\lambda'}))$ naturally respects Eq. (16), and it is symmetric with respect to the 180° -plane and 360° -periodic. It implies that the friction between streams is maximal for head-on flow, and that the friction grows most rapidly at an intersection angle of $\varphi = 90^\circ$, i.e., when the behavioral regime changes from ‘leader-follower’ to ‘collision avoidance’ (Bierlaire and Robin, 2009). Within each of these behavioral regimes, the friction still grows with an increasing intersection angle, but not as much as at the transitional angle $\varphi = 90^\circ$, where the slope amounts to $d\gamma/d\varphi = \beta$. Wong et al. (2010) propose the same relationship to describe the γ - φ -dependency, whereas Xie and Wong (2015) consider a specification that is not symmetric with respect to the 180° -plane.

Bibliography

- Al-Gadhi, S. A. H., Mahmassani, H. S., 1990. Modelling crowd behavior and movement: application to Makkah pilgrimage. *Transportation and Traffic Theory 1990*, 59–78.
- Alahi, A., Bagnato, L., Chanel, D., Alahi, A., 2013a. Technical report for SBB network of sensors. Tech. rep., VisioSafe SA, Switzerland.
- Alahi, A., Ramanathan, V., Fei-Fei, L., 2013b. Socially-aware large-scale crowd forecasting. In: *Proceedings of the IEEE Conference on Computer Vision and Pattern Recognition*. pp. 2203–2210.
- Amacker, K., 2012. SBB Facts and Figures. Annual report, Swiss Federal Railways (SBB-CFF-FFS), Bern, Switzerland.
- Anken, N., Hänseler, F. S., Bierlaire, M., 2012. Flux piétonniers dans la gare de Lausanne: Vers l'estimation d'une matrice OD à l'aide des extrapolations voyageurs des CFF. Internal report (unpublished), Ecole Polytechnique Fédérale de Lausanne.
- Antonini, G., Bierlaire, M., Weber, M., 2006. Discrete choice models of pedestrian walking behavior. *Transportation Research Part B: Methodological* 40 (8), 667–687.
- Asano, M., Sumalee, A., Kuwahara, M., Tanaka, S., 2007. Dynamic cell transmission-based pedestrian model with multidirectional flows and strategic route choices. *Transportation Research Record: Journal of the Transportation Research Board* 2039 (1), 42–49.
- Ashok, K., Ben-Akiva, M. E., 2000. Alternative approaches for real-time estimation and prediction of time-dependent origin–destination flows. *Transportation Science* 34 (1), 21–36.

- Bai, J., 1999. Likelihood ratio tests for multiple structural changes. *Journal of Econometrics* 91 (2), 299–323.
- Bauer, D., Brändle, N., Seer, S., Ray, M., Kitazawa, K., 2009. Measurement of pedestrian movements: A comparative study on various existing systems. In: Timmermans, H. (Ed.), *Pedestrian Behavior: Models, Data Collection and Applications*. Emerald Group Publishing, Bingley, U.K.
- Ben-Akiva, M. E., Bergman, M. J., Daly, A. J., Ramaswamy, R., 1984. Modeling inter-urban route choice behaviour. In: *Proceedings of the 9th International Symposium on Transportation and Traffic Theory*. VNU Press, Utrecht, The Netherlands, pp. 299–330.
- Ben-Akiva, M. E., Bierlaire, M., 2003. Discrete choice models with applications to departure time and route choice. In: Hall, R. W. (Ed.), *Handbook of Transportation Science*. Springer, Berlin, Germany, pp. 7–37.
- Ben-Akiva, M. E., Lerman, S. R., 1985. *Discrete choice analysis: Theory and application to predict travel demand*. Vol. 9. MIT Press.
- Benmoussa, M., Ducommun, F., Khalfi, A., Kharouf, M., Koymans, A., Nguyen, M., Raies, A., Vidaud, M., Birchler, C., 2011. *Analyse des flux piétonniers en gare de Lausanne*. Tech. rep., Ecole Polytechnique Fédérale de Lausanne.
- Besag, J., 1975. Statistical analysis of non-lattice data. *The statistician*, 179–195.
- Bierlaire, M., Crittin, F., 2004. An efficient algorithm for real-time estimation and prediction of dynamic OD tables. *Operations Research* 52 (1), 116–127.
- Bierlaire, M., Crittin, F., 2006. Solving noisy, large-scale fixed-point problems and systems of nonlinear equations. *Transportation Science* 40 (1), 44–63.
- Bierlaire, M., Robin, T., 2009. Pedestrians choices. In: Timmermans, H. J. P. (Ed.), *Pedestrian Behavior. Models, Data Collection and Applications*. Emerald Group Publishing, Bingley, U.K., pp. 1–26.

- Bierlaire, M., Toint, P. L., 1995. Meuse: An origin-destination matrix estimator that exploits structure. *Transportation Research Part B: Methodological* 29 (1), 47–60.
- Bierlaire, M., Toint, P. L., Tuyttens, D., 1991. On iterative algorithms for linear least squares problems with bound constraints. *Linear Algebra and its Applications* 143, 111–143.
- Blue, V. J., Adler, J. L., 2001. Cellular automata microsimulation for modeling bi-directional pedestrian walkways. *Transportation Research Part B: Methodological* 35 (3), 293–312.
- Borgers, A., Timmermans, H., 1986. A model of pedestrian route choice and demand for retail facilities within inner-city shopping areas. *Geographical analysis* 18 (2), 115–128.
- Bottom, J. A., 2000. Consistent anticipatory route guidance. Ph.D. thesis, Massachusetts Institute of Technology.
- Brilon, W., 2001. Handbuch für die Bemessung von Straßenverkehrsanlagen (HBS). Forschungsgesellschaft für Straßen und Verkehrswesen, Köln, Germany.
- Buchmüller, S., Weidmann, U., 2008. Handbuch zur Anordnung und Dimensionierung von Fussgängeranlagen in Bahnhöfen. IVT Projekt Nr. C-06-07. Institute for Transport Planning and Systems, ETH Zürich, Switzerland.
- Caillaud, L., 2011. Extraction des données ASE/TL/Transitec. Presentation, Swiss Federal Railways (SBB-CFF-FFS), Lausanne, Switzerland.
- Cascetta, E., 1984. Estimation of trip matrices from traffic counts and survey data: A generalized least squares estimator. *Transportation Research Part B: Methodological* 18 (4), 289–299.
- Cascetta, E., Improta, A. A., 2002. Estimation of travel demand using traffic counts and other data sources. *Applied Optimization* 63, 71–91.
- Cascetta, E., Inaudi, D., Marquis, G., 1993. Dynamic estimators of origin-destination matrices using traffic counts. *Transportation Science* 27 (4), 363–373.

- Cascetta, E., Nguyen, S., 1988. A unified framework for estimating or updating origin/destination matrices from traffic counts. *Transportation Research Part B: Methodological* 22 (6), 437–455.
- Cascetta, E., Nuzzolo, A., Russo, F., Vitetta, A., 1996. A modified logit route choice model overcoming path overlapping problems: Specification and some calibration results for interurban networks. In: *Proceedings of the 13th International Symposium on Transportation and Traffic Theory*. Pergamon, Oxford, U.K., pp. 697–711.
- Cascetta, E., Papola, A., Marzano, V., Simonelli, F., Vitiello, I., 2013. Quasi-dynamic estimation of o-d flows from traffic counts: Formulation, statistical validation and performance analysis on real data. *Transportation Research Part B: Methodological* 55, 171–187.
- Cascetta, E., Postorino, M. N., 2001. Fixed point approaches to the estimation of O/D matrices using traffic counts on congested networks. *Transportation Science* 35 (2), 134–147.
- Casey, H. J., 1955. Applications to traffic engineering of the law of retail gravitation. *Traffic Quarterly* 9 (1), 23–35.
- Chattaraj, U., Seyfried, A., Chakroborty, P., 2009. Comparison of pedestrian fundamental diagram across cultures. *Advances in Complex Systems* 12 (03), 393–405.
- Chen, M., Bärwolff, G., Schwandt, H., 2014. Modeling pedestrian dynamics on triangular grids. *Transportation Research Procedia* 2, 327–335.
- Cheung, C. Y., Lam, W. H. K., 1998. Pedestrian route choices between escalator and stairway in MTR stations. *Journal of Transportation Engineering* 124 (3), 277–285.
- Colombo, R. M., Rosini, M. D., 2005. Pedestrian flows and non-classical shocks. *Mathematical Methods in the Applied Sciences* 28 (13), 1553–1567.
- Cooper, G. A., 2014. A multi-class framework for a pedestrian cell transmission model accounting for population heterogeneity. Master's thesis, Ecole Polytechnique Fédérale de Lausanne.

- Courant, R., Friedrichs, K., Lewy, H., 1967. On the partial difference equations of mathematical physics. *IBM Journal of Research and Development* 11 (2), 215–234.
- Cule, B., Goethals, B., Tassenoy, S., Verboven, S., 2011. Mining train delays. In: *Advances in Intelligent Data Analysis X*. Springer, pp. 113–124.
- Daamen, W., 2004. Modelling passenger flows in public transport facilities. Ph.D. thesis, Delft University of Technology.
- Daamen, W., Bovy, P. H. L., Hoogendoorn, S. P., 2005. Influence of changes in level on passenger route choice in railway stations. *Transportation Research Record: Journal of the Transportation Research Board* 1930 (1), 12–20.
- Daamen, W., Hoogendoorn, S. P., 2003. Controlled experiments to derive walking behaviour. *European Journal of Transport and Infrastructure Research* 3 (1), 33–59.
- Daganzo, C. F., 1994. The cell transmission model: A dynamic representation of highway traffic consistent with the hydrodynamic theory. *Transportation Research Part B: Methodological* 28 (4), 269–287.
- Daganzo, C. F., 1995. The cell transmission model, Part II: Network traffic. *Transportation Research Part B: Methodological* 29 (2), 79–93.
- Daly, P. N., McGrath, F., Annesley, T. J., 1991. Pedestrian speed/flow relationships for underground stations. *Traffic Engineering & Control* 32 (2), 75–78.
- Danalet, A., 2015. Activity choice modeling for pedestrian facilities. Ph.D. thesis, Ecole Polytechnique Fédérale de Lausanne.
- Danalet, A., Farooq, B., Bierlaire, M., 2014. A Bayesian approach to detect pedestrian destination-sequences from WiFi signatures. *Transportation Research Part C: Emerging Technologies* 44, 146–170.
- Davidich, M., Geiss, F., Mayer, H. G., Pfaffinger, A., Royer, C., 2013. Waiting zones for realistic modelling of pedestrian dynamics: A case study using two major German railway stations as examples. *Transportation Research Part C: Emerging Technologies* 37, 210–222.

- Dial, R. B., 1971. A probabilistic multipath traffic assignment model which obviates path enumeration. *Transportation Research* 5 (2), 83–111.
- Dijkstra, E. W., 1959. A note on two problems in connexion with graphs. *Numerische Mathematik* 1 (1), 269–271.
- Djukic, T., Barceló, J., Bullejos, M., Montero, L., Cipriani, E., van Lint, H., Hoogendoorn, S. P., 2015. Advanced traffic data for dynamic od demand estimation: The state of the art and benchmark study. In: 94th Annual Meeting of the Transportation Research Board, Washington, USA, 11-15 January 2015.
- Djukic, T., Flötteröd, G., van Lint, H., Hoogendoorn, S. P., 2012. Efficient real time od matrix estimation based on principal component analysis. In: 15th International IEEE Conference on Intelligent Transportation Systems (ITSC). IEEE, pp. 115–121.
- Dodge, Y., 2006. *The Oxford dictionary of statistical terms*. Oxford University Press, Oxford, U.K.
- Drake, J. S., Schofer, J. L., May, A. D., 1967. A statistical analysis of speed-density hypotheses. In: *Proceedings of the Third International Symposium on the Theory of Traffic Flow*. New York, pp. 112–117.
- Duives, D. C., Daamen, W., Hoogendoorn, S. P., 2013. State-of-the-art crowd motion simulation models. *Transportation Research Part C: Emerging Technologies* 37 (12), 193–209.
- Eddie, L. C., 1963. *Discussion of traffic stream measurements and definitions*. Port of New York Authority, New York, USA.
- Fernández, R., Valencia, A., Seriani, S., 2015. On passenger saturation flow in public transport doors. *Transportation Research Part A: Policy and Practice* 78, 102–112.
- Fisk, C. S., 1988. On combining maximum entropy trip matrix estimation with user optimal assignment. *Transportation Research Part B: Methodological* 22 (1), 69–73.
- Florian, M., Chen, Y., 1995. A Coordinate Descent Method for the Bi-level O-D Matrix Adjustment Problem. *International Transactions in Operational Research* 2 (2), 165–179.

- Fonseca, J. M., 2015. Specification testing of fundamental diagrams for an anisotropic pedestrian network loading model. Bachelor's thesis, Ecole Polytechnique Fédérale de Lausanne.
- Frejinger, E., Bierlaire, M., 2007. Capturing correlation with subnetworks in route choice models. *Transportation Research Part B: Methodological* 41 (3), 363–378.
- Frejinger, E., Bierlaire, M., Ben-Akiva, M., 2009. Sampling of alternatives for route choice modeling. *Transportation Research Part B: Methodological* 43 (10), 984–994.
- Fruin, J. J., 1971. *Pedestrian planning and design*. Metropolitan Association of Urban Designers and Environmental Planners, Michigan, USA.
- Ganansia, F., Carincotte, C., Descamps, A., Chaudy, C., 2014. A promising approach to people flow assessment in railway stations using standard CCTV networks. In: *Transport Research Arena*, Paris, France.
- Gendre, G., Zulauf, C., 2010. *Gare de Lausanne: Analyse des flux piétonniers*. Internal report (I-PM-LS; unpublished), Swiss Federal Railways (SBB-CFF-FFS), Lausanne, Switzerland.
- Gentili, M., Mirchandani, P. B., 2012. Locating sensors on traffic networks: Models, challenges and research opportunities. *Transportation Research Part C: Emerging Technologies* 24, 227–255.
- Geroliminis, N., Daganzo, C. F., 2008. Existence of urban-scale macroscopic fundamental diagrams: Some experimental findings. *Transportation Research Part B: Methodological* 42 (9), 759–770.
- Goatin, P., Colombo, R. M., Rosini, M. D., 2009. A macroscopic model for pedestrian flows in panic situations. In: *Current Advances in Nonlinear Analysis and Related Topics*. Vol. 32. pp. 255–272.
- Gourieroux, C., Monfort, A., Renault, E., 1993. Indirect inference. *Journal of Applied Econometrics* 8, S85–S85.
- Gourieroux, C., Monfort, A., Trognon, A., 1984. Pseudo maximum likelihood methods: Theory. *Econometrica: Journal of the Econometric Society*, 681–700.

- Goverde, R. M. P., 2007. Railway timetable stability analysis using max-plus system theory. *Transportation Research Part B: Methodological* 41 (2), 179–201.
- Guo, R. Y., Huang, H. J., Wong, S. C., 2011. Collection, spillback, and dissipation in pedestrian evacuation: A network-based method. *Transportation Research Part B: Methodological* 45 (3), 490–506.
- Hänseler, F. S., Bierlaire, M., Farooq, B., Mühlematter, T., 2014a. A macroscopic loading model for time-varying pedestrian flows in public walking areas. *Transportation Research Part B: Methodological* 69, 60–80.
- Hänseler, F. S., Lederrey, G., 2015. Java implementation of anisotropic pedestrian loading model.
URL <https://github.com/flurinus/AnisoPedCTM>
- Hänseler, F. S., Molyneaux, N. A., 2015. Python implementation of pedestrian OD demand estimator for train stations.
URL <https://github.com/flurinus/DemEstMeth>
- Hänseler, F. S., Molyneaux, N. A., Bierlaire, M., 2015. Estimation of pedestrian origin-destination demand in train stations. *TRANSP-OR Report Nr. 150703*, Ecole Polytechnique Fédérale de Lausanne.
- Hänseler, F. S., Mühlematter, T., Farooq, B., 2014b. Java implementation of PedCTM.
URL <https://github.com/flurinus/PedCTM>
- Hazelton, M. L., 2000. Estimation of origin–destination matrices from link flows on uncongested networks. *Transportation Research Part B: Methodological* 34 (7), 549–566.
- Hazelton, M. L., 2003. Some comments on origin–destination matrix estimation. *Transportation Research Part A: Policy and Practice* 37 (10), 811–822.
- Helbing, D., 2001. Traffic and related self-driven many-particle systems. *Reviews of modern physics* 73 (4), 1067.
- Helbing, D., Buzna, L., Johansson, A., Werner, T., 2005. Self-organized pedestrian crowd dynamics: experiments, simulations, and design solutions. *Transportation Science* 39 (1), 1–24.

- Helbing, D., Farkas, I., Molnar, P., Vicsek, T., 2002. Simulation of pedestrian crowds in normal and evacuation situations. *Pedestrian and evacuation dynamics* 21.
- Helbing, D., Molnár, P., 1995. Social force model for pedestrian dynamics. *Physical Review E* 51 (5), 4282–4286.
- Helbing, D., Molnar, P., Farkas, I. J., Bolay, K., 2001. Self-organizing pedestrian movement. *Environment and Planning B* 28 (3), 361–384.
- Hermant, L. F. L., 2012. Video data collection method for pedestrian movement variables & development of a pedestrian spatial parameters simulation model for railway station environments. Ph.D. thesis, Stellenbosch University.
- Higgins, A., Kozan, E., 1998. Modeling train delays in urban networks. *Transportation Science* 32 (4), 346–357.
- Highway Capacity Manual, 2000. Transportation Research Board. Washington, DC.
- Hoogendoorn, S. P., 2015. Unraveling urban traffic flows. Presentation held on December 2, 2015, The University of Melbourne.
- Hoogendoorn, S. P., Bovy, P. H. L., 2002. Normative pedestrian behaviour theory and modelling. *Transportation and Traffic Theory* 15, 219–245.
- Hoogendoorn, S. P., Bovy, P. H. L., 2004. Pedestrian route-choice and activity scheduling theory and models. *Transportation Research Part B: Methodological* 38 (2), 169–190.
- Hoogendoorn, S. P., Daamen, W., 2004. Design assessment of Lisbon transfer stations using microscopic pedestrian simulation. In: *Computers in railways IX (Congress Proceedings of CompRail 2004)*. pp. 135–147.
- Hoogendoorn, S. P., Daamen, W., 2007. Microscopic calibration and validation of pedestrian models: Cross-comparison of models using experimental data. In: *Traffic and Granular Flow '05*. Springer, pp. 329–340.

- Hoogendoorn, S. P., van Wageningen-Kessels, F., Daamen, W., Duives, D. C., Sarvi, M., 2015. Continuum theory for pedestrian traffic flow: Local route choice modelling and its implications. *Transportation Research Part C: Emerging Technologies* 59, 183–197.
- Hoogendoorn, S. P., van Wageningen-Kessels, F. L. M., Daamen, W., Duives, D. C., 2014. Continuum modelling of pedestrian flows: From microscopic principles to self-organised macroscopic phenomena. *Physica A: Statistical Mechanics and its Applications* 416, 684–694.
- Huang, L., Wong, S. C., Zhang, M., Shu, C. W., Lam, W. H. K., 2009. Revisiting Hughes' dynamic continuum model for pedestrian flow and the development of an efficient solution algorithm. *Transportation Research Part B: Methodological* 43 (1), 127–141.
- Hughes, R. L., 2002. A continuum theory for the flow of pedestrians. *Transportation Research Part B: Methodological* 36 (6), 507–535.
- Jiang, C. S., Deng, Y. F., Hu, C., Ding, H., Chow, W. K., 2009a. Crowding in platform staircases of a subway station in China during rush hours. *Safety Science* 47 (7), 931–938.
- Jiang, Y., Xiong, T., Wong, S. C., Shu, C. W., Zhang, M., Zhang, P., Lam, W. H. K., 2009b. A reactive dynamic continuum user equilibrium model for bi-directional pedestrian flows. *Acta Mathematica Scientia* 29 (6), 1541–1555.
- Jin, W. L., Zhang, H. M., 2003. On the distribution schemes for determining flows through a merge. *Transportation Research Part B: Methodological* 37 (6), 521–540.
- Johansson, A., Helbing, D., Shukla, P. K., 2007. Specification of the social force pedestrian model by evolutionary adjustment to video tracking data. *Advances in Complex Systems* 10 (2), 271–288.
- Kaakai, F., Hayat, S., El Moudni, A., 2007. A hybrid Petri nets-based simulation model for evaluating the design of railway transit stations. *Simulation Modelling Practice and Theory* 15 (8), 935–969.
- Khisty, C. J., 1994. Evaluation of pedestrian facilities: beyond the level-of-service concept. *Transportation Research Record* 1438, 45–50.

- Kim, K. M., Hong, S. P., Ko, S. J., Kim, D., 2015. Does crowding affect the path choice of metro passengers? *Transportation Research Part A: Policy and Practice* 77, 292–304.
- Kirkpatrick, S., Gelatt, C. D., Vecchi, M. P., 1983. Optimization by simulated annealing. *Science* 220 (4598), 671–680.
- Kretz, T., Grünebohm, A., Kaufman, M., Mazur, F., Schreckenberg, M., 2006. Experimental study of pedestrian counterflow in a corridor. *Journal of Statistical Mechanics: Theory and Experiment* 2006 (10), P10001.
- Krzywinski, M., Schein, J., Birol, Í., Connors, J., Gascoyne, R., Horsman, D., Jones, S. J., Marra, M. A., 2009. Circos: an information aesthetic for comparative genomics. *Genome research* 19 (9), 1639–1645.
- Lam, W. H. K., Cheung, C. Y., 2000. Pedestrian speed/flow relationships for walking facilities in Hong Kong. *Journal of Transportation Engineering* 126 (4), 343–349.
- Lam, W. H. K., Cheung, C. Y., Lam, C. F., 1999. A study of crowding effects at the Hong Kong light rail transit stations. *Transportation Research Part A: Policy and Practice* 33 (5), 401–415.
- Lam, W. H. K., Lee, J. Y. S., Cheung, C. Y., 2002. A study of the bi-directional pedestrian flow characteristics at Hong Kong signalized crosswalk facilities. *Transportation* 29 (2), 169–192.
- Lam, W. H. K., Wu, Z. X., Chan, K. S., 2003. Estimation of transit origin–destination matrices from passenger counts using a frequency-based approach. *Journal of Mathematical Modelling and Algorithms* 2 (4), 329–348.
- Lavadinho, S., 2012. Compréhension fine des stratégies piétonnières en gare de Lausanne. Internal report (unpublished), Swiss Federal Railways (SBB-CFF-FFS), Lausanne, Switzerland.
- Lawson, C. L., Hanson, R. J., 1974. Solving least squares problems. Vol. 161. Society for Industrial and Applied Mathematics.
- Lebacque, J.-P., 1996. The Godunov scheme and what it means for first order traffic flow models. In: *International Symposium on Transportation and Traffic Theory*. pp. 647–677.

- Lederrey, G., 2015. A macroscopic loading model for dynamic, anisotropic and congested pedestrian flows: Implementation, calibration and case study analysis. Semester thesis, Ecole Polytechnique Fédérale de Lausanne.
- Lee, H. Y., Yang, I. T., Lin, Y. C., 2012. Laying out the occupant flows in public buildings for operating efficiency. *Building and Environment* 51, 231–242.
- Lee, J. Y. S., Lam, W. H. K., 2003. Levels of service for stairway in Hong Kong underground stations. *Journal of Transportation Engineering* 129 (2), 196–202.
- Lee, J. Y. S., Lam, W. H. K., Wong, S. C., 2001. Pedestrian simulation model for Hong Kong underground stations. In: *Intelligent Transportation Systems*. IEEE, pp. 554–558.
- Lighthill, M. J., Whitham, G. B., 1955. On kinematic waves. II. A theory of traffic flow on long crowded roads. *Proceedings of the Royal Society of London. Series A. Mathematical and Physical Sciences* 229 (1178), 317–345.
- Løvås, G. G., 1994. Modeling and simulation of pedestrian traffic flow. *Transportation Research Part B: Methodological* 28 (6), 429–443.
- Marzano, V., Papola, A., Simonelli, F., 2009. Limits and perspectives of effective o-d matrix correction using traffic counts. *Transportation Research Part C: Emerging Technologies* 17 (2), 120–132.
- Molyneaux, N. A., Hänseler, F. S., Bierlaire, M., 2014. Modeling of train-induced pedestrian flows in railway stations. In: *Proceedings of the 14th Swiss Transport Research Conference*. Locarno, Switzerland.
- Montero, L., Codina, E., Barceló, J., 2015. Dynamic od transit matrix estimation: formulation and model-building environment. In: *Progress in Systems Engineering*. Springer, Berlin, Germany, pp. 347–353.
- Moreira, M. J., 2003. A conditional likelihood ratio test for structural models. *Econometrica* 71 (4), 1027–1048.

- Mōri, M., Tsukaguchi, H., 1987. A new method for evaluation of level of service in pedestrian facilities. *Transportation Research Part A: General* 21 (3), 223–234.
- Moussaïd, M., Perozo, N., Garnier, S., Helbing, D., Theraulaz, G., 2010. The walking behaviour of pedestrian social groups and its impact on crowd dynamics. *PLoS One* 5 (4), e10047.
- Mustafa, M., Ashaari, Y., 2015. Assessing pedestrian behavioral pattern at rail transit terminal: State of the art. In: *Proceedings of the International Civil and Infrastructure Engineering Conference*. Springer, Berlin, Germany, pp. 1245–1254.
- Naini, F. M., Dousse, O., Thiran, P., Vetterli, M., 2011. Population size estimation using a few individuals as agents. In: *International Symposium on Information Theory Proceedings (ISIT)*. IEEE, pp. 2499–2503.
- Navin, F. P., Wheeler, R. J., 1969. Pedestrian flow characteristics. *Traffic Engineering* 39.
- Nguyen, S., Morello, E., Pallottino, S., 1988. Discrete time dynamic estimation model for passenger origin/destination matrices on transit networks. *Transportation Research Part B: Methodological* 22 (4), 251–260.
- Nikolić, M., Bierlaire, M., 2014. Pedestrian-oriented flow characterization. *Transportation Research Procedia* 2, 359–366.
- Nikolić, M., Bierlaire, M., Farooq, B., de Lapparent, M., 2015. Probabilistic speed-density relationship for pedestrian traffic: a data-driven approach. Technical report, Ecole Polytechnique Fédérale de Lausanne.
- Nio, I., 2012. Het station als publieke ruimte (in Dutch). Tech. rep., Bureau Spoorbouwmeester, Amsterdam, The Netherlands.
- Older, S. J., 1968. Movement of pedestrians on footways in shopping streets. *Traffic Engineering & Control* 10 (4), 160–163.
- Pettersson, P., 2011. Passenger waiting strategies on railway platforms: Effects of information and platform facilities. Master's thesis, KTH, Sweden.

- Plaue, M., Bärwolff, G., Schwandt, H., 2014. On measuring pedestrian density and flow fields in dense as well as sparse crowds. In: *Pedestrian and Evacuation Dynamics 2012*. Springer, pp. 411–424.
- Polus, A., Schofer, J. L., Ushpiz, A., 1983. Pedestrian flow and level of service. *Journal of Transportation Engineering* 109 (1), 46–56.
- Powell, M. J. D., 2009. The BOBYQA algorithm for bound constrained optimization without derivatives. Report DAMTP 2009/NA06, Department of Applied Mathematics and Theoretical Physics, Cambridge University, Cambridge, U.K.
- PTV, 2013. VISSIM 5.40 User Manual.
URL <http://vision-traffic.ptvgroup.com>
- Rabasco, J., 2014. Demand/supply coupling in pedestrian traffic estimation. Bachelor's thesis, Ecole Polytechnique Fédérale de Lausanne.
- Richards, P. I., 1956. Shock waves on the highway. *Operations Research* 4 (1), 42–51.
- Rindsfüser, G., Klügl, F., 2007. Agent-based pedestrian simulation: A case study of Bern Railway Station. *The Planning Review* 170, 9–18.
- Robin, T., Antonini, G., Bierlaire, M., Cruz, J., 2009. Specification, estimation and validation of a pedestrian walking behavior model. *Transportation Research Part B: Methodological* 43 (1), 36–56.
- Rojas-Lombarte, E., 2014. A two-step approach for estimating pedestrian demand in a congested network. Bachelor's thesis, Ecole Polytechnique Fédérale de Lausanne.
- Sayir, M. B., Dual, J., Kaufmann, S., 2008. *Ingenieurmechanik*. Springer.
- SBB-Infrastruktur, 2013. Le processus de l'élaboration de l'horaire. Internal report (unpublished), Swiss Federal Railways (SBB-CFF-FFS), Bern, Switzerland.
- Seer, S., Bauer, D., Brandle, N., Ray, M., 2008. Estimating pedestrian movement characteristics for crowd control at public transport facilities. In: *Intelligent Transportation Systems*. IEEE, pp. 742–747.

- Seneviratne, P. N., Morrall, J. F., 1985. Analysis of factors affecting the choice of route of pedestrians. *Transportation Planning and Technology* 10 (2), 147–159.
- Solak, S., Clarke, J.-P. B., Johnson, E. L., 2009. Airport terminal capacity planning. *Transportation Research Part B: Methodological* 43 (6), 659–676.
- Srikukenthiran, S., Shalaby, A., Morrow, E., 2014. Mixed logit model of vertical transport choice in Toronto subway stations and application within pedestrian simulation. *Transportation Research Procedia* 2, 624–629.
- Starmans, M., Verhoeff, L., van den Heuvel, J. P. A., 2014. Passenger transfer chain analysis for reallocation of heritage space at Amsterdam Central station. *Transportation Research Procedia* 2, 651–659.
- Stubenschrott, M., Kogler, C., Matyus, T., Seer, S., 2014. A dynamic pedestrian route choice model validated in a high density subway station. *Transportation Research Procedia* 2, 376–384.
- Tajima, Y., Takimoto, K., Nagatani, T., 2001. Scaling of pedestrian channel flow with a bottleneck. *Physica A: Statistical Mechanics and its Applications* 294 (1), 257–268.
- Ton, D., 2014. NAVISTATION: A study into the route and activity location choice behaviour of departing pedestrians in train stations. Master's thesis, Delft University of Technology.
- Tregenza, P., 1976. *The design of interior circulation*. Van Nostrand Reinhold, New York, USA.
- Treuille, A., Cooper, S., Popović, Z., 2006. Continuum crowds. In: *ACM Transactions on Graphics (TOG)*. Vol. 25. ACM, pp. 1160–1168.
- Turner, S., Middleton, D., Longmire, R., Brewer, M., Eureka, R., 2007. *Testing and evaluation of pedestrian sensors*. Monograph, Texas Transportation Institute, Texas A&M University.
- U.S. Department of Transportation, 2013. *Traffic monitoring guide*. Tech. rep., Federal Highway Administration.

- van den Heuvel, J. P. A., Hoogenraad, J. H., 2014. Monitoring the performance of the pedestrian transfer function of train stations using automatic fare collection data. *Transportation Research Procedia* 2, 642–650.
- van Hagen, M., 2011. Waiting experience at train stations. Ph.D. thesis, Universiteit Twente.
- van Wageningen-Kessels, F., Daamen, W., Hoogendoorn, S., 2015a. The two-dimensional Godunov scheme and what it means for macroscopic pedestrian flow models. Submitted manuscript, Delft University of Technology.
- van Wageningen-Kessels, F. L. M., Leclercq, L., Daamen, W., Hoogendoorn, S. P., 2015b. The lagrangian coordinate system and what it means for two-dimensional crowd flow models. *Physica A: Statistical Mechanics and its Applications*.
- van Zuylen, H. J., Willumsen, L. G., 1980. The most likely trip matrix estimated from traffic counts. *Transportation Research Part B: Methodological* 14 (3), 281–293.
- Versichele, M., Neutens, T., Delafontaine, M., Van de Weghe, N., 2012. The use of Bluetooth for analysing spatiotemporal dynamics of human movement at mass events: A case study of the Ghent Festivities. *Applied Geography* 32 (2), 208–220.
- Viti, F., Rinaldi, M., Corman, F., Tampère, C. M. J., 2014. Assessing partial observability in network sensor location problems. *Transportation Research Part B: Methodological* 70, 65–89.
- Weidmann, U., 1992. *Transporttechnik der Fussgänger*. Schriftenreihe des IVT Nr. 90. Institute for Transport Planning and Systems, ETH Zürich, Switzerland.
- Willumsen, L. G., 1981. An entropy maximising model for estimating trip matrices from traffic counts. Ph.D. thesis, University of Leeds.
- Wilson, A. G., 1970. *Entropy in urban and regional modelling*. Pion, London, U.K.

- Wong, S. C., Leung, W. L., Chan, S. H., Lam, W. H. K., Yung, N. H. C., Liu, C. Y., Zhang, P., 2010. Bidirectional pedestrian stream model with oblique intersecting angle. *Journal of Transportation Engineering* 136 (3), 234–242.
- Wong, S. C., Tong, C., 1998. Estimation of time-dependent origin-destination matrices for transit networks. *Transportation Research Part B: Methodological* 32 (1), 35–48.
- Wong, S. C., Tong, C. O., Wong, K. I., Lam, W. H. K., Lo, H. K., Yang, H., Lo, H. P., 2005. Estimation of multiclass origin-destination matrices from traffic counts. *Journal of Urban Planning and Development* 131 (1), 19–29.
- Xia, Y., Wong, S. C., Zhang, M., Shu, C. W., Lam, W. H. K., 2008. An efficient discontinuous Galerkin method on triangular meshes for a pedestrian flow model. *International Journal for Numerical Methods in Engineering* 76 (3), 337–350.
- Xie, S., Wong, S. C., 2015. A Bayesian inference approach to the development of a multidirectional pedestrian stream model. *Transportmetrica A: Transport Science* 11 (1), 61–73.
- Xu, X. Y., Liu, J., Li, H. Y., Hu, J. Q., 2014. Analysis of subway station capacity with the use of queueing theory. *Transportation Research Part C: Emerging Technologies* 38, 28–43.
- Yang, H., 1995. Heuristic algorithms for the bilevel origin-destination matrix estimation problem. *Transportation Research Part B: Methodological* 29 (4), 231–242.
- Yoshimura, Y., Sobolevsky, S., Ratti, C., Girardin, F., Carrascal, J. P., Blat, J., Sinatra, R., 2014. An analysis of visitors' behavior in the louvre museum: a study using bluetooth data. *Environment and Planning B: Planning and Design* 41 (6), 1113–1131.
- Zhang, J., Klingsch, W., Schadschneider, A., Seyfried, A., 2012. Ordering in bidirectional pedestrian flows and its influence on the fundamental diagram. *Journal of Statistical Mechanics: Theory and Experiment* 2012 (02), P02002.

- Zhang, J., Seyfried, A., 2014. Comparison of intersecting pedestrian flows based on experiments. *Physica A: Statistical Mechanics and its Applications* 405, 316–325.
- Zhang, Q., Han, B., Li, D., 2008. Modeling and simulation of passenger alighting and boarding movement in Beijing metro stations. *Transportation Research Part C: Emerging Technologies* 16 (5), 635–649.
- Zhou, X., Mahmassani, H. S., 2007. A structural state space model for real-time traffic origin–destination demand estimation and prediction in a day-to-day learning framework. *Transportation Research Part B: Methodological* 41 (8), 823–840.

Flurin S. Hänseler

23.03.1988, Zürich, Switzerland

flurin.haenseler@epfl.ch

Education

- 11.2011 – 03.2016 **EPFL**, Switzerland
Ph.D. in Civil and Environmental Engineering
Ph.D. thesis: ‘Modeling and estimation of pedestrian flows in train stations’
Jury: Michel Bierlaire (thesis director), Nikolas Geroliminis, Serge P. Hoogendoorn, William H.K. Lam, Ulrich Weidmann
July – December 2014: Visiting Ph.D. student, The Hong Kong Polytechnic University, Prof. William H.K. Lam
- 09.2006 – 10.2011 **ETH Zürich**, Switzerland
MSc in Process Engineering (GPA: 5.93/6)
Specializing in Transport Processes and Reactions
Master thesis: ‘Semiconductor Nanocrystal Formation in Tubular Microreactors’, Prof. Klavs Jensen, MIT, USA
BSc in Mechanical Engineering (GPA: 5.74/6)
Specializing in Energy, Flows and Processes

Relevant publications and technical reports

- Vetter et al. (2013), *Modeling Nucleation, Growth, and Ostwald Ripening in Crystallization Processes: A Comparison between Population Balance and Kinetic Rate Equation*, Crystal Growth & Design.
- Hänseler et al. (2014), *A macroscopic loading model for time-varying pedestrian flows in public walking areas*, Transportation Research Part B.
- Hänseler et al. (2015), *Estimation of pedestrian origin-destination demand in train stations*, Technical report (under second review at Transportation Science).
- Hänseler et al. (2015), *A dynamic network loading model for anisotropic and congested pedestrian flows*, Technical report (submitted).
- Hänseler et al. (2015), *Assessing the usage and level-of-service of pedestrian facilities in train stations: A Swiss case study*, Technical report (currently being revised for resubmission at Transportation Research Part A).

Awards and distinctions

- SNSF scholarship for six-month research period at PolyU Hong Kong (2014)
- ETH Medal, ETH Zürich (2012)
- Master Thesis Award, Micro and Nano Science Platform, ETH Zürich (2011)
- Ernest Solvay scholarship for six-month research period at MIT (2011)
- Fellowship of the Swiss Study Foundation (2008 – 2016)
- Outstanding D-MAVT Bachelor Award, ETH Zürich (2007 and 2010)

Open-source software (on GitHub)

- PedCTM (2014): Pedestrian cell transmission model, in Java
- AnisoPedCTM (2015): Multi-directional pedestrian loading model, in Java
- DemEstMeth (2015): Pedestrian OD demand estimator for train stations, in Python

